高等植物における脂肪酸β酸化系酵素の細胞生物学的研究

林　潤

要旨

カボチャなどの脂肪性種子において、発芽したばかりの光合成能を持たない黄化子葉は、細胞内のリピッドボディに蓄えられた貯蔵脂肪を糖に変えることによって生長のためのエネルギー及び炭素源としている。この変換を触媒するものがマイクロボディに存在する脂肪酸β酸化系とグリオキシル酸サイクルの諸酵素である。高等植物において、このβ酸化系酵素のうちacyl-CoA oxidaseは長鎖、中鎖、短鎖の鎖長特異性の異なる3種類のアイソザイムを持つことが報告されている。しかし、これまでの報告は生化学的な解析のみであり、分子的実体が明らかにされていなかった。事実、acyl-CoA oxidaseの高次構造は多様であり、ラット肝のacyl-CoA oxidaseは同一タンパク質が全長と特定部位が切断されて生じた2種類のサブユニットにより構成されている。

ミトコンドリアとマイクロボディにおいて脂肪酸β酸化が行われる動物とは異なり、高等植物の場合、ミトコンドリアにおけるβ酸化活性が非常に低く、脂肪酸β酸化の存在にはまだ議論の余地はある。そのため、高等植物では主にマイクロボディで脂肪酸を代謝していると考えられており、マイクロボディの脂肪酸代謝システムは非常に重要である。マイクロボディの脂肪酸β酸化系の諸酵素のうち、基質特異性のあるacyl-CoA oxidaseはβ酸化系のスパイラルに入るための初発酵素である。現在まで、脂肪酸β酸化系を構成する他の酵素についての知見はあるが、acyl-CoA oxidaseに関してはその解析が進んでいない。そこで、筆者はacyl-CoA oxidaseの分子的実体を明らかにするためcDNAクローニングを試みた。

第1章でカボチャのcDNAライブラリーより高等植物で初めてacyl-CoA oxidaseのcDNAを単離、同定した(*J.Biol.Chem.*, 273: 8301-8307, 1998)。その解析の結果、このタンパク質はマイクロボディへのターゲティングシグナルとしてN末端に延長配列をもつことが判明した。動物のacyl-CoA oxidaseは全てC末端にターゲティングシグナルをもつ形で合成されるので、機能の同一なacyl-CoA oxidaseが植物と動物において輸送シグナルを異にすることが判明した。また、発現パターンが同じβ酸化系酵素のthiolaseと同様の挙動を示すことよりβ酸化系の諸酵素が同じ機構で制御されている可能性が示唆された。また、この

acyl-CoA oxidase の基質特異性を解析したところ長鎖、中鎖のアシル CoA に特異的な長鎖特異的 acyl-CoA oxidase であることが明らかとなった。

次に第 2 章では、現在知られている分子量 60,000-70,000 の acyl-CoA oxidase より計算分子量が小さい 47,000 の acyl-CoA oxidase と推測されるタンパク質について解析を行った。バキュロウイルス発現システムを使用して、活性を保ったまま発現させて精製を行った。精製タンパク質の解析から、C8 以下の短鎖アシル CoA に基質特異性をもつ、高等真核生物で初めて分子的実体が報告される短鎖特異的 acyl-CoA oxidase であることを明かにした (*J.Biol.Chem.*, 274: 12715-12721, 1999)。動物では短鎖アシル CoA はミトコンドリアに輸送されて代謝されるため、短鎖特異的 acyl-CoA oxidase は存在しない。このことは、短鎖長のアシル CoA がミトコンドリアに輸送され ATP 生成に利用される動物細胞と異なり、植物細胞では脂肪酸がマイクロボディ内で完全に分解されてアセチル CoA になり、糖新生の基質として利用されていることを示している。

これら長鎖、短鎖 acyl-CoA oxidase の解析により、高等植物における acyl-CoA oxidase の炭素鎖長特異性がタンパク質自身に由来するものであり、高等植物のマイクロボディ β 酸化系には、長鎖、短鎖の基質特異性の異なる 2 種類の acyl-CoA oxidase が存在していることが明らかになった。このことにより、マイクロボディ内で脂肪酸が長鎖から短鎖まで完全に代謝されていることが分子レベルで初めて明らかにされた。

略号

AcNPV	:*Autographa californica* Nuclear Polyhedrosis virus
cDNA	:complementary DNA
CoA	:coenzyme A
c.p.m.	:counts per minute
BSA	:bovine serum albumin
dATP	:deoxyadenosine 5'-triphosphate
dCTP	:deoxycytidine 5'-triphosphate
DNA	:deoxyribonucleic acid
DTT	:dithiothreitol
dNTPs	:deoxynucleoside 5'-triphosphates
EDTA	:ethylenediaminetetraacetic acid
EST	:expressed sequence tag
FAD	:flavin adenine dinucleotide
FBS	:fetal bovine serum
FMN	:flavin mononucleotide
FPCoA	:β-(2-furyl)propionyl-CoA
GM	:germination medium
GUS	:β-glucuronidase
HEPES	:*N*-2-hydroxyethylpiperazine-*N*'-2-ethanesulfonic acid
IgG	:immunoglobulin G
kDa	:kilodalton
mRNA	:messenger RNA
M.O.I.	:multiplicity of infection
MOPS	:3-(*N*-morpholino)propanesulfonic acid
MS	:Murashige and Skoog medium
PBS	:phosphate buffered saline
PCR	:polymerase chain reaction
PFU	:plaque forming unit
PMSF	:phenylmethanesulfornyl fluoride
poly(A)$^+$RNA	:polyadenylated RNA
PPAR	:peroxisome proliferator-activator receptor
PPRE	:peroxisome proliferator-receptor element
PTS	:peroxisomal targeting signal
PVDF	:polyvinylidene difluoride
RNA	:ribonucleic acid
SDS	:sodium dodecyl sulfate
SDS-PAGE	:SDS-polyacrylamide gel electrophoresis
Sf9 cell	:*Spodoptera frugiperda* 9 insect cell
TCA	:tricarboxylic acid
TNM-FH	:Trichoplusia ni Medium-Formulation Hink
Tris	:tris(hydoxymethyl)aminomethane

その他、核酸、アミノ酸の略号として１文字及び３文字表記を用いた。

目次

序論

植物は光合成によりエネルギーを得る独立栄養生物である。しかし、種子が発芽する段階では光合成を行うことができない。そのため、植物細胞は発芽時に備えて細胞内に栄養物を蓄えることによって、光合成を行う能力が獲得されるまでに必要なエネルギー源を確保している。カボチャなどの脂肪性種子において、発芽したばかりの光合成能を持たない黄化子葉は、細胞内のリピッドボディに蓄えられた貯蔵脂肪を糖に変換することによって生長のためのエネルギー及び炭素源としている。発芽後、芽生えが展開して光照射を受け緑化すると、緑化子葉は光合成により生長に必要なエネルギーを獲得するようになる。このように、発芽種子では黄化子葉が緑化し、光合成能を獲得する間に、エネルギー源を種子貯蔵物から光合成産物に切り替える。このエネルギー源の変換は細胞内にも大きな影響を与える。高等植物細胞は、オルガネラの機能を変換することによりこの変化に対応している。エチオプラストは光合成を行う葉緑体となり、ミトコンドリアは光呼吸におけるグリシンの酸化を行うようになる。マイクロボディは発芽時の貯蔵脂肪の分解から光呼吸への関与にその機能を変換する (Titus and Becker 1985, Nishimura et al. 1986)。

1) マイクロボディとは

マイクロボディは真核細胞に広く分布する直径 0.1-2.0μm の球状ないし楕円形の一重膜の細胞内小器官 (オルガネラ) である。Rhodin らはマウス腎臓尿細管上皮細胞の電子顕微鏡観察より微小顆粒状のマトリクスを持つ新しいオルガネラを観察し、形態学的名称としてマイクロボディ (microbody) と命名した (Rhodin 1954)。しかし、このマイクロボディは局在する組織及び機能により様々な名称がある。de Duve らは、ラット肝細胞由来のオルガネラ中に過酸

化水素の生成を伴う酸化酵素群とこの有毒な過酸化水素を分解する catalase を検出し、機能的名称としてパーオキシソームと呼ぶことを提唱し、現在ではこの名称が広く用いられている (de Duve and Baudhuin 1966)。高等植物では、脂肪性種子の発芽時に子葉において一過性に発現するマイクロボディにはグリオキシル酸サイクルが存在することから、この特殊なマイクロボディはグリオキシソームと名付けられた (Breidenbach and Beevers 1967)。

2）マイクロボディターゲティングシグナル

マイクロボディはミトコンドリア、葉緑体と異なりそれ自身の DNA を有しておらず、マイクロボディタンパク質は核ゲノムにコードされている。このため、マイクロボディタンパク質はサイトゾルからマイクロボディへ移行するためのシグナルを保持しており、サイトゾルの遊離ポリソームで生合成された後、マイクロボディへ輸送される。近年、遺伝子工学的手法を用いてターゲティングシグナルの探索が主に動物培養細胞を用いて精力的に行われた。その結果、移行シグナルはパーオキシソームターゲティングシグナル (Peroxisomal Targeting Signal : PTS) と呼ばれ、現在までに大きく分けて 3 種類 (PTS1, PTS2, mPTS) のマイクロボディ移行シグナルが同定されている。PTS は酵母から動物、植物細胞まで広く保存されているが、そのアミノ酸特異性は種により変化していることが明らかになっている (Subramani 1993, Hayashi et al. 1996, Kato et al. 1996)。

3）マイクロボディの機能変換

先程述べたように、黄化子葉においてマイクロボディは、β酸化系とグリオキシル酸サイクルをもつグリオキシソームとして、主に貯蔵脂肪を分解す

る役割を果たしている。脂肪性種子の黄化子葉が光照射により緑化する際、マイクロボディは脂肪酸β酸化系とグリオキシル酸サイクルが存在するグリオキシソームから緑葉パーオキシソームにその機能を大きく変換する。マイクロボディ内の酵素群もマイクロボディの機能に合致するように大幅に変動する。このとき、malate synthase, isocitrate lyase は特異的に分解される。そして、緑葉パーオキシソーム酵素である glycolate oxidase, hydroxypyruvate reductase が新たに合成されてマイクロボディに輸送される。また、子葉の老化時には緑葉パーオキシソームはグリオキシソームに変換される (Nishimura et al. 1986)。

4）マイクロボディの脂肪酸β酸化系

脂肪酸β酸化系の概念は、イヌにω炭素をフェニル基でラベルした脂肪酸を与え、その尿を解析したところ、偶数炭素の脂肪酸を与えたときには常にフェニル酢酸が、奇数炭素を与えた場合は、常に安息香酸が観察されたことより、脂肪酸が C-2 位と C-3 位の共有結合の酸化的切断により分解されること（β酸化）が示されたことに始まる。当初、動物の肝細胞において、脂肪酸β酸化はミトコンドリアのみで行われていると考えられていた。脂肪酸β酸化により生成されたアセチル CoA は TCA サイクルの基質になること、及び呼吸鎖の酸化的リン酸化に共役することから、ミトコンドリアで脂肪酸β酸化が行われると考えることが合理的であった。しかし、高等植物において、グリオキシル酸サイクルが存在するグリオキシソームにその基質となるアセチルCoAを供給する脂肪酸β酸化系が局在することが明らかになった (Cooper and Beevers 1969)。

グリオキシソームβ酸化系の発見は、脂肪酸β酸化系がミトコンドリア以

外のオルガネラにも存在することを示している。また、同一のオルガネラに脂肪酸β酸化系とグリオキシル酸サイクルが存在することは、糖新生にとって効率が良い。その後、ラット肝細胞由来のマイクロボディも脂肪酸β酸化能を持つことが示された。ラット肝細胞ではβ酸化系が抗高脂血薬剤などのパーオキシソーム増殖剤の投与により、マイクロボディの増殖が10倍以上亢進することが示された (Lazarow and de Duve 1976)。また、酵母ではアルカンを炭素源として発育させるとマイクロボディが著しく増殖し、脂肪酸β酸化系が誘導されることが明らかになった (Osumi et al. 1975)。このように、当初、マイクロボディにおける脂肪酸β酸化系は植物において先行して発見されたが、その後、分子遺伝学的手法での解析が容易な酵母、遺伝子疾患の研究が精力的に行われている動物細胞において脂肪酸β酸化系の諸酵素の解析が進んでいる (Picataggio et al. 1991, van den Bosch et al. 1992)。

5）脂肪酸β酸化系 (Fig.1)

自然界に分布する脂肪酸の多くは偶数個の炭素原子を持つ直鎖脂肪酸であるのでβ酸化の繰り返しにより最終的にはアセチル CoA に分解される。また、不飽和脂肪酸、奇数個の炭素原子を含む脂肪酸、分枝脂肪酸から生じるプロピオニル CoA や短鎖分枝脂肪酸は、β酸化に加えてそれぞれ特殊な代謝系を経て、最終的にはアセチル CoA と二酸化炭素に分解される。

マイクロボディのβ酸化系酵素はacyl-CoA oxidase、 2-enoyl-CoA hydratase及び 3-hydroxyacyl-CoA dehydrogenase の活性を有する多機能酵素、3-ketoacyl-CoA thiolase（以下 thiolase と呼ぶ）により構成される。ミトコンドリアの脂肪酸β酸化系は acyl-CoA dehydrogenase、2-enoyl-CoA hydratase、 3-hydroxyacyl-CoA dehydrogenase、3-ketoacyl-CoA thiolase により構成されている。どちらの

系の場合でも脂肪酸分解は acyl-CoA synthetase による脂肪酸の活性化によって触媒される。

Acyl-CoA synthetase

Acyl-CoA synthetase は、ATP を AMP とピロリン酸に加水分解するエネルギーを利用して脂肪酸のカルボキシル基と CoA の間にチオエステルを形成する。この反応は、脂肪酸のカルボキシル基に AMP が結合する反応と、生成した脂肪酸-AMP が CoA に置換する反応の 2 段階よりなる。

Acyl-CoA oxidase, Acyl-CoA dehydrogenase (Fig.2)

脂肪酸 β 酸化の最初の反応は、アシル CoA の 2,3 位の炭素原子間に trans の二重結合を導入しエノイル CoA にする反応である。この反応は原核生物や真核生物のミトコンドリアでは acyl-CoA dehydrogenase、真核生物のマイクロボディでは acyl-CoA oxidase により行われる。両酵素はどちらも FAD を補酵素として利用する。しかし、acyl-CoA dehydrogenase が電子受容体として電子伝達フラビンタンパク質 (ETF) による電子伝達系を利用して呼吸鎖と共役して ATP 生成に関与するのに対し、acyl-CoA oxidase は分子状酸素を電子受容体として用い、生じた過酸化水素を catalase で消去している点が異なっている。

2-enoyl-CoA hydratase, 3-hydroxyacyl-CoA dehydrogenase, Thiolase

エノイル CoA は、2-enoyl-CoA hydratase、 3-hydroxyacyl-CoA dehydrogenase 及び thiolase により炭素数が 2 つ短いアシル CoA とアセチル CoA に分解される。

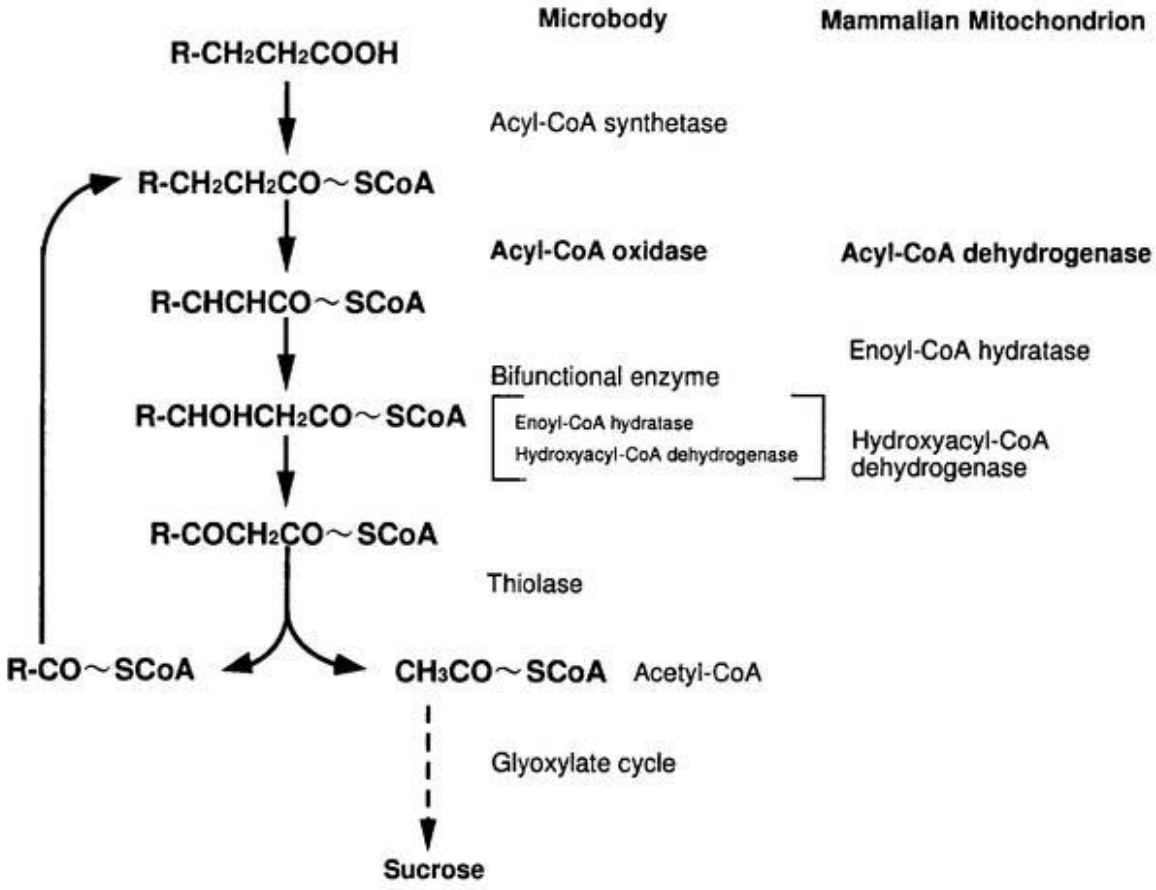

Fig. 1 Fatty acid β-oxidation

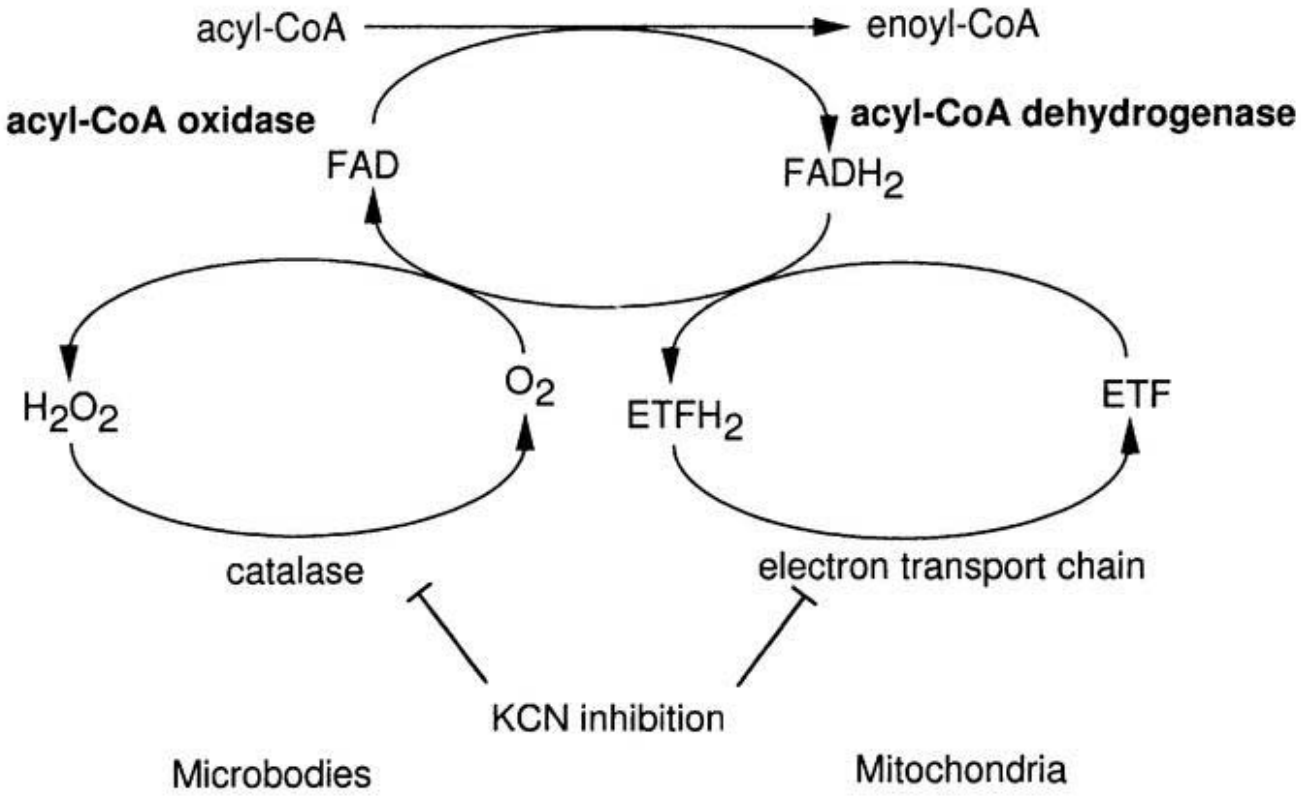

Fig. 2 Comparison of peroxisomal and mitochondrial β-oxidation.

しかし、不飽和脂肪酸を分解する場合は、enoyl-CoA isomerase、hydroxyacyl-CoA epimerase などが必要とされる。これらの酵素活性は 2 つまたは 3 つの活性を兼ねた多機能酵素などの形でも存在する。

6）マイクロボディβ酸化系とミトコンドリアβ酸化系

動物ではマイクロボディとミトコンドリアに脂肪酸β酸化系が存在する。主に、脂肪酸代謝を行っているのは ATP 生成と共役しているミトコンドリアで、マイクロボディはミトコンドリアでは代謝されにくい極長鎖脂肪酸や薬剤の代謝、及び胆汁酸合成をする (Furuta et al. 1981, Shultz 1991)。この両オルガネラのβ酸化の異なる点は、

a) マイクロボディ膜には極長鎖 acyl-CoA synthetase と長鎖 acyl-CoA synthetase が存在する。通常、炭素鎖長数 22 以上 (C22) の脂肪酸を極長鎖脂肪酸という。ヒトの遺伝病であるパーオキシソーム病で蓄積する脂肪酸の炭素鎖長は主に C22、C24、C26 である。これに対し、ミトコンドリア外膜には長鎖 acyl-CoA synthetase のみが存在する。しかし、近年、極長鎖 acyl-CoA dehydrogenase が発見されたことからミトコンドリアにも極長鎖 acyl-CoA synthetase が存在することが示唆されている (Izai et al. 1992)。

b) マイクロボディにはミトコンドリア内膜に存在する carnitine palmitoyl-transferase、 carnitine/acylcarnitine translocase のような長鎖アシル CoA 輸送機構は存在しない。

c) ミトコンドリアの脂肪酸β酸化系は呼吸鎖と共役しているのでシアンで阻害されるが、マイクロボディの脂肪酸β酸化系はシアンで阻害されない。但し、catalase が阻害されて過酸化水素が蓄積する。

d) 動物の acyl-CoA oxidase は炭素鎖長に特異性を示さず、極長鎖から中鎖まで全て代謝する（酵母、高等植物には炭素鎖長特異性はある）。ミトコンドリアの acyl-CoA dehydrogenase は炭素鎖長による基質特異性を示すアイソザイムが少なくとも 5 種類見つかっている (Ikeda et al. 1983, Izai et al. 1992)。(極長鎖特異的 acyl-CoA dehydrogenase、長鎖特異的 acyl-CoA dehydrogenase、中鎖特異的 acyl-CoA dehydrogenase、短鎖特異的 acyl-CoA dehydrogenase、分枝短鎖特異的 acyl-CoA dehydrogenase)

7）植物の脂肪酸β酸化系

動物の脂肪酸β酸化はミトコンドリアとマイクロボディの両方のオルガネラで機能している。動物のマイクロボディでは脂肪酸炭素鎖長の短縮は中鎖 (C8) までしか行われず、C8 以下のアシル CoA はミトコンドリアに輸送されて代謝される (Schulz 1991)。これに対して、高等植物ではマイクロボディの脂肪酸β酸化系は脂肪酸を長鎖から短鎖まで完全に代謝する能力があり、脂肪酸β酸化系において初発酵素である acyl-CoA oxidase は、炭素鎖長による基質特異性を持ちアシル CoA の炭素鎖長を識別する (Gerhardt 1992, Kirsh et al.1986)。しかし、これらの知見は生化学的な解析のみであり、分子レベルでの解析はされていない。また、ミトコンドリアにおける脂肪酸β酸化能は動物のミトコンドリアの脂肪酸β酸化活性と比較して著しく低く、ミトコンドリアの脂肪酸β酸化系の存在にはまだ議論の余地がある (Gerhardt 1992)。
このように植物のマイクロボディ脂肪酸β酸化は脂肪酸代謝に重要な役割を果たしている。しかし、解析の進んでいる動物のミトコンドリア、マイクロボディの脂肪酸β酸化と比較して、高等植物の脂肪酸β酸化に関する知見は限られている。現在までに、多機能酵素、thiolase については酵素活性、cDNA クローニングの知見が報告されているが、高等植物の acyl-CoA oxidase

は cDNA クローニングがまだ報告がされていなかった。高等植物の acyl-CoA oxidase は動物のマイクロボディβ酸化系との大きな相違点である基質特異性のある酵素であり、acyl-CoA oxidase の cDNA を同定し解析することは高等植物において脂肪酸β酸化の生理的役割を明らかにするためにも重要である。

第 1 章において、カボチャ発芽子葉のグリオキシソーム膜結合タンパク質の N 末端アミノ酸配列を基にその cDNA クローニングを行い、塩基配列を決定してその解析を行った。その結果、このタンパク質は動物の acyl-CoA oxidase とは異なる PTS を持つ長鎖特異的 acyl-CoA oxidase であることが明らかになった。

第2章では、アラビドプシス短鎖特異的 acyl-CoA oxidase の同定をバキュロウイルス発現システムを用いて行い、その酵素特性を解析した。短鎖特異的 acyl-CoA oxidase は酵母の知見があるが、動物ではまだ報告例がなく、高等真核細胞で初めて報告されるものである。また、酵母の短鎖特異的 acyl-CoA oxidase はこれまでに知られていた acyl-CoA oxidase と同じ一次構造を示しているのに対し、アラビドプシスの短鎖特異的 acyl-CoA oxidase は一次構造上 acyl-CoA dehydrogenase と高い類似性を示すユニークな acyl-CoA oxidase であることが明らかになった。

引用文献

Breidenbach, R.W. and Beevers, H. (1967) Biochem. Biophys. Res. Commun. 27:462-429

Cooper, T.G. and Beevers, H. (1969) J. Biol. Chem. 244:3507-3513

de Duve, C. and Baudhuin, P. (1966) Physiol. Rev. 46:323-357

Furuta, S., Miyazawa, S. and Hashimoto, T. (1981) J. Biochem. (Tokyo) 90:1739-1750

Gerhardt, B. (1992) Prog. Lipid Res. 31:417-446

Hayashi, M., Aoki, M., Kato, A., Kondo, M. and Nishimura, M. (1996) Plant J. 10:225-234

Ikeda, Y., Dabrowski, C. and Tanaka, K. (1983) J. Biol. Chem. 258:1066-1076

Izai, K., Uchida, Y., Orii, T., Yamamoto, S. and Hashimoto, T. (1992) J. Biol. Chem. 267:1027-1033

Kato, A., Hayashi, M., Kondo, M. and Nishimura, M. (1996) Plant Cell 8:1601-1611

Kirsch, T., Löffler, H. -G. and Kindl, H. (1986) J. Biol. Chem. 261: 8570-8575

Lazarow, P.B. and de Duve, C. (1976) Proc. Natl. Acad. Sci. USA 73:2043-2046

Nishimura, M., Yamaguchi, J., Mori, H., Akazawa, T. and Yokota, S. (1986) Plant Physiol. 81:313-316

Nishimura, M., Hayashi, M., Kato, A., Yamaguchi, K. and Mano, S. (1996) Cell Struct. Funct. 21:387-393

Osumi, M., Fukuzumi, F., Teranishi, Y., Tanaka, A. and Fukui, F. (1975) Arch Microbiol. 103:1-11

Picataggio, S., Deanda, K. and Mielenz, J. (1991) Mol. Cell. Biol. 11:4333-4339

Reddy, J.K.and Krishnakantha, T.P. (1975) Science 190:787-789

Rhodin, J. (1954) Ph. D. thesis. Aktiebolaget Goduil, 76

Schulz, H. (1991) Biochim. Biophys. Acta 1081:109-120

Subramani, S. (1993) Annu. Rev. Cell Biol. 9:445-478

Titus, D.E. and Becker, W.M. (1985) J. Cell Biol. 101:1288-1299

van den Bosch, H., Schutgens, R.B., Wanders, R.J. and Tager, J.M. (1992) Annu. Rev. Biochem. 61:157-197

第１章

カボチャ子葉の 73kD グリオキシソーム膜結合タンパク質の cDNA クローニングとその解析

材料及び方法

実験材料

実験材料としてはカボチャの種子 (*Cucurbita sp.* Kurokawa Amakuri) を用いた。種子は表皮をつけたまま、流水に 12 時間浸した後、湿らせた粒状ロックウール（日東紡績）上に播種し、暗所下 25℃ において発芽、生育させた。また、発芽後 5 日間暗所で生育させた黄化芽生えを白色光下に移し、25℃で生育させたものを緑化芽生えとした。

発芽カボチャ子葉 cDNA ライブラリーの作製

暗所下で 4 日間発芽、生育させた黄化子葉から、SDS /フェノール法 (Ausubel et al., 1987) により全 RNA を抽出した。この全 RNA をオリゴ (dT) セルロースカラムクロマトグラフィー (Aviv and Leder, 1972) に供し、poly(A)$^+$ RNA を調製した。cDNA synthesis system plus (Amersham Pharmacia, Japan)、λgt 11 cDNA library synthesis kit (Amersham Pharmacia, Japan) を用いて、poly(A)$^+$RNA から λgt 11 phage library を構築した。

ポリメラーゼチェーン反応 (PCR, Saiki et al., 1985)

反応液は、1μM primer、160μM dNTPs, 1.5mM $MgCl_2$, 1 x PCR 緩衝液、2units Taq DNA polymerase (Promega, U.S.A.) を含み、全量を 25μl とした。プレート上から 1 プラークを寒天培地ごとパスツールピペットで吸い取り、50μl の滅菌水に懸濁した。このうちの 2μl を増幅反応液中に加えた。増幅反応は、94℃ 2分間の前処理の後、94℃ 1 分間、55℃ 1 分間、72℃ 2 分間のサイクルを 30 回繰り返した後、さらに 72℃ 10 分間の後処理を行った。反応液 5μl を 1 %アガロース電気泳動に供して生成物の大きさを確認した。ファージクローンの cDNA インサートの長さを確認するためには、λgt 11 のリバースプライマー (5'-TTGACACCAGACCAACTGGTAATG-3') とフォワードプライマー (5'-GGTGGCGACGACTCCTGGAGCCCG-3') を用いて PCR を行った。

塩基配列の決定

ファージクローン中の cDNA インサートは制限酵素 *Eco* RI で切り出した後、Bluescript II プラスミドベクター (Stratagene, U.S.A.) に連結した。ディリーションクローンの作製には Kirosequence deletion kit (Takara, Japan) を使用した。塩基配列の同定は ABI PRISM サイクルシークエンシングキットによるジデオキシ法 (Sanger et al. 1977) を用いた。

特異抗体の調製

スクリーニングにより得られた cDNA を発現ベクター pET32b (Novagen, U.S.A.) に連結したプラスミドを作製し、大腸菌に導入して長鎖特異的 acyl-CoA oxidase と

6xhistidine による融合タンパク質 (LACOX-6xhis) を大腸菌内で生産した。超音波処理により大腸菌を破壊し、3,000xg の遠心により可溶性画分と不溶性画分に分離させ、その不溶性画分を 6M 尿素で処理し、3,000xg の遠心を行い、その6M尿素可溶性画分をニッケルレジンカラムにより精製した。0.5mg の LACOX-6xhistidine 融合タンパク質を含む 1 ml の滅菌水に、等量の Freund's complete adjuvant (Difco Laboratories, U.S.A.) を加えて良く乳化後、ウサギ背部に皮下注射して第 1 回目の免疫感作とした。4 週間後、同量の融合タンパク質を含む1mlの滅菌水に等量の incomplete adjuvant を加えて乳化し、第 2 回目の免疫感作として皮下注射とした。以後、1 週間毎に第 5 回まで免疫感作を行った。第 1 回目の免疫感作の直前に少量採血し、前血清とした。第 2 回目以降の免疫感作から 1 週間後に耳の動脈より採血を行い抗血清を調製して使用した。

カボチャ黄化子葉ホモジネイトのショ糖密度勾配遠心

発芽後 4 日目のカボチャ黄化子葉、15gを 10ml の緩衝液 (150mM Tricine-KOH、pH 7.5, 1mM EDTA, 0.5M ショ糖, 1% BSA) とともに氷上のペトリ皿内でカミソリ刃により約 5 分間破砕し、これを4層のガーゼで弱く絞って濾過した後、核、プラスチド等を除くため JA-20 アングルローター (Beckman, U.S.A.) で 1,500xg、10 分間遠心した。上清 2ml を 16ml のショ糖密度勾配溶液 [30 %-60 % (w/w), 1mM EDTA] に上層して、SW 28.1 スイングローター (Beckman, U.S.A.) で、21,000 rpm 、3 時間遠心した。遠心終了後、直ちに fractionator (model 185: ISCO, U.S.A.) で 0.5ml 毎に分画し、それぞれの画分において指標酵素の活性測定を行った。すべての操作は 4℃ で行った。

カボチャ黄化子葉からの無傷グリオキシソームの単離

発芽後 5 日目のカボチャ黄化子葉、100g を 200ml の緩衝液 I (20mM ピロリン酸ナ

トリウム、pH 7.5, 1mM EDTA, 0.3M マンニトール) とともに破砕し、これを 4 層のガーゼで濾過し、強く絞った。この操作を再度繰り返した後、これらの抽出液を合わせて 1,500xg で 15 分間遠心し、核、プラスチド等を除き、さらに上清を 10,000xg で 20 分間遠心した。この沈澱を 200ml の緩衝液 I に懸濁した後、1,500xg の遠心、続いて 10,000xg の遠心を繰り返した。ここで得られた沈澱を 10-20ml の緩衝液 II (10mM HEPES-KOH, pH 7.2, 1mM EDTA, 0.3 M マンニトール) に懸濁し、そのうちの 4ml を 30ml のパーコール溶液 [28% (w/w) パーコール (Amersham Pharmacia, Japan), 10mM HEPES-KOH,pH 7.2, 1mM EDTA, 0.3M ラフィノース]に上層した。40,000xg で 30 分間遠心後、遠心管の底部にバンド状に集まったグリオキシソームを駒込ピペットで回収した。得られたグリオキシソームは 5 倍量の緩衝液IIを加えてパーコールを希釈し、4,800xg, 10 分間遠心して沈澱として回収した。

グリオキシソーム膜結合タンパク質の調製

5 日間暗所で培養したカボチャの黄化子葉より無傷グリオキシソームを単離した。これを 5,000xg, 10 分間遠心後、沈澱を 200µl の抽出液 (10mM HEPES-KOH, pH7.2) で懸濁した。100,000xg, 30 分間遠心後、その上清をグリオキシソーム可溶性画分とした。沈澱は 200µl の抽出液で懸濁後、 0.2M Na_2CO_3 を等量加えて再度懸濁した後、100,000xg, 30 分間遠心を行い、上清をグリオキシソーム膜結合タンパク質画分とした。すべての操作は 4℃ で行った。

N末端アミノ酸配列の決定

長鎖特異的 acyl-CoA oxidase の N 末端アミノ酸配列は Matsudaira (1987) の方法に従って決定した。グリオキシソーム膜結合タンパク質画分を SDS-PAGE で分離、染色

した後、PVDF 膜 (Perkin-Elmer, Japan) に転写した。約 73kD に相当するバンドを切り出して、自動アミノ酸配列決定装置 (model 473A, Perkin-Elmer, Japan) により分析した。

cDNA 塩基配列の解析

cDNA 塩基配列の解析にはコンピュータソフトウェア、GeneWorks (IntelliGenetics, Inc., U.S.A.) を使用し、アミノ酸配列の同一性を調べるために BLAST e-mail server (Altschul et al., 1990) を経由して cDNA (GenBank) 及びタンパク質データベース (Gepept, Swissprot) にアクセスした。アミノ酸配列の解析及び分子系統樹の作製には CLUSTAL W プログラム (Higgins et al., 1992) を使用した。

長鎖特異的アシル CoA オキシダーゼ cDNA のスクリーニング

プラークハイブリダイゼイションは Sambrook et al. (1989) の方法に従った。プローブはランダムプライマー法 (Feinberg and Vogelstein, 1984) を用いて [α-^{32}P] dATP (Amersham Pharmacia, Japan) で放射標識した。

フェニルセファロースカラムクロマトグラフィー

5 日間暗所下で発芽、生育したカボチャの黄化子葉を 3 倍量(W/V)の緩衝液 A (150mM Tris-HCl, pH7.8, 10mM KCl, 1mM DDT, 10μM FAD, 0.1mM PMSF, 10% glycerol) で磨砕し、そのホモジネイトを15,000xg、4℃、20分間遠心した。その上清を等量の緩衝液 C [50mM sodium phosphate, pH 7.0, 3.4 M $(NH_4)_2SO_4$] を加えてフェニルセファロースカラム (Amersham Pharmacia, Japan) にかけた。緩衝液 D [50mM sodium phosphate, pH 7.0, 1.7M $(NH_4)_2SO_4$] で洗浄後、緩衝液 B (50mM sodium phosphate, pH 7.0, 60% ethyleneglycol) により濃度勾配をかけて抽出した。

ノザンブロット解析

全 RNA はカボチャ芽生えより RNA/DNA 抽出キット ISOGEN (Nippon gene, Japan) を使用して調製した。10μg の全 RNA を 0.66M ホルムアミドと10mM MOPS, pH 7.5 を含むアガロースゲルで電気泳動した。泳動後、ゲル中の RNA はナイロンメンブレン (Hybond N^+, Amersham Pharmacia, Japan) に転写した。50ml の 2xSSC (SSC: 150mM NaCl, 15mM sodium citrate, pH 7.0) で固定、乾燥した。プレハイブリダイゼイション、ハイブリダイゼイションは、ハイブリダイゼイション溶液中 [0.12M $NaPO_4$, pH 7.2, 0.25M NaCl, 1mM EDTA, 7% (w/w) SDS, 50% (w/v) ホルムアミド] , 42℃ で行った。プローブは長鎖特異的 acyl-CoA oxidase の cDNA を用いた。Megaprime DNA labeling kit (Amersham Pharmacia, Japan) を用いて [α -^{32}P] dATP で放射標識し、放射活性が $1x10^6$ c.p.m./ml になるようにハイブリダイゼイション液に加えた。プレハイブリダイゼイションは 42℃ 15 分間、ハイブリダイゼイションは 42℃ 18 時間行った。ハイブリダイゼイション後、洗浄は 1xSSC/0.1% SDS で 15 分間、0.1xSSC/0.1% SDSで15分間行った。洗浄後、余分な水分を除いてサランラップで覆い、増感板を用いて -80℃ 下で X 線フィルムとコンタクトした。

イムノブロット解析

各発育段階において採取したカボチャ子葉は、抽出緩衝液 (100mM Tris-HCl, pH 8.0, 1mM EDTA, 1mM PMSF, 1% SDS) とともに磨砕し、抽出液を遠心後、上清を SDS-PAGE で分離した。SDS-PAGE はLaemmli (1970) の方法に、ナイロン膜への転写はTowbin et al. (1979) の方法に従った。

酵素活性の測定

Acyl-CoA oxidase の活性測定は Gerhardt (1987) の方法に従った。反応溶液 (acyl-CoA oxidase, 200mM Tris-HCl, pH8.5, 1mM 4-aminoantyphyrine, 100mM *p*-hydroxyaminobenzonic acid, 20μM FAD, 1mM NaN_3, 4U horse-radish peroxidase) 1 ml 中に 50μM もしくは 25μM のアシル CoA を基質として加えた。オルガネラの指標酵素である catalase は Aebi (1965) の方法に、cytochrome *c* oxidase は Hodges and Loenald (1974) の方法に従って測定した。

その他の方法

プラスミド DNA の調製、制限酵素による DNA の切断、DNA のアガロースゲル電気泳動等の基本的操作は Sambrook らの方法 (1989) に準じた。

結果

1）長鎖特異的 acyl-CoA oxidase の cDNA クローニングと塩基配列の決定

現在知られている acyl-CoA oxidase は分子量が約 60,000-80,000 であることより、分子量が 75,000 の acyl-CoA oxidase の可能性のあるグリオキシソーム膜結合型タンパク質の同定を行った。カボチャの種子を暗所で 5 日間生育させた黄化子葉を採取して、グリオキシソーム画分を調製した。このグリオキシソーム画分を抽出液Iでよく懸濁してグリオキシソームを破砕した後、100,000xg, 4℃, 30 分間遠心した。この沈澱を 0.1M Na_2CO_3 で可溶化し、再度、遠心した。この上清を膜結合型タンパク質画分とした。この画分を SDS-PAGE にかけ、分離、染色した後 (Fig.3)、まだ、機能の判明していない約 73KDa に相当するバンドの N 末端アミノ酸配列の決定を試みたところ, A-A-G-K-A-K-A-K-I-E-V-D-M-G-S-L-S-L-Y-M-R-G-K-H-R-E-I-Q-E-R-V-F-E-Y-F-N というアミノ酸配列が得られた (Fig.3)。このアミノ酸配列をデータベースにより検索すると動物の acyl-CoA oxidase に同一性があることが明らかになった。そこで、このグリオキシソーム膜結合型タンパク質をコードする cDNA を得るため、以下のようにスクリーニングを行った。

得られた N 末端アミノ酸配列を基にしてディジェネレイトプライマー (primer 1, [5'-GC(A/T/C/G) GG(A/T/C/G) (A/C)A(A/G) GC(A/T/C/G) AA(A/G) GC-3']; primer 2 [5'-AT(A/C/T) GA(A/G) GT(A/T/C/G) GA(C/T) ATG GG-3']) を作製し (Fig.4A)、カボチャプラスミド cDNA ライブラリー (pTTQ) を鋳型として PCR を行った。最初に T3 primer-primer 1, T7 primer-primer 1 の組み合わせで PCR を行った結果、T7 primer-primer 1 の組み合わせで増幅した断片が得られた。この増幅断片を鋳型として T7 primer-primer 2 の組み合わせで PCR を行い、約 1.6kbp の増幅断片を得た。この増幅断片の両端の塩基配列を決定したところ、先に決定した N 末端アミノ酸配列をコードする塩基配

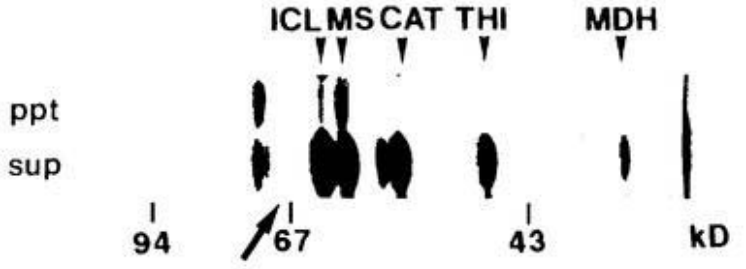

(A/Q)AGK/(Q/A)KAKIEVDMGSLSLYMRGKH(K/R)EIQ(E)RVFE(Q)YFN

Fig. 3 N-terminal amino acid sequence of alkali-soluble glyoxysomal membrane binding protein.

The abbreviations used are: ppt, precipitate fraction; sup, supernatant fraction in 0.1 M Na_2CO_3 treatment; ICL, isocitrate lyase; MS, malate synthase; CAT, catalase; THI, thiolase; MDH, malate dehydrogenase.

A.

AAGKAKAKIEVDMGSLSLYMRGKHREIQERVFEYFN

primer 1 primer 2

primer 1 [5'-GC(A/T/C/G) GG(A/T/C/G) (A/C)A(A/G) GC(A/T/C/G) AA(A/G) GC-3']
primer 2 [5'-AT(A/C/T) GA(A/G) GT(A/T/C/G) GA(C/T) ATG GG-3'])

B.

IEVDMGSLSLYMRGKHREIQERVFEYFN----

primer 3 primer 4

primer 3 [5'-CACAGGGAGATTCAAGA-3']
primer 4 [5'-TCGGATCGAATGTAGCT-3']

Fig. 4 A. Design of the degenerate primers based on 72kD glyoxysomal membrane binding protein in pumpkin etiolated cotyledons that were used for PCR as a template of pumpkin plasmid cDNA library.
B. Design of the primers for PCR, in which PCR product was used as a probe for screening of pumpkin phage cDNA library.

列を持つことが判明した。

さらに全長の cDNA を得るため、得られた PCR 断片の塩基配列を基にしてプライマーを作製し (Fig. 4B, primer 3, [5'-CACAGGGAGATTCAAGA-3']; primer 4, [5'-TCGGATCGAATGTAGCT-3'])、PCR により増幅させた約 400bp の断片をスクリーニング用プローブとして使用した。カボチャファージ cDNA ライブラリー (λ gt 11) を用いてスクリーニングを試みた結果、約 2.4kbp のインサートを含む cDNA クローンを得た。この cDNA クローンのマルチクローニングサイト中の制限酵素 *Eco*RI サイトで切断後、pBluescript にサブクローニングし、全塩基配列を決定した。その結果、Figure 5 に示される cDNA の塩基配列を決定した。インサートの全長は 2313bp であり、2073bp のオープンリーディングフレームをもち、690 アミノ酸残基をコードしていること明らかになった。この cDNA にコードされているタンパク質の計算分子量は 77,319 になる。しかし、cDNA がコードするアミノ酸配列の N 末端より46アミノ酸残基目より、先に決定された N 末端アミノ酸配列が存在した (Fig.3、及びFig.5、下線部分)。このことは、Figure 5 の二重下線領域は延長配列であること示している。延長配列を取り除いた成熟体タンパク質部分の計算分子量は 72,414 となり、膜結合型タンパク質画分の SDS-PAGE による推定分子量 73,000 とほぼ同じ分子量となった。この成熟体タンパク質の計算分子量は先に精製されたキュウリの長鎖特異的 acyl-CoA oxidase の分子量 72,000 とほぼ同じものである (Kirsch et al., 1986)。

2）一次構造解析

GenBank データベースより、得られた cDNA に同一性のあるものを検索した結果、コチョウランより単離された acyl-CoA oxidase ホモログとして登録されている cDNA とアミノ酸レベルにおいて 76% 同一であることが分かった (Do and Huang 1997)。また、現在知られている acyl-CoA oxidase とアミノ酸レベルで比較を行った結果、全体

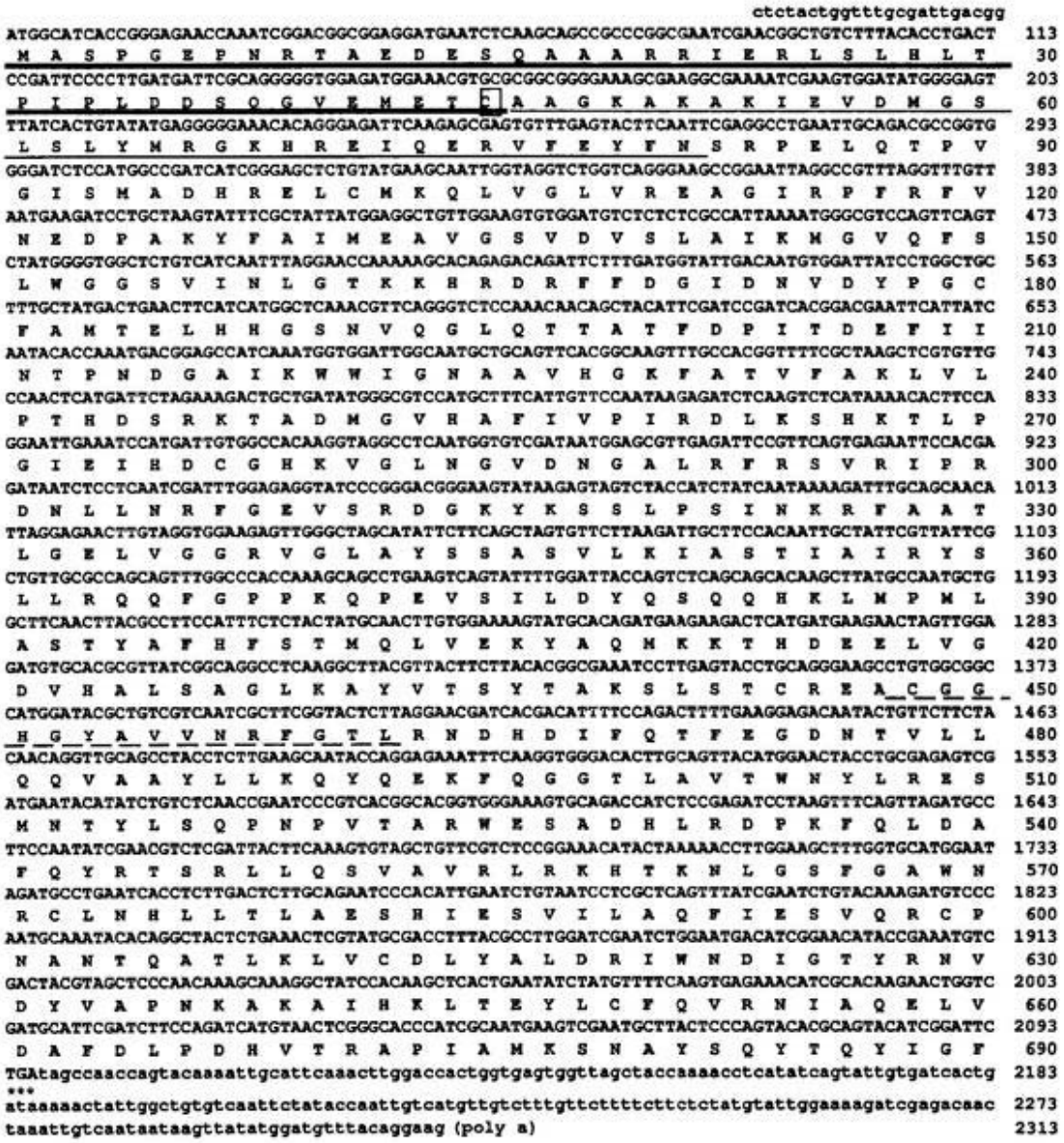

Fig. 5 Nucleotide and deduced amino acid sequences of the pumpkin acyl-CoA oxidase cDNA.

The amino-terminal amino acid sequence of the mature protein, as determined by Edman degradation, is single-underlined; the putative presequence is double-underlined; the dotted line marks the putative FMN binding motif. The amino acid residue of the processing site is marked with an open box.

として動物の acyl-CoA oxidase とは同一性が低かった。最も同一性が高いラットの pristanoyl-CoA oxidase に対して 30% の同一性であり、次いでラットの trihydroxycoprostanoyl-CoA とは 29%、一般的な acyl-CoA oxidase であるラットの palmitoyl-CoA oxidase に対して 28% の同一性であった (Osumi and Hashimoto 1978, Van Veldhoven et al. 1992, Van Veldhoven et al. 1994)。

カボチャ、コチョウランの acyl-CoA oxidase 及び pristanoyl-CoA oxidase とのアミノ酸配列の比較を Figure 6 に示している。動物のパーオキシソームに局在する pristanoyl-CoA oxidase はメチル化された側鎖脂肪酸の CoA エステルを酸化する acyl-CoA oxidase で側鎖のない長鎖脂肪酸 CoA エステルも酸化する (Van veldhoven et al. 1994)。この 3 種の acyl-CoA oxidase の全長にわたるアミノ酸配列に対する同一性は低く見える。しかしながら、部分的に高い同一性を持つ領域が存在する (Fig.6、下線部)。この領域はラットの trihydroxycoprostanoyl-CoA、palmitoyl-CoA oxidase においても存在する。また、この領域はフラビンモノヌクレオチド結合サイトと推定される領域を含んでいる (Fig.5、点線部 Dubourdieu et al. 1977)。動物のミトコンドリアのβ酸化系酵素で acyl-CoA oxidase と同様の機能を果たす acyl-CoA dehydrogenase に共通して存在するとされている protein signature 1 (PS1: [GAC]-[LIVM]-[ST]-E-x(2)-[GSAN]-G-S-D-x(2)-[GSA], Bairoch et al. 1995) は 9 アミノ酸残基中 7 残基、protein signature 2 (PS2:[QE]-x(2)-G-[GS]-x-G-[LIVMFY]-x(2)-[DEN]-x(4)-[KR]-x(3)-[DE], Bairoch et al. 1995) は 8 アミノ酸残基中 6 残基がカボチャ acyl-CoA oxidase においても保存されていることが確認された (Fig. 6、アステリスク)。これらの領域は FAD や基質であるアシル CoA の結合部位になっている可能性が示唆される。

いくつかのペルオキソームタンパク質 (malate dehydrogenase, thiolase, citrate synthase) は高分子量の前駆体として合成されることが知られている (Kato et al.1995, 1996a, 1998)。これらの前駆体型タンパク質はタンパク質の N 末端側が切断され成熟体にな

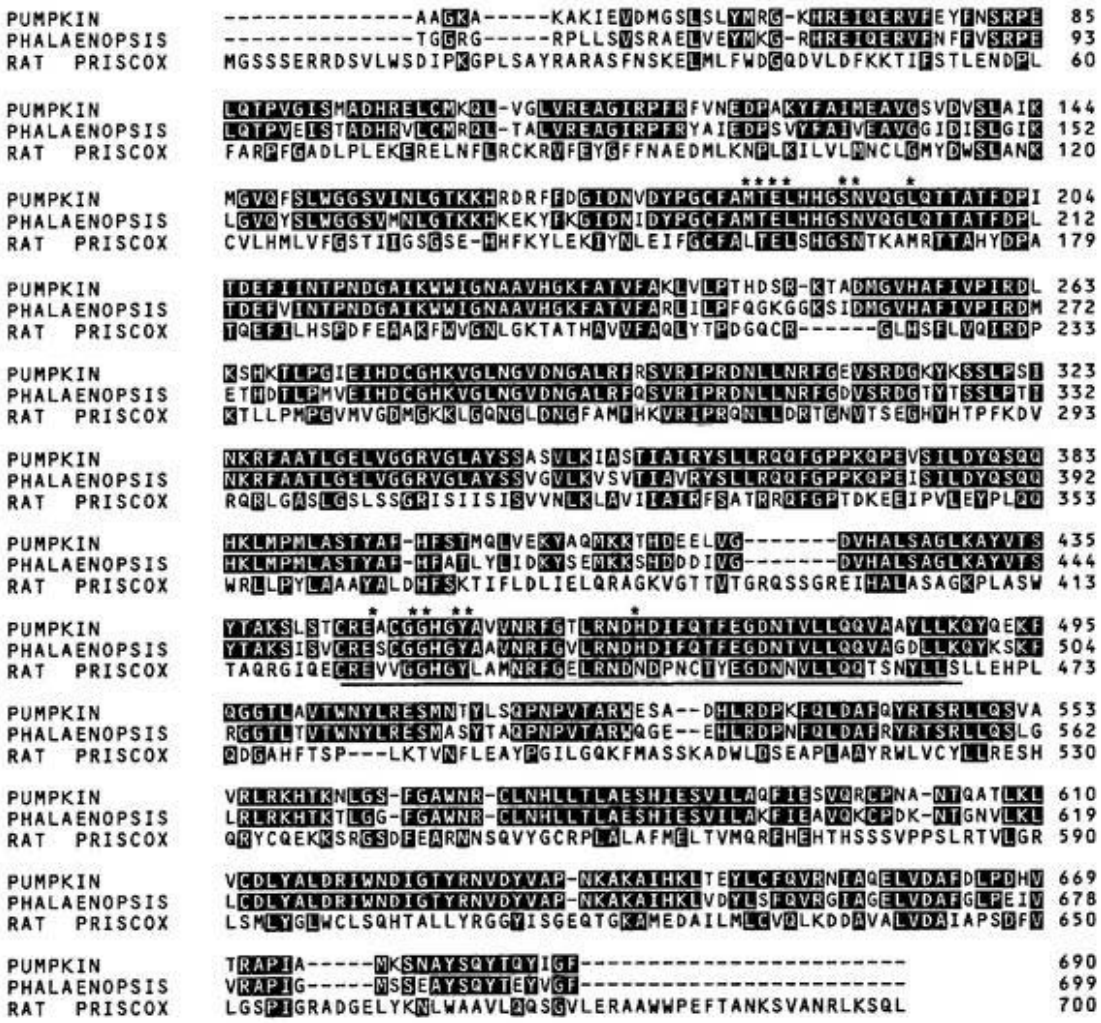

Fig. 6 Alignment of amino acid sequences of pumpkin acyl-CoA oxidase (pumpkin), *Phalaenopsis* acyl-CoA oxidase (*Phalaenopsis*), and rat Pristanoyl-CoA oxidase (rat PRISCOX). The region of high homology is underlined, asterisks mark amino acids common to the two protein signatures of acyl-CoA dehydrogenase (protein signature 1 and protein signature 2, respectively).

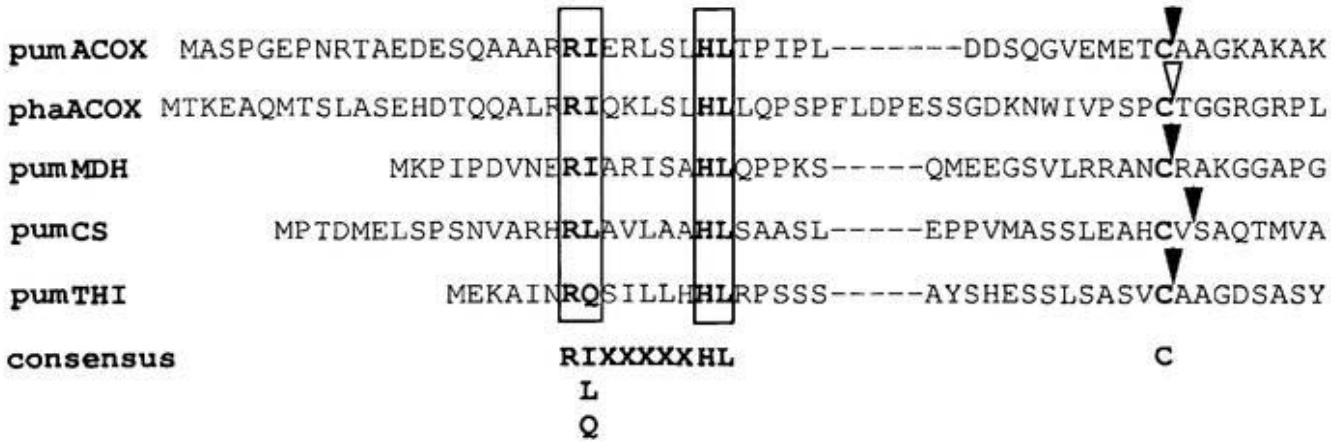

Fig. 7 Alignment of the amino-terminal presequence of pumpkin acyl-CoA oxidase with other presequences of microbody proteins that are synthesized as larger precursors: pumACOX, pumpkin acyl-CoA oxidase; phaACOX, *Phalaenopsis* acyl-CoA oxidase (Do, Y.Y. et al., 1997); pumMDH, pumpkin glyoxysomal malate dehydrogenase (Kato, A. et al., 1997); pumCS, pumpkin glyoxysomal citrate synthase (Kato, A. et al., 1995); pumTHI, pumpkin glyoxysomal 3-keto-acyl-CoA thiolase (Kato, A. et al., 1996a). Conserved amino acids are shown in bold. Processing sites of presequences, determined by sequencing of the amino-terminal amino acids of mature proteins, are shown by arrowheads.

る。当研究室を含めた最近の知見より、前駆体型で合成される他のマイクロボディタンパク質のN末端延長配列はシステイン残基のC末端側で切断されることがすでに明らかになっている。また、マイクロボディタンパク質のN末端延長配列がターゲティングシグナル(PTS2)として働くことも報告されている(Subramani 1993, Kato et al. 1996b)。先に決定されたN末端アミノ酸配列より(Fig.3, Fig.5 下線部分)、カボチャacyl-CoA oxidaseは45番目のシステインのカルボキシル側で切断され、成熟体型タンパク質になることが示された。Figure 7にカボチャ、コチョウランのacyl-CoA oxidase、及び前駆体で合成されるカボチャマイクロボディタンパク質のN末端領域を示した(Kato et al.1995, 1996a, 1998, Do and Huang 1997)。コチョウランの場合、cDNAが単離されているだけなので、その切断部位は推定したものを示している。これらのタンパク質のアミノ末端領域には、高等植物のPTS2として同定されている配列(R-[ILQ]-x5-H-L)が存在している。このことより、カボチャacyl-CoA oxidaseはPTS2タイプのターゲティングシグナルを持っていることが示唆される。

3）カボチャ黄化子葉のacyl-CoA oxidase活性

得られたcDNAが、実際にacyl-CoA oxidaseであるかを調べるために以下の実験を行った。発芽後5日間暗所で生育させたカボチャの黄化子葉を破砕し、15,000xg、4℃、20分間遠心後、その上清をフェニルセファロースカラムにかけ、そのフラクションのacyl-CoA oxidase活性を調べた(Fig.8A)。その結果、炭素鎖長特異性の異なる3種のacyl-CoA oxidase活性が検出された。1つは短鎖長のアシルCoAであるヘキサノイルCoA (C6)に特異的な短鎖特異的acyl-CoA oxidaseと思われる活性を示している。他の2つは重複しており、長鎖長のパルミトイルCoA (C16)と中鎖長のデカノイルCoA (C10)に対する活性を示している。このことは長中鎖に特異的なacyl-CoA oxidaseが存在することを示している。大腸菌に発現させたカボチャacyl-CoA oxidase

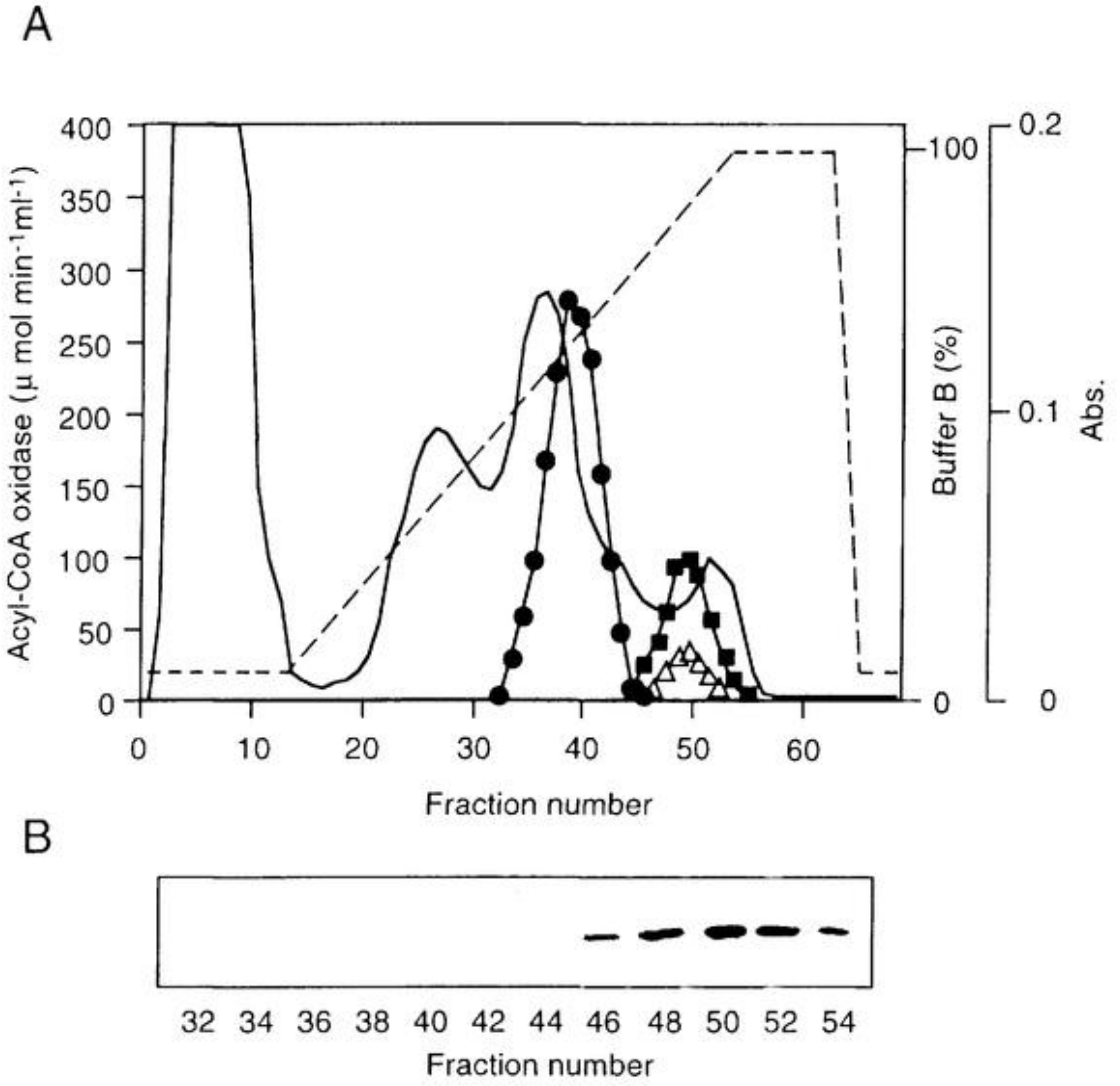

Fig. 8 A. Separation of acyl-CoA oxidase isoenzymes by hydrophobic interaction chromatography. A crude extract from 5-day dark-grown pumpkin cotyledons was loaded onto a Phenyl Sepharose High Performance HiTrap column (1 ml) and proteins were eluted by increasing the concentration of buffer B (50 mM sodium phosphate, pH 7.0, containing 60 % ethylene glycol) from 0 to 100 %. Protein (—, A_{280}) and acyl-CoA oxidase activities with different substrates (hexanoyl-CoA, ●; decanoyl-CoA, Δ; palmitoyl-CoA, ■) were determined. The dotted line represents the concentration (%) of Buffer B.

B. Immunodetection of acyl-CoA oxidase in fractions from the hydrophobic interaction chromatography. 25 µl of the fractions indicated were subjected to SDS-PAGE (10 % acrylamide) and immunoblotted.

に対するポリクローナル抗体を作製してフェニルセファロースカラムの各フラクションに対し、イムノブロット解析を行った。その結果、長中鎖 acyl-CoA oxidase の活性があったフラクションにのみ分子量約 73,000 のバンドが検出された (Fig. 8B)。これまでの生化学的解析により植物の acyl-CoA oxidase は精製された長鎖特異的 acyl-CoA oxidase が分子量 72,000 であり、中鎖特異的 acyl-CoA oxidase が分子量 62,000 であることが報告されている (Kirsch et al. 1986, Hooks et al. 1996)。以上のことより、このカボチャ acyl-CoA oxidase は長鎖特異的 acyl-CoA oxidase であると同定した。

4）カボチャ黄化子葉における長鎖特異的 acyl-CoA oxidase の局在性

スクリーニングにより得られた cDNA がコードする acyl-CoA oxidase の細胞内局在性を調べるために、ショ糖密度勾配遠心によりオルガネラを分画後、イムノブロット解析及び酵素活性の測定を行った (Fig.9)。発芽後 4 日間暗所で生育した黄化子葉をカミソリ刃を用いて抽出緩衝液中で裁断し、これを 4 層のガーゼで濾過後、抽出液を 1,500xg の遠心にかけて核、プラスチド等を除去した。この上清を 30-60% (w/v) のショ糖密度勾配遠心で分画した。catalase をグリオキシソームの指標酵素に、cytochrome *c* oxidase をミトコンドリアの指標酵素として活性を測定した。Acyl-CoA oxidase 活性はcatalaseと同様に上清及びグリオキシソームに検出された (Fig.9A)。また、おなじβ酸化系酵素の thiolase をグリオキシソームの指標酵素として各画分のイムノブロット解析を行った結果、Acyl-CoA oxidase は thiolase と同様に上清とグリオキシソームに検出された (Fig.9B)。グリオキシソームは一重膜で囲まれたオルガネラであるため、分画中に壊されやすい。そのため、上清に検出された活性及びタンパク質は破壊されたグリオキシソームより漏れ出たものと考えられる。また、ミトコンドリアにもわずかな酵素活性が検出されたが、グリオキシソームの混入によるものではないかと推測している。以上の結果より、acyl-CoA oxidase はグリオキシソー

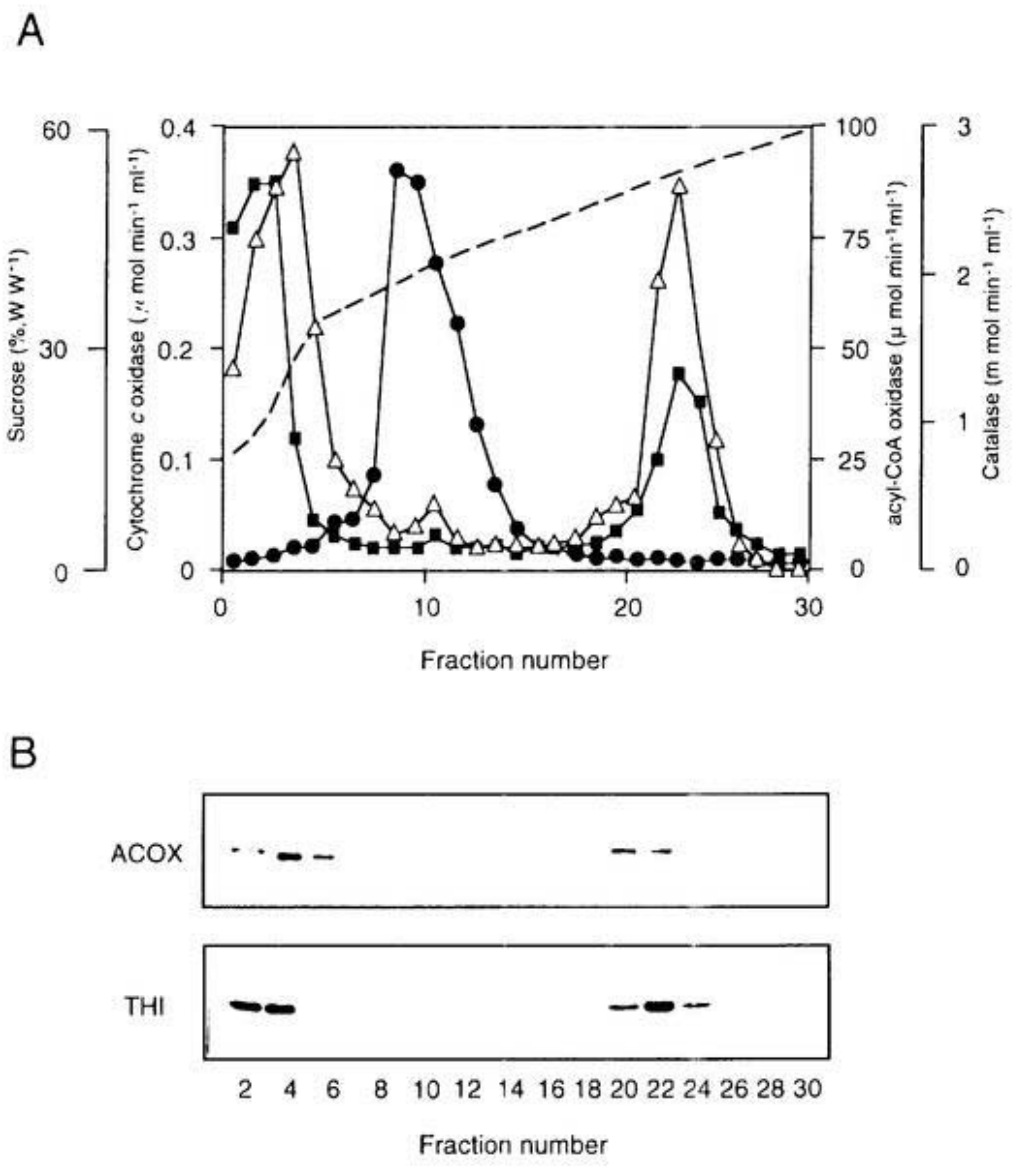

Fig. 9 Subcellular localization of acyl-CoA oxidase in etiolated pumpkin cotyledons. An extract from 5-day-old etiolated cotyledons was fractionated by sucrose density gradient centrifugation. A. Enzyme activities: Cytochrome *c* oxidase (●), catalase (■), and acyl-CoA oxidase (Δ). Sucrose concentration w/w (—). B. Immunological detection of pumpkin acyl-CoA oxidase. 5 μl from each odd-numbered fraction was subjected to SDS-PAGE (10 % acrylamide) and immunoblotted.

ムに局在し、N 末端延長配列に存在する PTS2 はターゲティングシグナルとして機能することが確認された。

5）発芽過程における mRNA 及びタンパク質の発現

脂肪性種子の黄化子葉が光照射により緑化する際、マイクロボディ内の酵素群も大きく変動する。脂肪酸β酸化系酵素である acyl-CoA oxidase も種子の発芽過程において大きく変化するものと思われる。そのため、発芽後の acyl-CoA oxidase の挙動を暗所下で生育させた場合、及び光照射し緑化させた場合に mRNA 及びタンパク質の挙動を解析した (Fig.10,11)。ノーザンブロット解析により acyl-CoA oxidase の mRNA 量の挙動を解析したものを Figure 10A に示している。長鎖特異的 acyl-CoA oxidase の mRNA は発芽初期より急速に発現量が増加し、発芽後、暗所生育3日目に最大値に達した後、急速に減少している。また、暗所で4日間培養後、光照射下に移して生育した緑化子葉とそのまま暗所下で生育させた黄化子葉を比較した場合は mRNA の発現量に変化が見られなかった。同じβ酸化系酵素である thiolase においても、同様の結果が得られている。但し、長鎖特異的 acyl-CoA oxidase は、その mRNA の発現量が thiolase と比較して低いものとなっている (Fig.10B)。

イムノブロット解析によるタンパク質量の変動を Figure 10 に示している。長鎖特異的 acyl-CoA oxidase のタンパク質の蓄積量は、発芽後、暗所生育 5 日目に最大になっており mRNA の発現ピークより遅くなっている。また、その減少過程も暗所生育下で mRNA のように急速に減少するのではなく徐々に減少している (Fig.11A)。この mRNA とタンパク質の発現パターンの違いは、thiolase においても同様の結果が観察される (Fig.11B)。これらの結果より、長鎖特異的 acyl-CoA oxidase は mRNA の転写レベルで調節を受けているばかりでなく、タンパク質レベルでも調節を受けていることが示している。しかし、光照射により緑化子葉になると長鎖特異的 acyl-CoA

oxidase、thiolase ともに急速に減少する。このことは光照射により長鎖特異的 acyl-CoA oxidase、thiolase の分解が誘導されていることを示している。

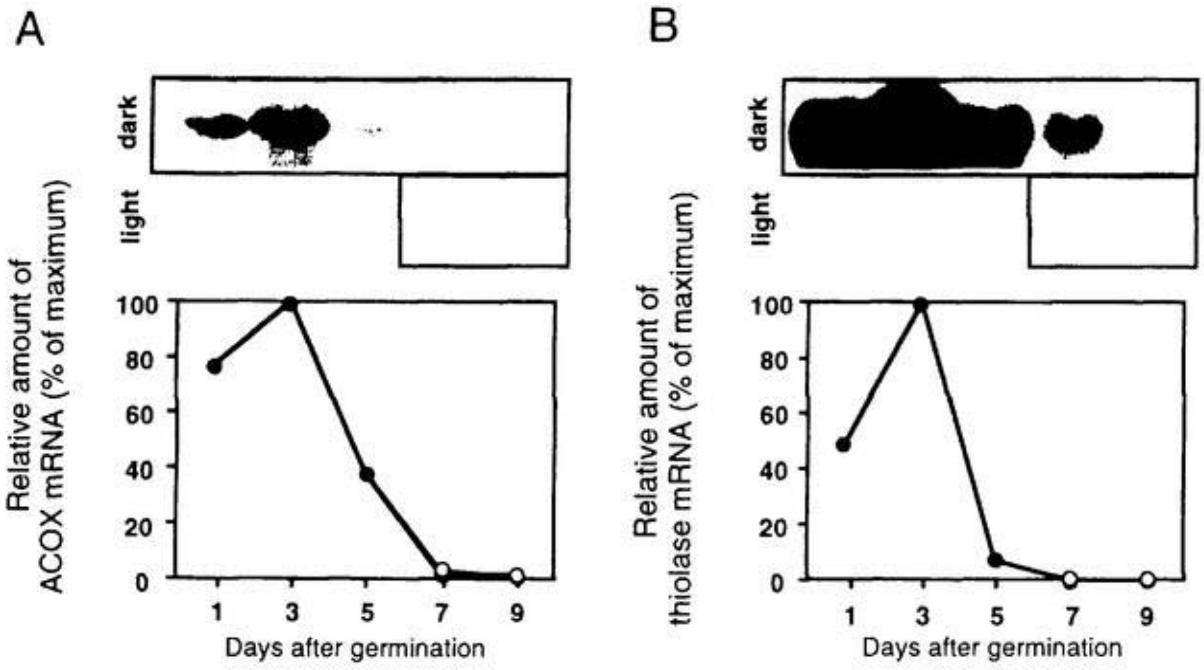

Fig. 10 Developmental changes in the level of mRNAs for pumpkin acyl-CoA oxidase (A) and thiolase (B).

Top panels, Northern blots of total RNA from one cotyledons of dark-grown seedlings. RNA was blotted on a nylon membrane and then the membrane was allowed to hybridize with specific probes. Middle panels, Northern blots of RNA of seedlings after being transferred to continuous illumination 5 days after the onset of germination. Bottom panels, quantification of spot intensives of dark-grown (●) and light-grown (O) seedlings.

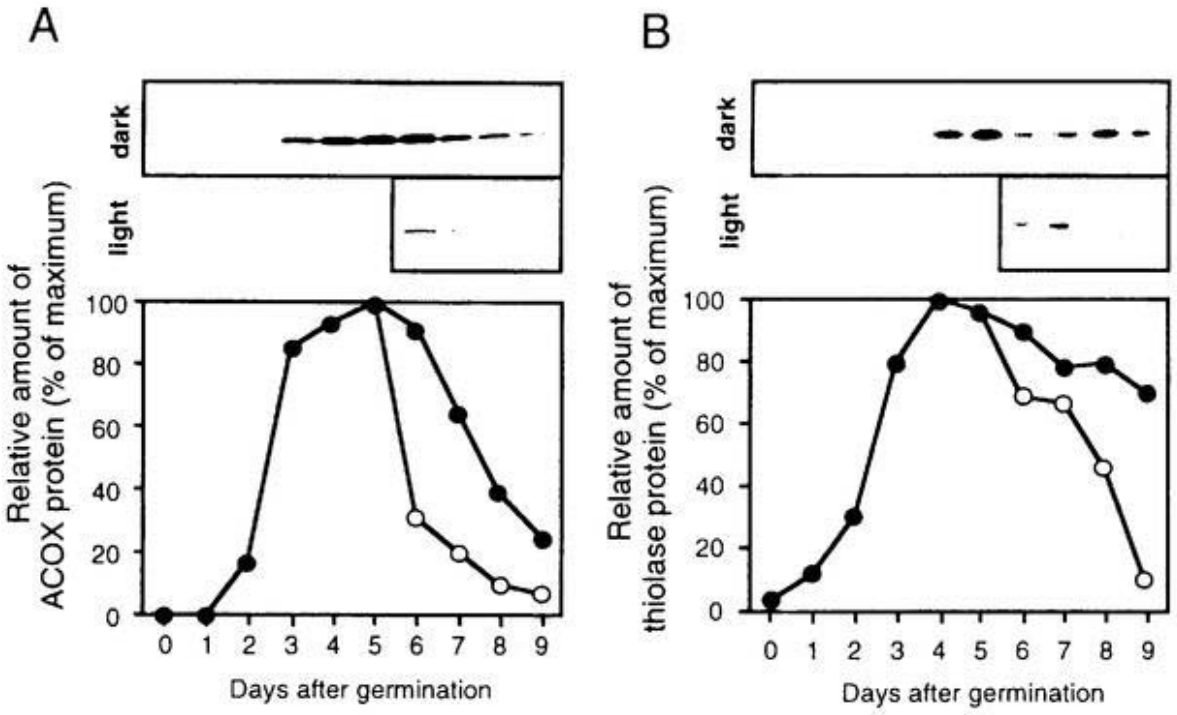

Fig. 11 Developmental changes in the level of proteins for pumpkin acyl-CoA oxidase (A) and thiolase (B).

Top panels, Western blots of 0.05 % of total homogenate from ten cotyledons of dark-grown seedlings. Total homogenate was blotted on a nylon membrane and then the membrane was allowed to hybridize with specific probes. Middle panels, Western blots of total homogenate of seedlings after being transferred to continuous illumination 5 days after the onset of germination. Bottom panels, quantification of spot intensives of dark-grown (●) and light-grown (○) seedlings.

考察

今回の解析により、カボチャ発芽子葉で発現が誘導されるグリオキシソーム膜結合型タンパク質の cDNA を同定、解析を行った結果、このタンパク質は 690 アミノ酸残基からなる前駆体として合成され、マイクロボディターゲティングシグナル (PTS2) となる延長配列をN末端に持つことが明らかになった。また、カラム分画及びオルガネラ分画の結果、このタンパク質が長鎖特異的 acyl-CoA oxidase であり、マイクロボディに局在することが明らかとなった。

発芽時における長鎖特異的 acyl-CoA oxidase の発現パターンについて

長鎖特異的 acyl-CoA oxidase mRNA は発芽直後からその蓄積量が認められ、暗所生育 3 日目の黄化子葉で最大の蓄積量となる。その後、5 日目より急激に減少して 7 日目以降、非常にわずかな mRNA 量で一定になる。暗所で 5 日間生育させた芽生えを光照射下で生育させた場合、長鎖特異的 acyl-CoA oxidase mRNA の蓄積量はそのまま暗所下で生育させたものとほとんど変わらない。このことは、種子発芽直後から長鎖特異的 acyl-CoA oxidase mRNA は誘導され、その転写抑制も発芽過程のかなり早い時期に始まることを示している。同じβ酸化系の酵素である thiolase mRNA は長鎖特異的 acyl-CoA oxidase と同様の挙動を示しているが、光照射により緑化させた場合、そのまま暗所下で生育させた黄化子葉の mRNA 量と比較して減少量が大きい。このことから、thiolase では光による転写抑制が行われていることが示唆される。これはグリオキシル酸サイクルの酵素であるカボチャ citrate synthase の mRNA の発現パターンとよく似ている (Kato et al. 1995)。カボチャのような脂肪性種子の発芽時には、貯蔵脂肪が脂肪酸β酸化系で分解され、生じるアセチル CoA はグリオキシル酸サイクルに取り込まれて糖新生の基質となる。このことから、脂肪酸β酸化系の酵素と

グリオキシル酸サイクルの酵素は同じ制御機構によりコントロールされている可能性が示唆されている (Kato et al. 1996a)。しかし、長鎖特異的 acyl-CoA oxidase mRNA は光による転写制御が働いていないように観察される。または、光照射以前の mRNA 量の減少が著しく、光照射による影響を確認できなかったとも考えられる。

長鎖特異的 acyl-CoA oxidase のタンパク質は mRNA よりもかなり遅く暗所生育 5 日目にその最大値になり、5 日目以降、徐々に減少していく。緑化子葉になると長鎖特異的 acyl-CoA oxidase のタンパク質量は急速に減少していく。このように、長鎖特異的 acyl-CoA oxidase のタンパク質は mRNA と異なり、光による影響がはっきりと確認できた。光照射によるタンパク質量の減少はグリオキシル酸サイクルの諸酵素においても確認されている。また、同時に行った thiolase も長鎖特異的 acyl-CoA oxidase と同様の挙動を示し、光照射下でタンパク質量が減少している。黄化子葉が緑化するとマイクロボディは、グリオキシソームから緑葉パーオキシソームに機能変換を行う。この光照射による acyl-CoA oxidase、thiolase の変動は、グリオキシソームの機能を支えるこれら脂肪酸 β 酸化系酵素が特異的に分解されていることを示す。この脂肪酸 β 酸化系酵素分解系は、光をシグナルとしていると思われる。

Acyl-CoA oxidase について

高等植物の脂肪酸 β 酸化と動物の脂肪酸 β 酸化は生理学上大きな違いがある。高等植物はグリオキシソーム中において長鎖脂肪酸を完全にアセチル CoA に分解する能力を持っている (Gerhardt 1992)。これに対し、動物の脂肪酸 β 酸化はミトコンドリアとパーオキシソームの分業体制になっている。パーオキシソームの脂肪酸 β 酸化系は短鎖のアシル CoA を酸化する能力を有しておらず、短鎖アシル CoA はミトコンドリアに輸送されて分解される (Schulz 1991)。

これまでに高等植物の acyl-CoA oxidase については、生化学的な解析が報告のみがされていた (Kirsh et al. 1986, Hooks et al. 1996)。これらの知見より、これまでに 3 種類の acyl-CoA oxidase がその酵素活性により精製され、長鎖、中鎖、短鎖のアシル CoAに特異的な acyl-CoA oxidase が存在することが明らかになっている。1 つはキュウリ黄化子葉より精製された acyl-CoA oxidase である。これは長中鎖のアシル CoA に活性を持つ長鎖特異的 acyl-CoA oxidase で、サブユニット分子量が 72,000、高次構造がホモテトラマーのタンパク質である。他の 2 つはトウモロコシより単離されており、中鎖特異的 acyl-CoA oxidase はモノマーで 62,000 の分子量を持ち、短鎖特異的 acyl-CoA oxidase は部分精製の結果であるが 15,000 のサブユニット分子量を持つホモテトラマータンパク質であることが報告されている。カボチャ黄化子葉のタンパク質抽出液をフェニルセファロースカラムにより分画した結果、長鎖特異的 acyl-CoA oxidase 活性と中鎖特異的 acyl-CoA oxidase 活性が重なっていた。現在知られている長鎖特異的 acyl-CoA oxidase、中鎖特異的 acyl-CoA oxidase の分子量より、この両活性は長鎖特異的 acyl-CoA oxidase のものと推論した。しかし、中鎖特異的 acyl-CoA oxidase 活性が他の独立したタンパク質に由来する可能性もあり、今後さらに生化学的な解析を行う必要がある。筆者が研究を始めた当時、植物において acyl-CoA oxidase をコードする cDNA は単離されておらず、その一次構造は不明であった。一方、動物の acyl-CoA oxidase は生化学的な解析のみならず、分子レベルでの解析も行われ、その一次構造も明らかになっていた。ラット肝より精製された palmitoyl-CoA oxidase は分子量 72,000 のサブユニットが生合成された後、パーオキシソーム内で特定の部位が切断を受けて分子量 51,000、21,000 サブユニットが生じ、分子量 72,000、51,000、21,000 のサブユニットが 5:1:1 の割合で結合した高次構造をとることが報告されている (Osumi et al. 1980, Miyazawa et al. 1987)。このように、高等植物と動物では acyl-CoA oxidase は異なる高次構造をとっており、その一次構造上においても同一

性が低いものと考えられる。

近年、コチョウランにおいて花弁の老化時に発現する遺伝子や大麦の乾燥ストレス応答遺伝子 (*cdr*29) が、acyl-CoA oxidase ホモログとして同定されている (Do and Huang 1997, Grossi et al. 1995)。大麦の報告では遺伝子 (*cdr*29) は部分長のみであったが、最近、全塩基配列が登録された。しかし、これらの報告は遺伝子の発現解析のみであり、同一性から acyl-CoA oxidase である可能性を示唆するのみにとどまっている。他の高等植物では、Graham のグループによりアラビドプシスで 2 種類の cDNA が acyl-CoA oxidase (ACX1, GenBank accesion No.AF057044, 分子量約 74,000; ACX2, No.AF057043, 分子量約 77,000) として登録されている。今回、明らかにしたカボチャ長鎖特異的 acyl-CoA oxidase (分子量約 77,000) はコチョウランの acyl-CoA oxidase ホモログ (分子量約78,000) とアミノ酸レベルで 79%、アラビドプシス ACX2 と 83% の同一性があり、この 2 つの acyl-CoA oxidase は長鎖特異的 acyl-CoA oxidase である可能性が高い。しかし、アラビドプシス ACX1、大麦の acyl-CoA oxidase ホモログ (分子量約 72,000) とは同一性が低く、それぞれ 21%、24% の同一性にすぎない。動物の acyl-CoA oxidasede では同一性が最も高いラットの pristanoyl-CoA oxidase である (Van Veldhoven et al. 1994)。この acyl-CoA oxidase は側鎖型メチル化脂肪酸 CoA エステル及び直鎖型長鎖脂肪酸 CoA エステルを酸化する。現在知られている他の動物の acyl-CoA oxidase としては、胆汁酸生成に関与するラットの trihydroxycoprostanoyl-CoA で 29% (Van Veldhoyen et al. 1992)、極長鎖から中鎖アシル CoA までを酸化する一般的な acyl-CoA oxidase である palmitoyl-CoA oxidase とは 28% の同一性を示す (Osumi and Hashimoto 1978)。これらの同一性の計算は成熟体のアミノ酸配列で行っている。高等植物と動物の acyl-CoA oxidase において進化系統樹を作製したところ、ACX1、大麦の acyl-CoA oxidase ホモログは動物の acyl-CoA oxidase により近いことが示された (Fig. 12)。また、アラビドプシス ACX1 および大麦の acyl-CoA oxidase ホモ

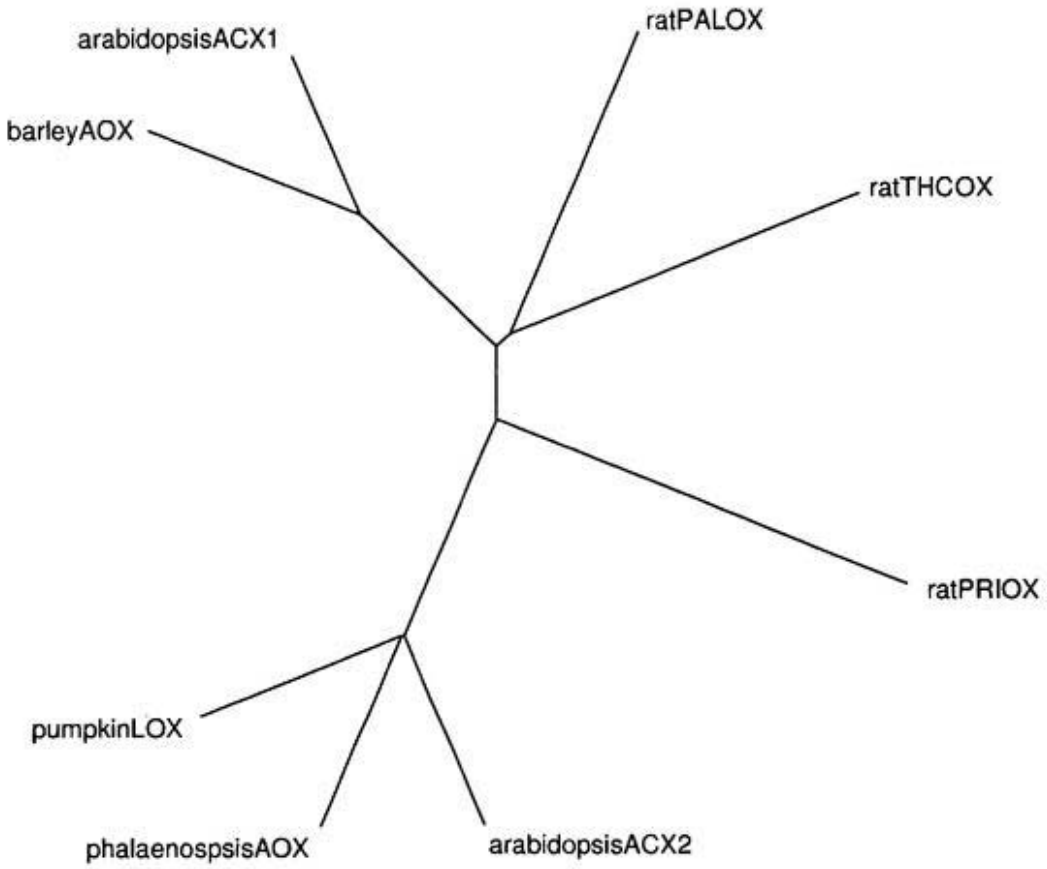

Fig. 12 Phylogenetic tree of acyl-CoA oxidases. Multiple sequence alignment of the protein sequences was performed using theCLUSTAL W program; the phylogenetic tree was constructed according to NJPLOTprogram. Known acyl-CoA oxidases were aligned: pumpkin LOX, pumpkin long-chain acyl-CoA oxidase (GenBank accession No. AF002016); phalaenopsis ACOX,*Phalaenopsis* putative acyl-CoA oxidase (No. U66299); barley AOX, barley putative acyl-CoA oxidase (NoAJ001341); arabidopsis ACX1,2,*Arabidopsis* acyl-CoA oxidase homolog(No. AF057044,AF057043); rat PRIOX, rat pristanoyl-CoA oxidase (No. X95188); rat PALOX, rat palmitoyl-CoA oxidase (No. P07872); rat THCOX, rat trihydroxycoprostanoyl-CoA oxidase (No. X95189);

ログは、長鎖特異的 acyl-CoA oxidase よりも動物の acyl-CoA oxidase に同一性が高く、長鎖特異的 acyl-CoA oxidase のホモログではない可能性が示唆される。短鎖特異的 acyl-CoA oxidase（分子量約 47,000）は第 2 章に記してあるように分子量の全く異なるタンパク質であるので、アラビドプシス ACX1、大麦の acyl-CoA oxidase ホモログは、中鎖特異的 acyl-CoA oxidase ではないかと推論される。

マイクロボディターゲティングシグナルについて

マイクロボディタンパク質の輸送機構の解析は酵母、及びヒトの培養細胞において研究が進んでいる。その知見によると、マイクロボディ輸送機構を構成するタンパク質はペルオキシン (*PEX*) と呼ばれるパーオキシソーム形成に関与するタンパク質群に属している。PTS1 タイプのマイクロボディタンパク質は *PEX5* がレセプターとなり、PTS2 タイプのマイクロボディタンパク質は *PEX7* がレセプターとなる。このように、PTS1 を持つマイクロボディタンパク質と PTS2 を持つマイクロボディタンパク質ではその輸送機構が異なる。

マイクロボディへのターゲティングシグナルとしては、C 末端に位置するシグナル配列として PTS1、N 末端に延長配列として合成されるシグナル配列として PTS2 が良く知られている。この両シグナル配列はそれぞれ独立に機能する。PTS1 は SKL を基本的モチーフとして構成される (Gould et al. 1987, Miyazawa et al. 1989, Hayashi et al. 1998)。一方、PTS2 は 30-50 アミノ酸よりなる延長配列からなり、その中に R-(I/H/L)-x5-H-L の保存配列が存在している (Kato et al. 1996b, Subramani 1993, 1996)。動物の acyl-CoA oxidase は全て PTS1 タイプであり、特に Miyazawa らはラット肝 acyl-CoA oxidase を PTS2 のモデルタンパク質として実験を行っている。また、酵母の acyl-CoA oxidase の PTS は不明で、acyl-CoA oxidase の内部に存在すると言われて

いる (Small et al. 1988)。高等植物では、カボチャ長鎖特異的 acyl-CoA oxidase 及びコチョウランの acyl-CoA oxidase ホモログ、アラビドプシス ACX2 は PTS2 タイプのターゲティングシグナルを持つ。興味深いことに、カボチャ長鎖特異的 acyl-CoA oxidase と同一性の低いアラビドプシス ACX1 及び大麦の acyl-CoA oxidase ホモログは動物の acyl-CoA oxidase と同様、マイクロボディターゲティングシグナルを C 末端に持つ PTS1 タイプであり、その N 末端配列を解析すると PTS2 は存在しない。この PTS1 タイプの acyl-CoA oxidase は PTS2 タイプの長鎖特異的 acyl-CoA oxidase とは同一性が低いことより、長鎖特異的 acyl-CoA oxidase ではなく他のアイソザイムであることが示唆されたが、異なるターゲティングシグナルを持つこともこの予想を支持する。1 つの酵素のアイソザイムが異なったシグナルを持っている例は珍しく、PTS が異なることは何か意味があるのだろうか？ PTS1 と PTS2 の輸送機構の違いにより使い分けているのだろうか？

Acyl-CoA oxidase のアイソザイム

同じ β 酸化系酵素である thiolase は、acyl-CoA oxidase に比べ種間の一次構造の保存性が高い。カボチャ、キュウリ、ラット肝、ヒト肝、パン酵母でクローニングが行われているが全ての thiolase が PTS2 をもつ形で合成されている。一方、高等植物の acyl-CoA oxidase は（少なくともアラビドプシスでは）分子量のよく似た PTS の異なる 2 種類の acyl-CoA oxidase が存在する。先ほど述べたように、PTS2 タイプの acyl-CoA oxidase が長鎖特異的acyl-CoA oxidaseであることより、PTS1 タイプの acyl-CoA oxidase は中鎖特異的 acyl-CoA oxidase ではないかと推測される。しかし、PTS1 タイプの acyl-CoA oxidase は中鎖特異的 acyl-CoA oxidase ではなく、長鎖特異的 acyl-CoA oxidase なのかもしれない。その根拠は分子量にある。PTS1 タイプの acyl-CoA

oxidase の分子量は約 72,000-74,000 でこれは分子量約 77,000-78,000 の PTS2 タイプの長鎖特異的 acyl-CoA oxidase の成熟体型分子量と変わらない。一方、Hooks らの報告によるとトウモロコシの中鎖特異的 acyl-CoA oxidase の分子量は約 62,000 である。長鎖特異的 acyl-CoA oxidase の分子量はトウモロコシ、キュウリで 72,000 であり、種間により分子量の違いはあまり大きくないものと思われる。分子量から推測すると PTS1 タイプと PTS2 タイプの acyl-CoA oxidase は、両方とも長鎖特異的 acyl-CoA oxidase である可能性が考えられる。この答えを得るためには、PTS1 タイプと PTS2 タイプの acyl-CoA oxidase の基質特異性を正確に解析することが必要であり、そのために、第 2 章の短鎖特異的 acyl-CoA oxidase の解析のように活性を持った形で cDNA のコードするタンパク質を発現させて基質特異性を解析しなければならない。

このように、分子量が大きく異なる短鎖特異的 acyl-CoA oxidase の他に分子量が同じ程度のターゲティングシグナルの異なった acyl-CoA oxidase が高等植物には存在している。現在のところ、これら PTS1 タイプと PTS2 タイプの acyl-CoA oxidase の基質特性は不明であるが、筆者はこの 2 種類のアイソザイムは全く別々の生理的機能を果たしているのではないかと考えている。進化系統樹の結果を考慮に入れると（Fig.12）、高等植物の PTS1 タイプの acyl-CoA oxidase（アラビドプシス ACX1、大麦の acyl-CoA oxidase ホモログ）は動物の acyl-CoA oxidase に相当する acyl-CoA oxidase ではないだろうか。そして、PTS2 タイプの acyl-CoA oxidase が動物にはない高等植物特有の生理機能に対応しているのではないかと考えている。今後、この生理機能の解明されることが期待される。

引用文献

Aebi, H. (1974) Methods of enzymatic analysis 2:673- 684, Academic Press, New York

Altschul, S.F., Gish, W., Miller, W., Myers, E.W. and Lipman, D.J. (1990) J. Mol. Biol. 215:403-410

Ausubel, F.M., Brent, R., Kingston, R.E., Moore, D.D., Seidman, J.G., Smith, J. and Struhl, K. (1987) in Current protocols in molecular biology, 4.3.1-4.3.3, John Wiley & Sons, New York

Aviv, H. and Leder, P. (1972) Proc. Natl. Acad. Sci. USA 69:1408-1412

Bairoch, A., Bucher, P. and Hofmann, K. (1996) Nucleic Acid Res. 24: 189-196

Do, Y.Y. and Huang, P.L. (1997) Arch. Biochem. Biophys. 344: 295-300

Dubourdieu, M. and Fox, J.L. (1977) J. Biol. Chem. 252:1453-1463

Feinberg, A.P. and Vogelstein, B. (1984) Anal. Biochem. 139: 266-267

Gerhardt, B. (1987) Methods Enzymol. 148: 516-525

Gerhardt, B. (1992) Prog. Lipid Res. 31:417-466

Gould, S. J., Keller, G.A. and Subramani, S. (1987) J. Cell Biol. 105: 2923-2931

Grossi, M., Gulli, M., Stanca, M. and Cattivelli, L. (1995) Plant Science 105:71-80

Hayashi, M., Toriyama, K., Kondo, M. and Nishimura, M. (1998) Plant Cell 2: 183-195

Higgins, D.G., Bleasby, C.J. and Fuchs, R. (1992) Compt. Appl. Biosci. 8:189-191

Hodges, T.K. and Leonard, R.T. (1974) Mehtods Enzymol. 32: 392-406

Hooks, M.A., Bode, K. and Couée, I. (1996) Biochem. J. 320: 607-614

Kato, A., Hayashi, M., Mori, H. and Nishimura, M. (1995) Plant Mol. Biol. 22: 843-852

Kato, A., Hayashi, M., Takeuchi, Y. and Nishimura, M. (1996a) Plant Mol. Biol. 27: 377-390

Kato, A., Hayashi, M., Kondo, M. and Nishimura, M. (1996b) Plant Cell 8: 1601-1611

Kato, A., Takeda-Yoshikawa, Y., Hayashi, M., Kondo, M., Hara-Nishimura, I. and Nishimura, M. (1998) Plant Cell Physiol. 39:186-195

Kirsch, T., Löffler, H.-G. and Kindl, H. (1986) J. Biol. Chem. 261: 8570-8575

Laemmli, U.K. (1970) Nature 227:680-685

Matsudaira, P. (1987) J. Biol. Chem. 262: 10035-10038

Miyazawa, S., Hayashi, H., Hijikata, M., Ishii, N., Furuta, S., Kagamiyama, H., Osumi, T. and Hashimoto, T. (1987) J. Biol. Chem. 262:8131-8137

Miyazawa, S., Osumi, T., Hashimoto, T., Ohno, K., Miura, S. and Fujiki, Y. (1989) Mol. Cell. Biol. 9:83-91

Osumi, T. and Hashimoto, T. (1978) Biochem. Biophys. Res. Commun. 83: 479-485

Osumi, T., Hashimoto, T. and Ui, N. (1980) J. Biochem. (Tokyo) 87:1735-1746

Saiki, R.K., Scharf, S., Faloona, F., Mullis, K.B., Horn, G.T., Erlich, H.A. and Arnheim, N. (1985) Science 230:1350-1354

Sambrook, J., Fritsch, E.F. and Maniatis, T. (1989) Cold Spring Habour Laboratory Press, New York

Sanger, F., Nicklen, S. and Coulson, A.R. (1977) Proc. Natl. Acad. Sci. USA 74: 5463-5467

Schulz, H. (1991) Biochim. Biophys. Acta 1081:109-120

Small, G.M., Szabo, J. and Lazarow, P.B. (1988) EMBO J. 7:1167-1173

Subramani, S. (1993) Annu. Rev. Cell Biol. 9: 445-478

Subramani, S. (1996) J. Biol. Chem. 271: 32483-32486

Towbin, H., Staehelin, T. and Gordon, J. (1979) Proc. Natl. Acad. Sci. USA 76: 4350-4354

Van Veldhoven, P.P., Vanhove, G., Asselberghs, S., Eyssen, H.J. and Mannaerts, G.P. (1992) J. Biol. Chem. 267: 20065-20074

Van Veldhoven, P.P., Van Rompuy, P., Fransen, M., De Béthune, B. and Mannaerts, G.P. (1994) Eur. J. Biochem. 222: 795-801

第２章

新規のアラビドプシス acyl-CoA oxidase の解析

材料及び方法

実験材料

実験材料としてはカボチャの種子 (*Cucurbita sp.* cv. Kurokawa Amakuri) を用いた。種子は表皮をつけたまま、流水に 12 時間浸した後、湿らせた粒状ロックウール（日東紡績）上に播種し、暗所下 25℃ において発芽、生育させた。また、発芽後 5 日間暗所で生育させた黄化芽生えを白色光下に移し、25℃ で生育させたものを緑化芽生えとした。

塩基配列の決定

塩基配列の同定は ABI PRISM サイクルシークエンシングキットによるジデオキシ法 (Sanger et al. 1977) を用いた。

プラスミド

Arabidopsis Expressed Sequence Tag (EST) の cDNA クローンを Arabidopsis Biological Resource Center (Ohio State University) より得た。

cDNA の解析

cDNA 塩基配列の解析にはコンピュータソフトウェア、Gene Works (Intelli Genetics Inc., U.S.A.) を使用し、アミノ酸配列の同一性を調べるために BLAST e-mail server (Altschul et al. 1990) を経由してタンパク質データベース (Gepept, Swissprot) にアクセ

スした。アミノ酸配列の解析及び分子系統樹の作製にはCLUSTAL Wプログラム (Higgins et al. 1992) を使用した。

特異抗体の調製

Arabidopsis Expressed Sequence Tag (EST) より得たcDNAクローンを制限酵素 *Kpn* I, *Eco*RIで切り出し、発現ベクターpET32a (Novagen, U.S.A.) にインフレームになるように連結した発現ベクターを作製し、大腸菌 (BL21DE3) に導入して短鎖特異的acyl-CoA oxidaseと6xhistidineによる融合タンパク質 (SACOX-6xhis) を大腸菌内で生産した。超音波処理により大腸菌を破壊し、3,000xgの遠心により可溶性画分と不溶性画分に分離させ、その可溶性画分を、再度3,000xgの遠心を行って沈殿物を完全に取り除いた後、可溶性画分をニッケルレジンカラムにより精製した。0.5mgのSACOX-6xhis融合タンパク質を含む1mlの滅菌水に、等量のFreund's complete adjuvant (Difco Laboratories, U.S.A.) を加えて良く乳化後、ウサギ背部に皮下注射して第1回目の免疫感作とした。4週間後、同量の融合タンパク質を含む1mlの滅菌水を等量のincomplete adjuvantを加えて乳化し、第2回目の免疫感作として皮下注射とした。以後、1週間毎に第5回まで免疫感作を行った。第1回目の免疫感作の直前に少量採血し、前血清とした。第2回目以降の免疫感作から1週間後に耳の動脈より採血を行い抗血清を調製して使用した。

短鎖特異的アシルCoAオキシダーゼのスクリーニング

プラークハイブリダイゼイションはSambrook et al. (1989) の方法に従った。プローブはランダムプライマー法 (Feinberg and Vogelstein 1984) を用いて [α-^{32}P] dATP (Amersham Pharmacia, Japan) で放射標識した。

カボチャ黄化子葉ホモジネイトのショ糖密度勾配遠心

発芽後4日目のカボチャ黄化子葉、15gを10mlの緩衝液 (150mM Tricine-KOH、pH 7.5, 1mM EDTA, 0.5M ショ糖, 1% BSA) とともに氷上のペトリ皿内でカミソリ刃により約5分間破砕し、これを4層のガーゼで弱く絞って濾過した後、核、プラスチド等を除くため JA-20 アングルローター (Beckman, U.S.A.) で 1,500xg、10 分間遠心した。上清 2ml を 16ml のショ糖密度勾配溶液 [30%-60% (w/w), 1 mM EDTA] に上層して、SW 28.1 スイングローター (Beckman, U.S.A.) で、21,000 rpm 、3 時間遠心した。遠心終了後、直ちに fractionator (model 185; ISCO, U.S.A.) で 0.5ml 毎に分画し、それぞれの画分において指標酵素の活性測定を行った。すべての操作は 4℃ で行った。

アラビドプシス黄化子葉ホモジネイトのショ糖密度勾配遠心

100mg の種子（約 5,000 粒）を培地中で 22 ℃、5 日間、暗所で生育させたアラビドプシスの黄化子葉を刈り取り、2ml の緩衝液 (150mM Tricine-KOH, pH 7.5, 1mM EDTA, 0.5M ショ糖, 1% BSA) とともに氷上のペトリ皿内でカミソリ刃により約 5 分間破砕し、これを cell strainer (Becton Dickinson, U.S.A.) を用いて、核、プラスチド等を除くため 600xg、10 分間遠心し濾過した。上清 2 ml を 16 ml のショ糖密度勾配溶液 [30%-60% (w/w), 1mM EDTA] に上層して、SW 28.1 スイングローター (Beckman, U.S.A.) で 25,000 rpm、2.5 時間遠心した。遠心終了後、直ちに fractionator (model 185; ISCO, U.S.A.) で 0.5ml 毎に分画し、それぞれの画分において指標酵素の活性測定を行った。すべての操作は 4℃ で行った。

短鎖鎖特異的 acyl-CoA oxidase、catalase の二重染色による免疫電子顕微鏡観察

アラビドプシスの発芽子葉は 3 日間暗所で生育した黄化子葉を用いて Nishimura et

al. (1993), Hayashi et al. (1998b) の方法に従って固定、脱水を行い、LR White resin (London Resin, England) に包埋した。超薄切片はニッケルグリッド上にマウントし、ダイヤモンドナイフを使ったウルトラミクロトーム (Leica, Germany) で調製し、ブロッキング液 (1% BSA in PBS) で処理した。カボチャカタラーゼ抗体による免疫染色はプロテインA一金コロイド (Amersham Pharmacia, Japan) による免疫ラベル法で行った。超薄切片を 1,000 倍に希釈したカボチャカタラーゼ抗体と一晩、4℃ でインキュベートし、洗浄後、30 倍に希釈した直径 10nm のプロテイン A一金コロイドにより 30 分間、室温でインキュベートした。短鎖特異的アシル CoA オキシダーゼ抗体による免疫染色は以下のように行った。1,000 倍に希釈した短鎖特異的アシル CoA オキシダーゼ抗体と超薄切片を一晩、4℃ でインキュベートし、洗浄後、20 倍に希釈した抗ウサギ IgG 特異的ビオチン化 2 次抗体で 1 時間、室温でインキュベートした。これを洗浄後、20 倍に希釈した直径 15nm のストレプトアビジン一金コロイドにより 30 分間、室温でインキュベートした。切片は透過型電子顕微鏡 (1200EX, JEOL)で観察した。

イムノブロット解析

各発育段階において採取したカボチャ子葉は、抽出緩衝液 (100mM Tris-HCl, pH 8.0, 1mM EDTA, 1mM PMSF, 1% SDS) とともに磨砕し、抽出液を遠心後、上清を SDS-PAGE で分離した。SDS-PAGE はLaemmli (1970) の方法に、ナイロン膜への転写はTowbin et al. (1979) の方法に従った。

バキュロウイルスシステムによる短鎖特異的アシル CoA オキシダーゼの発現及び精製

Max Bac 2.0 kit (Invitrogen, U.S.A.) を用い、そのプロトコールに従った。固着培養によりグレース培地で培養した対数増殖期にある Sf9 昆虫細胞を 75cm^2 フラスコ 20 個より集めた。新鮮なグレース培地によって洗浄後、最適 M.O.I. になるように短鎖特異的 acyl-CoA oxidase を組み込んだバキュロウイルス (AcNPV) を感染させた。感染 4 日間後に昆虫細胞を 10% FBS 入り TNM-FH で洗浄した後、固着した細胞をピペッティングによりフラスコより剥がし、600xg の遠心により細胞を集め、PBSで細胞が破壊されないように懸濁、遠心を行った後、カラム緩衝液 A (50mM sodium phosphate, pH 6.7, 10mM NaCl, 100μg/ml PMSF, 10μM FAD, 10% glycerol) で洗浄、遠心を行った。集めた昆虫細胞に 8ml の抽出液を加え、懸濁し、細胞を超音波破砕機で破壊した (1min sonication x3, 20min interval on ice)。15,000xg, 4℃, 30 分間遠心後、その上清を粗抽出液としてカラム精製を行った。粗抽出液を 4℃ で 1 晩、カラム緩衝液 A 中で透析し、HiTrap SP column (Amersham Pharmacia, Japan) にかけた。10-500mM NaCl の濃度勾配により分画後、acyl-CoA oxidase 活性のある分画を回収して Centricon 30 concentrator (Amicon, U.S.A.) によって濃縮し、カラム緩衝液 B (10mM sodium phosphate,pH 7.2, 250mM NaCl, 100μg/ml PMSF, 10μM FAD, 10% glycerol) により平衡化した Superose 12 HR 10/30 column (Amersham Pharmacia, Japan) により 0.5ml 毎に分画した。

酵素活性の測定

Acyl-CoA oxidase の活性測定は Gerhardt (1987) の方法に従った。反応溶液 (acyl-CoA oxidase, 200mM Tris-HCl, pH8.5, 1mM 4-aminoantyphyrine, 100mM *p*-

hydroxyaminobenzonic acid, 0.02mM FAD, 1mM NaN_3, 4U horse-radish peroxidase) 1ml 中に 50μM もしくは 25μM のアシル CoA を基質として加えた。Acyl-CoA dehydrogenase の活性測定は Dommes and Kunau (1976) 及び Furuta et al. (1986) の方法に従った。オルガネラの指標酵素である catalase は Aebi (1974) の方法に、cytochrome *c* oxidase は Hodges and Loenald (1974) の方法に従って測定した。

その他の方法

プラスミド DNA の調製、制限酵素による DNA の切断、DNA のアガロースゲル電気泳動等の基本的操作は Sambrook らの方法 (1989) に準じた。

結果

1）塩基配列の決定

長鎖特異的 acyl-CoA oxidase を Genebank DNA データベース上で検索した結果、アラビドプシスの acyl-CoA dehydrogenase ホモログとして登録されている cDNA クローン (Grellet F., Gaubier P., Wu H. -J., Laudie M., Berger C., and Delseny M., GenBank accession No. U72505) と同一性があることが判明した。このクローンと同じ塩基配列を持つ cDNA クローンを *Arabidopsis* Expressed Sequence Tag (EST) database 上で検索し、*Arabidopsis* Biological Resource Center (Ohio State University) より得た。この EST cDNA クローンの塩基配列を決定して Delseny らの cDNA クローンと同じ塩基配列を持つものであることを確認した。この cDNA にコードされるタンパク質は 436 アミノ酸残基からなり、計算分子量約 47,000 のタンパク質をコードする。Delseny らの cDNA クローンに付けられた説明には、動物の acyl-CoA dehydrogenase と同一性があると書かれていた。しかし、現在まで、高等植物において、acyl-CoA dehydrogenase の存在は確認されておらず、cDNA も単離されていない。Acyl-CoA dehydrogenaseはミトコンドリアに局在する酵素であり、この cDNA にコードされるタンパク質もミトコンドリアに局在するものと考えられた。しかし、その一次構造を解析したところ、通常のミトコンドリアタンパク質の N 末端延長配列に見られるミトコンドリアターゲティングシグナルとして働く両親媒性 α ヘリックス構造が見つからなかった。その代わりに、マイクロボディターゲティングシグナルである PTS1 (peroxisome targeting signal) がその C 末端に存在することを発見した (Gould et al. 1987) (Fig.13 box)。マイクロボディの β 酸化系には acyl-CoA dehydrogenase は存在せず、acyl-CoA dehydrogenase のカウンターパートとして acyl-CoA oxidase がその役割を果たしている (Schulz 1991)。しかし、現在までに知られている acyl-CoA oxidase はサブユニットの

```
MAVLSSADRASNEKKVKSSYFDLPPMEMSV   30
AFPQATPASTFPPCTSDYYHFNDLLTPEEQ   60
AIRKKVRECMEKEVAPIMTEYWEKAEFPFH   90
ITPKLGAMGVAGGSIKGYGCPGLSITANAI  120
ATAEIARVDASCSTFILVHSSLGMLTIALC  150
GSEAQKEKYLPSLAQLNTVACWALTEPDNG  180
SDASGLGTTATKVEGGWKINGQKRWIGNST  210
FADLLIIFARNTTTNQINGFIVKKDAPGLK  240
ATKIPNKIGLRMVQNGDILLQNVFVPDEDR  270
LPGVNSFQDTSKVLAVSRVMVAWQPIGISM  300
GIYDMCHRYLKERKQFGAPLAAFQLNQQKL  330
VQMLGNVQAMFLMGWRLCKLYETGQMTPGQ  360
ASLGKAWISSKARETASLGRELLGGNGILA  390
DFLVAKAFCDLEPIYTYEGTYDINTLVTGR  420
EVTGIASFKPATRSRL                436
```

Fig. 13 Deduced amino acid sequence of *Arabidopsis* short-chain acyl-CoA oxidase.

The peroxisomal targeting signal (PTS1) is marked with an open box. The GenBank Accession Number for *Arabidopsis* short-chain acyl-CoA oxidase is AB017643.

分子量が 60,000 から 70,000 であり、この cDNA にコードされるタンパク質のように分子量 47,000 というものは知られていない (Hayashi et al. 1998a)。このことから、この cDNA にコードされるタンパク質は今まで知られている acyl-CoA oxidase とは異なる機能をもつ acyl-CoA oxidase ではないかと推測した。

2）バキュロウイルス発現システムによる発現、精製及びその解析

この cDNA にコードされるタンパク質が acyl-CoA oxidase の活性を持つか確かめるために、活性を持つ形で発現させる必要があった。まず最初に、大腸菌による発現を試みた。その結果、cDNA にコードされるタンパク質の発現には成功したが、発現タンパク質は活性を保持していなかった。そのため、発現タンパク質は抗体の作製にのみ使用した。次に、バキュロウイルス発現システムを用いてこのcDNAの発現を試みた。 発現システムは Invitrogen のキット (Max Bac 2.0 kit) を用いた。このキットではトランスファーベクターに cDNA を組み込み、線状のバキュロウイルスDNAとともに Sf9 昆虫細胞を形質転換すると、相同組み換えにより cDNA を組み込んだバキュロウイルスが昆虫細胞内で作られる。その後、野生型ウイルスを除くため、β-galactosidase によるカラーセレクションを行い、組み換えバキュロウイルスを単離した。単離されたバキュロウイルスを鋳型にしてトランスファーベクター内に設定されたプライマーによる PCR を行った。増幅されたPCR断片と組み込んだ cDNA の長さの比較により、組み換えウイルスのみが単離されていることを確認した。純化されていることが確認されたバキュロウイルスを昆虫細胞に感染させて、ウイルスを増幅させ、高い感染力価 (10^9PFU/ml)を持つバキュロウイルス液を作製した。この高力価バキュロウイルス液を使用して cDNA がコードするタンパク質を発現させた。

まず、発現させたタンパク質が acyl-CoA oxidase 活性をもつか否かを調べた。感染

させた昆虫細胞のホモジネイトを遠心し、その上清を用いて長鎖 (C16)、中鎖 (C10)、短鎖 (C6) のアシル CoA を基質として活性を調べた（データは示さない）。その結果、この上清は短鎖長 (C6) のアシルCoAに対して活性があることが分かった。次に、発現させたタンパク質を精製するため、感染させた昆虫細胞を大量培養してそのホモジネイトを遠心後、4℃ で 1 晩、カラム緩衝液 A 中で上清を透析した後、HiTrap SP column (Amersham Pharmacia, Japan) にかけた。Acyl-CoA oxidase 活性のある分画を回収して Centricon 30 concentrator (Amicon, U.S.A.) によって濃縮後、Superose 12 HR 10/30 column (Amersham Pharmacia, Japan) により精製した。精製の結果は Table1 に示している。Figure 14 に各精製段階の SDS-PAGE (Fig.14A) 及びイムノブロット (Fig.14B) の結果を示している。Figure 14B には 5 日間暗所で生育させたアラビドプシス黄化子葉のタンパク質抽出液によるイムノブロット解析も併せて示している。Figure 14A に示している精製段階の CBB パターンから発現タンパク質がこれらの精製ステップを行うことにより、完全に精製されていることが分かる。また、Figure 14B より、アラビドプシスの黄化子葉と同じ分子量の位置に精製タンパク質が検出されることより、精製されたタンパク質がアラビドプシスの分子量が 47,000 のタンパク質に相当することが確認された。

Figure 15 に基質特異性の解析結果を示している。その結果、このタンパク質は butyryl-CoA (C4) から octanoyl-CoA (C8) に特異的に活性を持つ acyl-CoA oxidase であることが明らかになった。このうち、hexanoyl-CoA (C6) に対して最大の活性を示し、その Km 値は 8.3μM であった。また、至適 pH は 8.5-9.0 であった。短鎖不飽和脂肪酸アシル CoA である crotonoyl-CoA (C4:1) 及びジカルボン酸アシル CoA である glutaryl-CoA に対しては活性を示さなかった。分枝短鎖脂肪酸エステルである isobutyryl-CoA に対しては低い活性があり (2.5 U/mg)、その Km 値は 67μM であった。

Table 1.

Purification of recombinant *Arabidopsis* short-chain acyl-CoA oxidase expressed employing the baculovirus expression system

Step	Activity (units)	Protein (mg)	Specific activity (units/mg)	Yield (%)	Purification (fold)
15000xg supernatant	23.5	3.3	7.1	100	1.0
HiTrap SP	16.1	0.58	27.8	68.5	3.9
Superose 12	3.4	0.031	109.8	14.5	15.5

Short-chain acyl-CoA oxidase activities were tested with hexanoyl-CoA as a substrate.

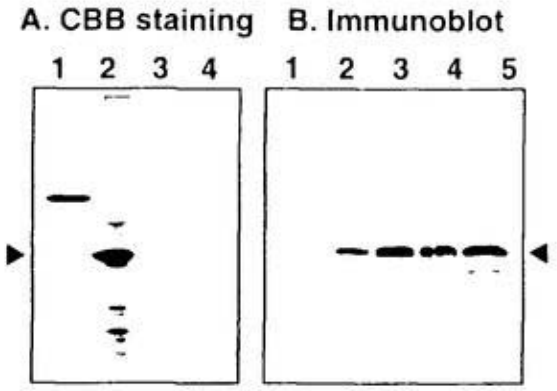

Fig. 14 SDS-PAGE and immunoblot analysis of samples taken at various steps during the purification of *Arabidopsis* short-chain acyl-CoA oxidase produced in the baculovirus expression system.

A. SDS-polyacrylamide gel stained with Coomassie Brilliant Blue dye.

B. Immunoblot analysis of polyclonal antibodies raised against recombinant *Arabidopsis* short-chain acyl-CoA oxidase. The arrowheads indicate the bands corresponding to the *Arabidopsis* short-chain acyl-CoA oxidase.

Lane 1. Homogenate (15,000xg supernatant) from insect cells infected with the wild-type baculovirus.

Lane 2. Homogenate (15,000xg supernatant) from insect cells infected with the recombinant baculovirus (harboring the *Arabidopsis* short-chain acyl-CoA oxidase cDNA).

Lane 3. HiTrap SP column fraction showing short-chain acyl-CoA oxidase activity.

Lane 4. Gel filtration fraction showing short-chain acyl-CoA oxidase activity.

Lane 5. Homogenate (15,000xg supernatant) from 5-day-old dark-grown *Arabidopsis* etiolated cotyledons.

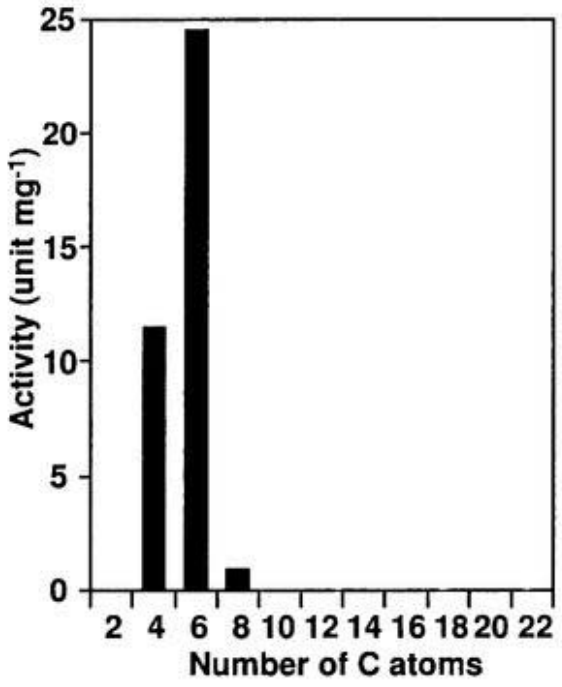

Fig. 15 Substrate specificity of *Arabidopsis* short-chain acyl-CoA oxidase produced in a baculovirus expression system.

The activity was monitored employing various acyl-CoAs as substrates at a concentration of 25 μM.

Table 2.

Properties of *Arabidopsis* Short-chain Acyl-CoA oxidase

subunit molecular mass	47 kDa
native molecular mass	180 kDa
pI	9.5
K_m	8.3 μM
optimal pH	8.5-9.0
isobutyryl-CoA	active
crotonoyl-CoA (unsaturated carboxylic ester)	inactive
glutaryl-CoA (dicarboxylic ester)	inactive
acyl-CoA dehydrogenase activity	none
Subcellular localization	peroxisomes

K_m and optimal pH values were determined employing hexanoyl-CoA as a substrate. acyl-CoA dehydrogenase activity was tested with hexanoyl-CoA, decanoyl-CoA and palmitoyl-CoA as substrates.

また、このタンパク質をコードしている cDNA は、acyl-CoA dehydrogenase ホモログとして登録されているので acyl-CoA dehydrogenase 活性を持つ可能性もある。そこで、hexanoyl-CoA (C6)、decanoyl-CoA (C10)、palmitoyl-CoA (C16) を基質にして acyl-CoA dehydrogenase 活性を測定したところ活性を示さなかった。これらのことより、この cDNA にコードされているタンパク質が短鎖特異的 acyl-CoA oxidase であることが判明した。この短鎖特異的 acyl-CoA oxidase は Superose 12 によるゲル濾過より、活性型で 180,000 の分子量であることが明らかになった。サブユニット分子量が 47,000 であることから、この短鎖特異的 acyl-CoA oxidase はホモテトラマーであることが示された。これらの短鎖特異的 acyl-CoA oxidase の酵素特性は Table2 に示している。

現在までに知られている acyl-CoA oxidase の分子量は 60,000 から 70,000、acyl-CoA dehydrogenase の分子量は 40,000 から 50,000 である。但し、極長鎖特異的 acyl-CoA dehydrogenase のみはその分子量が約 71,000 であり他の acyl-CoA dehydrogenase と異なっている。短鎖特異的 acyl-CoA oxidase は分子量が 47,000 であり、TritonX-100 に対して非感受性であることなど acyl-CoA oxidase より acyl-CoA dehydrogenase に近い性質を持っている。短鎖特異的 acyl-CoA oxidase にはカボチャの長鎖特異的 acyl-CoA oxidase (Hayashi et al, 1998a) と同様に動物の acyl-CoA dehydrogenase で保存されている PS1 と PS2 が存在する (Bairoch et al, 1997)。第 1 章より、カボチャ長鎖特異的 acyl-CoA oxidase はprotein signature 1 (PS1: [GAC]-[LIVM]-[ST]-E-x(2)-[GSAN]-G-S-D-x(2)-[GSA], Bairoch et al. 1995) は 9 アミノ酸残基中 7 残基、protein signature 2 (PS2: [QE]-x(2)-G-[GS]-x-G-[LIVMFY]-x(2)-[DEN]-x(4)-[KR]-x(3)-[DE], Bairoch et al. 1995) は 8 アミノ酸残基中 6 残基が保存されていることが確認された (Fig. 6、アステリスク)。しかし、アラビドプシス短鎖特異的 acyl-CoA oxidase は PS1, PS2 ともに完全に保存されている (Fig. 16A)。また、動物の acyl-CoA dehydrogenase において活性に大きな影響を与えるグルタミン酸残基も保存されている (Fig.16A、アステリスク)

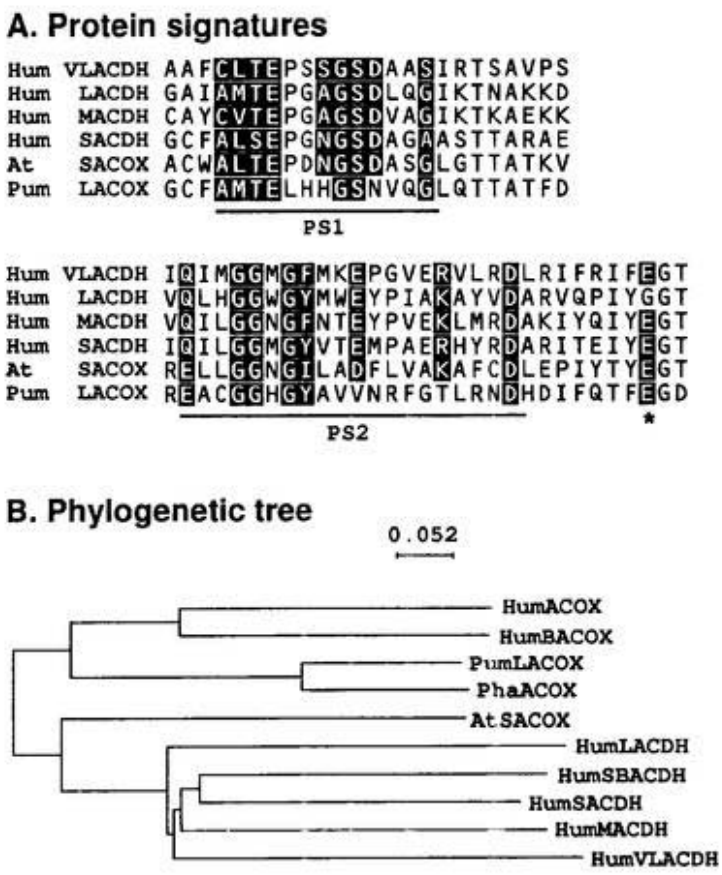

Fig. 16 (A) Partial alignment of acyl-CoA oxidases and acyl-CoA dehydrogenases. (B) Phylogenetic tree of acyl-CoA oxidases and acyl-CoA dehydrogenases.

White letters indicated to corresponding to PS1 and PS2 amino acids and underlines indicate the PS1 and PS2 regions. PS1:[GAC]-[LIVM]-[ST]-E-x(2)-[GSAN]-G-S-D-x(2)-[GSA], PS2:[QE]-x(2)-G-[GS]-x-G-[LIVMFY]-x(2)-[DEN]-x(4)-[KR]-x(3)-[DE] (Bairoch, M. et al., 1997).

Multiple sequence alignments of the protein sequences were performed using the CLUSTAL W program. The phylogenetic tree was constructed according to the NJPLOT program.

At SACOX,*Arabidopsis* short-chain acyl-CoA oxidase (GenBank Accession Number AB017643); Pum LACOX, Pumpkin long-chain acyl-CoA oxidase (AF002016);Pha ACOX,*Phalaenopsis* acyl-CoA oxidase (U66299); Hum ACOX, Human acyl-CoA oxidase (S69189); Hum BACOX, Human branched-chain acyl-CoA oxidase (X95190); Hum VLACDH, Human very long-chain acyl-CoA dehydrogenase (D43682); Hum LACDH, Human long-chain acyl-CoA dehydrogenase (M74096); Hum MACDH, Human medium-chain acyl-CoA dehydrogenase (M16827); Hum SACDH, Human short-chain acyl-CoA dehydrogenase (M26393).

(Bross et al. 1990, Kim et al. 1993, Battaile et al. 1996, Srivastava and Peterson 1998)。さらに、ヒトの acyl-CoA oxidase、acyl-CoA dehydrogenase と植物の acyl-CoA oxidase で進化系統樹を作製した結果、アラビドプシス短鎖特異的 acyl-CoA oxidaseはacyl-CoA oxidase ではなく、acyl-CoA dehydrogenase の系統樹の近くに配置された (Fig.16B)。これらのことより、このcDNAにコードされているタンパク質は、その分子構造上は acyl-CoA dehydrogenase と同一性はあるが acyl-CoA dehydrogenase 活性はもたない、短鎖アシルCoAに特異的な acyl-CoA oxidase であることが判明した。

3）細胞内局在性

短鎖特異的 acyl-CoA oxidase の細胞内局在性を調べるためにショ糖密度勾配遠心によりオルガネラを分画後、イムノブロット解析及び酵素活性の測定を行った(Fig.17)。5 日間、暗所で生育させたアラビドプシスの黄化子葉を用いて第 1 章と同様に行った。アラビドプシス黄化子葉の分画は酵素活性の測定が困難なため、イムノブロット解析のみを行った。そのため、同時に、発芽後 4 日目のカボチャ黄化子葉を用いてオルガネラ分画を行い、catalase をマイクロボディの指標酵素に、cytochrome *c* oxidase をミトコンドリアの指標酵素として活性を測定した。アラビドプシスとカボチャ黄化子葉の分画において、短鎖特異的 acyl-CoA oxidase、catalase は 21-23 番目のマイクロボディ画分に検出された。上清画分に検出された短鎖特異的 acyl-CoA oxidase、catalase はホモジネイト調製及びオルガネラ分画中に生じた破壊されたマイクロボディより漏れ出たものと推測される。カボチャ黄化子葉の分画において短鎖特異的 acyl-CoA oxidase 活性を測定すると、イムノブロット解析と同様にマイクロボディ画分にのみ活性が検出された。さらに、短鎖特異的 acyl-CoA oxidase 抗体と catalase 抗体の二重染色による免疫電子顕微鏡観察を発芽後 3 日間暗所で生育した黄化子葉を用いて行った (Fig.18)。

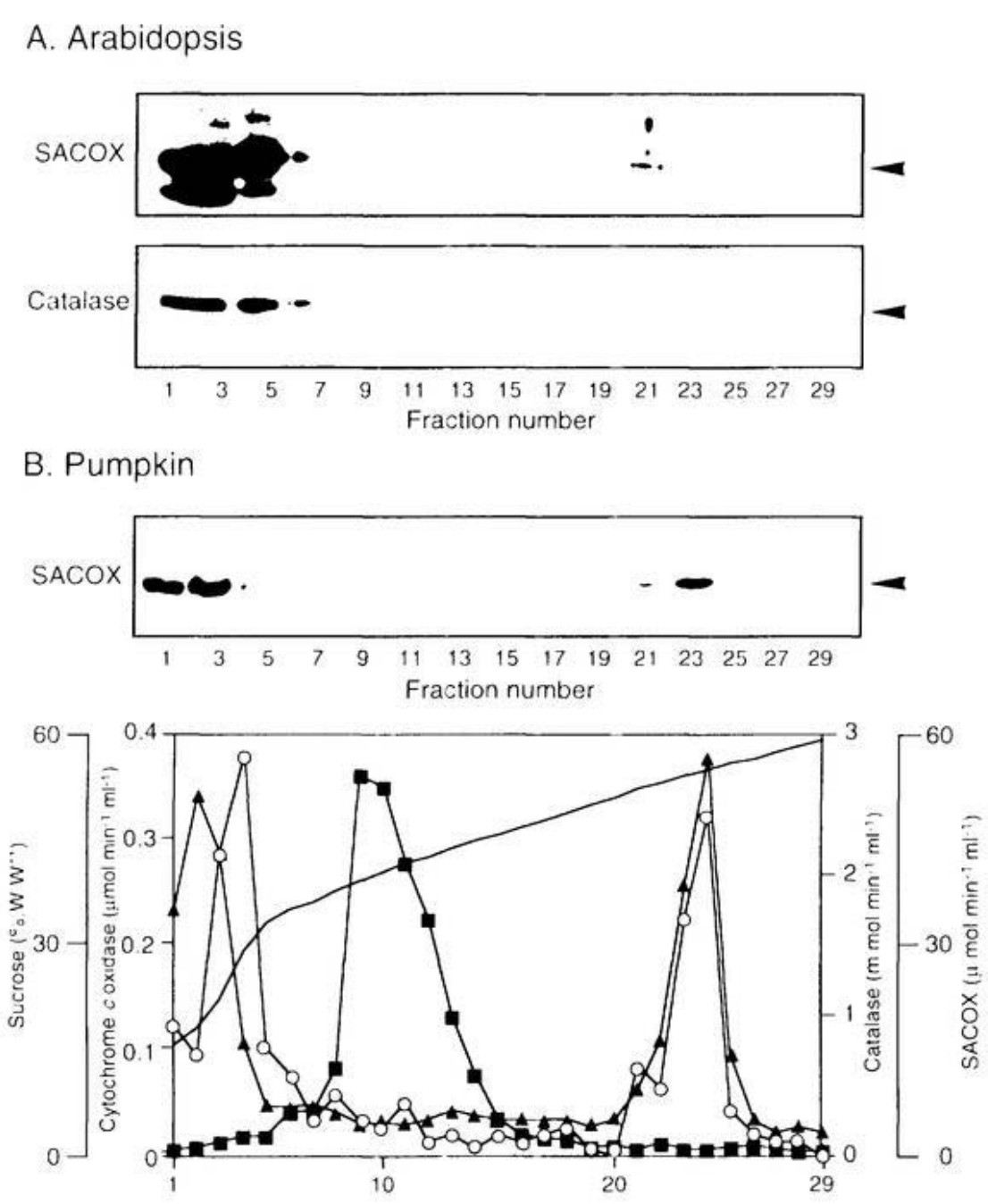

Fig. 17 Subcellular localization of short-chain acyl-CoA oxidase in *Arabidopsis* (A) and pumpkin (B) etiolated cotyledons.

Both extracts from 5-day-old etiolated cotyledons were fractionated by sucrose density gradient centrifugation. The arrowheads indicate the bands corresponding to the short-chain acyl-CoA oxidase.

A. Immunological detection of *Arabidopsis* short-chain acyl-CoA oxidase and catalase.

B. Immunological detection of pumpkin short-chain acyl-CoA oxidase and enzyme activities: short-chain acyl-CoA oxidase (O), catalase (▲), and cytochrome *c* oxidase (■). Sucrose concentration w/w (—). 20 μl (*Arabidopsis* short-chain acyl-CoA oxidase) and 5 μl (pumpkin short-chain acyl-CoA oxidase and catalase) of samples from each odd-numbered fraction was subjected to SDS-PAGE (10 % acrylamide) and immunoblot.

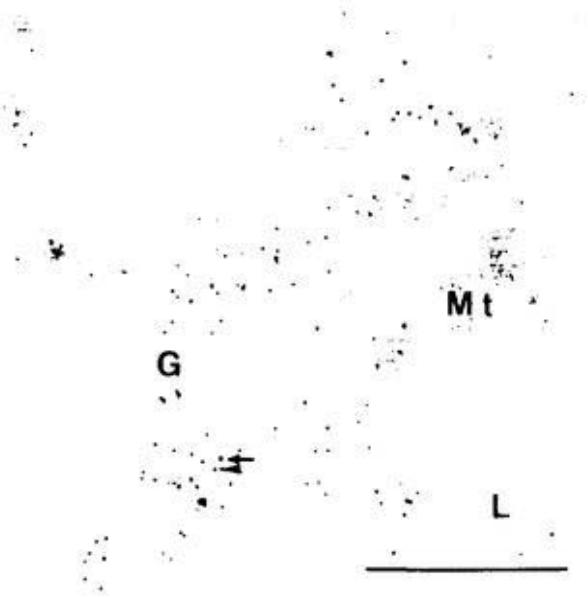

Fig. 18 Immunoelectron microscope analysis of the localization of *Arabidopsis* cotyledons of 3-day-old dark-grown seedlings using polyclonal antibodies against *Arabidopsis* short-chain acyl-CoA oxidase and pumpkin catalase.

Mt: mitochondria, G: glyoxysome, L: lipid body, Arrow: short-chain acyl-CoA oxidase (15-nm gold particles) Arrowhead: catalase (10-nm gold particles)

Bar: 1 μm

短鎖特異的 acyl-CoA oxidase 抗体の金粒子（直径15nm）を矢印、catalase 抗体の金粒子（直径10nm）を矢頭で示している。両抗体の金粒子ともマイクロボディに観察され、ミトコンドリアには観察されなかった。以上の結果より、短鎖特異的 acyl-CoA oxidase はマイクロボディに局在することが確かめられた。

4）発芽過程における短鎖特異的 acyl-CoA oxidase タンパク質の発現

Figure 19 は、アラビドプシス種子の発芽から芽生えの段階における短鎖特異的 acyl-CoA oxidase タンパク質の変動をイムノブロット解析により示したものである。短鎖特異的 acyl-CoA oxidase は、同じβ酸化系酵素の thiolase と同様に暗所生育 5 日目から 7 日目に最大のタンパク質量が検出された。これらの酵素の減少は緩やかで、9 日間暗所下で生育してもかなりのタンパク質量が蓄積している。4 日間、暗所生育後、光照射下に移した緑化子葉とそのまま暗所下で生育させた黄化子葉を比較した場合、急激にタンパク質量が減少する。しかし、光照射下で 3 日間生育させても緑化子葉中にもわずかに検出される。これに対し、グリオキシル酸サイクルの酵素である isocitrate lyase は短鎖特異的 acyl-CoA oxidase や thiolase と異なりタンパク質量の蓄積は暗所生育 3 日目の段階で最大値に達し、その後、減少して暗所生育 9 日目には観察されない。

5）短鎖特異的 acyl-CoA oxidase タンパク質の組織特異的発現

アラビドプシスの各組織における短鎖特異的 acyl-CoA oxidase のイムノブロット解析の結果を Figure 20 に示した。5 日間暗所下で生育した黄化子葉において最もタンパク質量が多く検出された。また、花、根、莢においても短鎖特異的 acyl-CoA oxidase は検出された。一方、緑化した子葉（4 日間暗所下で生育後、3 日間光照射下で生育）、ロゼット葉、茎では検出されなかった。

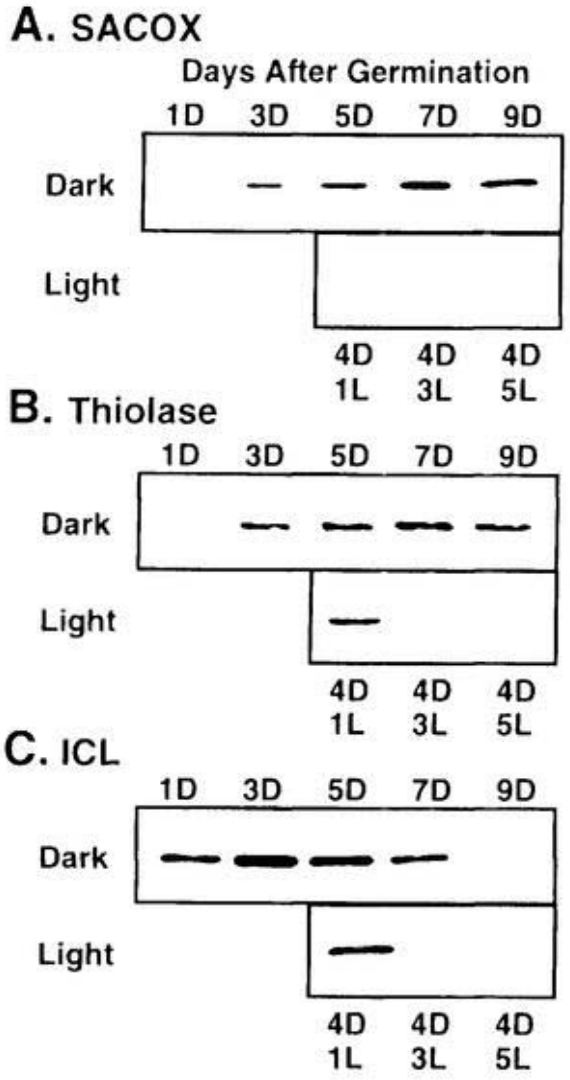

Fig. 19 Developmental changes in the level of short-chain acyl-CoA oxidase, thiolase and isocitrate lyase in *Arabidopsis* cotyledons.

D indicates the days of growth in the dark. L indicates the days of continuous illumination following 4-days in the dark.

Each lane was loaded with 10 μg (short-chain acyl-CoA oxidase) or 5 μg (thiolase, isocitrate lyase) of total proteins extracted from *Arabidopsis* cotyledons.

Electrophoresed proteins were blotted on a nylon membrane and then the membrane was allowed to hybridize with polyclonal antibodies raised against recombinant *Arabidopsis* short-chain acyl-CoA oxidase (A), against pumpkin thiolase (B) or against castor bean isocitrate lyase (C).

Thiolase のイムノブロット解析の結果も短鎖特異的 acyl-CoA oxidase と同様であるが、緑化した子葉、ロゼット葉、茎でのタンパク質量は短鎖特異的 acyl-CoA oxidase より多く検出された。 Isocitrate lyase は黄化子葉のみに検出されることから、 isocitrate lyase は他の組織では存在しないか、あるいは検出限界以下のタンパク質量であること明らかになった。

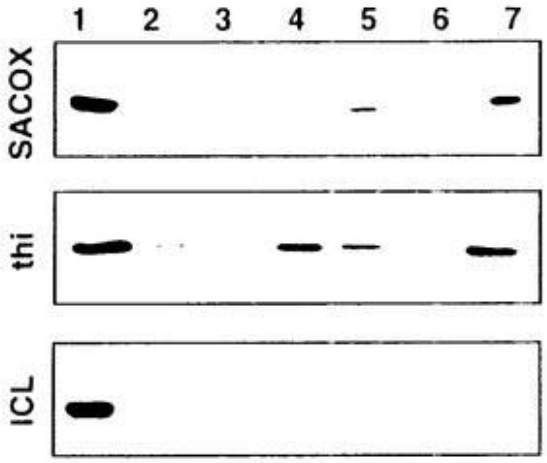

Fig. 20 Short-chain acyl-CoA oxidase, thiolase and isocitrate lyase expression in various *Arabidopsis* tissues.

Each lane was loaded with 10 μg total proteins. The tissues indicated were excised from 5-week-old plants except cotyledons which were excised after 5 or 7 days from sowing.

SACOX: short-chain acyl-CoA oxidase, thi: thiolase, ICL: isocitrate lyase.

Lane 1. *Arabidopsis* etiolated cotyledons from plants grown in the dark for 5 days.

Lane 2. Green *Arabidopsis* cotyledons from plants grown in the dark for 4 days followed by 3 days in the light.

Lane 3. Rosette leaves.

Lane 4. Flowers.

Lane 5. Roots.

Lane 6. Stems.

Lane 7. Siliques.

考察

新規の acyl-CoA oxidase

動物の脂肪酸β酸化系がマイクロボディとミトコンドリアの両方に局在していることは生化学的な知見からも分子生物学的解析からも確認されている。しかし、高等植物の場合、ミトコンドリアでの脂肪酸β酸化活性はマイクロボディにおける脂肪酸β酸化に比べ非常に弱く、しばしばマイクロボディの脂肪酸β酸化系酵素の混入によるものと判断され、その存在自体が疑問視されてきた (Gerhrtdt 1992)。ミトコンドリアの脂肪酸β酸化系はその初発酵素が acyl-CoA dehydrogenase で呼吸鎖と共役している。一方、マイクロボディの脂肪酸β酸化系は acyl-CoA dehydrogenase ではなく acyl-CoA oxidase がその役割を担っている (Schulz 1991)。このように、acyl-CoA dehydrogenase はミトコンドリアに局在、acyl-CoA oxidase はマイクロボディに局在する。

当初、我々はカボチャ長鎖特異的 acyl-CoA oxidase の他のタンパク質との同一性を調べるため、GenBank DNA データベース上で検索を行った。その結果、上位にはカボチャ長鎖特異的 acyl-CoA oxidase と同一性の高い cDNA として動物の acyl-CoA oxidase が、下位には acyl-CoA dehydrogenase が多数検索された。その acyl-CoA dehydrogenase を調べているとアラビドプシスの acyl-CoA dehydrogenase ホモログと書かれている cDNA が見つかった。この cDNA クローンがコードするアミノ酸配列を解析した結果、ミトコンドリアへの移行に必要なシグナルをもっておらず、逆にマイクロボディターゲティングシグナルであるPTS1が存在していた。前章のカボチャ長鎖特異的 acyl-CoA oxidase の解析の結果、高等植物と動物では acyl-CoA oxidase は全く違う高次構造をとっており、その一次構造上においても同一性が低く、高等植物と動物では acyl-CoA oxidase は一次構造があまり保存されていない可能性が示唆さ

れた。このアラビドプシスの cDNA が acyl-CoA dehydrogenase ホモログとして登録されている理由は、動物の acyl-CoA dehydrogenase との同一性より acyl-CoA dehydrogenase であると判断されているだけである。しかしながら、ミトコンドリアへのターゲティングシグナルがなく、マイクロボディへの移行シグナルを持っていることより、我々はこのタンパク質がマイクロボディタンパク質ではないかと推論した。また、コードされるタンパク質の分子量を計算すると約 47,000 で、分子量が 60,000 から 70,000 の acyl-CoA oxidase より 40,000 から 50,000 の acyl-CoA dehydrogenase に近い。ヒト acyl-CoA dehydrogenase と 25% 前後の同一性があるのに対し、カボチャ長鎖特異的 acyl-CoA oxidase とは 15% の同一性しかない。これらのことより、この cDNA がコードするタンパク質は acyl-CoA dehydrogenase に一次構造上似ている新しいタイプの acyl-CoA oxidase ではないかと推測した。

新規の acyl-CoA oxidase は短鎖特異的 acyl-CoA oxidase か？

高等植物の場合、特に、発芽種子においては脂肪酸 β 酸化が完全にグリオキシソームで行われていることが示唆されていた。脂肪酸 β 酸化においてアシルCoAの炭素鎖長を認識する acyl-CoA oxidase には、生化学的な解析により長鎖特異的 acyl-CoA oxidase、中鎖特異的 acyl-CoA oxidase、短鎖特異的 acyl-CoA oxidase のアイソザイムが報告されている (Kirsch et al. 1986, Hooks et al. 1996)。このうち、長鎖特異的 acyl-CoA oxidase、中鎖特異的 acyl-CoA oxidase はサブユニット分子量がそれぞれ 72,000、62,000 であることが明らかになっている。Hooks らによりトウモロコシから単離された短鎖特異的 acyl-CoA oxidase は、そのサブユニット分子量が 15,000 のホモテトラマーであると報告されているが、これは部分精製において acyl-CoA oxidase 活性を測定しており、確定的な知見ではない (Hooks et al. 1996)。そこで、この未同定な短

鎖特異的 acyl-CoA oxidase が、現在までに知られていない acyl-CoA oxidase ではないかと推論した。β酸化系酵素の解析が進んでいる動物の場合、マイクロボディの脂肪酸β酸化はアシル CoA を中鎖までしか代謝せず、短鎖長 (C8) のアシル CoA はミトコンドリアに輸送されてミトコンドリアのβ酸化系により代謝されている (Lazarow 1978, Osumi and Hashimoto 1978)。このため、動物のマイクロボディには極長鎖から中鎖までのアシル CoA を酸化する鎖長特異性のない acyl-CoA oxidase が存在するのみで、短鎖アシル CoA を酸化する acyl-CoA oxidase は存在しない。一方、酵母では、マイクロボディのみで脂肪酸β酸化が行われていることが確認されている (Ueda et al. 1985)。代謝する脂肪酸の炭素鎖長は C20-C4 と広範囲で植物と同様に基質特異性のある acyl-CoA oxidase が存在している。酵母の acyl-CoA oxidase は分子量が 70,000-80,000 であり酵母間で 40-60% の同一性がある。現在知られているアイソザイムのうち、*Candida tropicalis*の POX4、*Yarowitica lysoritica*の ACO3 が短鎖特異的 acyl-CoA oxidase であることが報告されている (Picataggio et al. 1991, Wang et al. 1998)。これらの短鎖特異的 acyl-CoA oxidase は分子量が 70,000 から 80,000 で他の acyl-CoA oxidaseと同じ分子量であり、アラビドプシス短鎖特異的 acyl-CoA oxidase ような acyl-CoA dehydrogenase との一次構造上の同一性は見られない。このことからも、アラビドプシス短鎖特異的 acyl-CoA oxidase は非常にユニークな acyl-CoA oxidase であるといえる。

Protein signature について

動物の acyl-CoA dehydrogenase において保存されている protein signature 1 (PS1: [GAC]-[LIVM]-[ST]-E-x(2)-[GSAN]-G-S-D-x(2)-[GSA]) 及び protein signature 2 (PS2: [QE]-x(2)-G-[GS]-x-G-[LIVMFY]-x(2)-[DEN]-x(4)-[KR]-x(3)-[DE], Bairoch et al. 1995) は

短鎖特異的 acyl-CoA oxidase においても完全に保存されていることが明らかになった。カボチャ長鎖特異的 acyl-CoA oxidase は PS1 が 9 アミノ酸残基中7残基、 PS2 が 8 アミノ酸残基中 6 残基が保存されている。このことも、短鎖特異的 acyl-CoA oxidase は分子構造上は acyl-CoA oxidase より acyl-CoA dehydrogenase に近いことを支持する。動物の acyl-CoA dehydrogenase の点変異による解析及び X 線構造解析の結果、中鎖特異的 acyl-CoA dehydrogenase 及び短鎖特異的 acyl-CoA dehydrogenase においてグルタミン酸残基（中鎖特異的 acyl-CoA dehydrogenase: Glu 376、短鎖特異的acyl-CoA dehydrogenase:Glu 368）が acyl-CoA dehydrogenase 活性に必要であることが報告されている (Bross et al. 1990, Kim et al. 1993, Battaile et al. 1996, Srivastava and Peterson 1998)。短鎖特異的 acyl-CoA oxidase 及びカボチャ長鎖特異的 acyl-CoA oxidase においても相当するグルタミン酸残基が保存されている (Figure 16A、アステリスク)。このことは、このグルタミン酸残基が acyl-CoA dehydrogenase 活性自体に必要なのではなく FAD への電子伝達に必要なのではないかと思われる。

短鎖特異的 acyl-CoA oxidase の発現制御

発芽過程において、短鎖特異的 acyl-CoA oxidase は同じβ酸化系酵素の thiolase と同様に暗所生育 5 日目から 7 日目に最大のタンパク質量が検出された。これに対し、グリオキシル酸サイクルの酵素である isocitrate lyase は暗所生育 3 日目に最大のタンパク質量が観察される。短鎖特異的 acyl-CoA oxidase、thiolase は 9 日間暗所生育してもタンパク質量の蓄積が確認されるが、isocitrate lyase は観察されない。前章の結果、カボチャ長鎖特異的 acyl-CoA oxidase も同じ挙動を示すことが明らかになった。これらのことより、β酸化系酵素は同じメカニズムにより発現が制御されていることが示唆される。一方、脂肪酸β酸化により生じたアセチル CoA を基質とするグリオキ

シル酸サイクル酵素は、β酸化系酵素と協調して発現していない。このことは、器官特異的な発現を解析した Figure 20 においても見られる。短鎖特異的 acyl-CoA oxidase、thiolase は花、根、莢の各器官においても発現しているが、isocitrate lyase はこれらの器官においては観察されない。このように、糖新生にのみ必要な isocitrate lyase と異なり、β酸化系の酵素は貯蔵脂肪の分解している黄化子葉にのみ発現しているのではなく、他の組織中にも発現していることを示している。カボチャ長鎖特異的 acyl-CoA oxidase についても同様の解析を行ったが、使用した抗体がアラビドプシスタンパク質に対して特異性が低く、考察できる結果が得られていない。

短鎖特異的 acyl-CoA oxidase の生化学的特性

このタンパク質は、新しいタイプの acyl-CoA oxidase なのか、それともマイクロボディ内で機能する acyl-CoA dehydrogenase なのであろうか。この問題を解析するために、この cDNA がコードするタンパク質を活性を持った形で発現させた。その結果、このタンパク質が octanoyl-CoA (C8) 以下のアシル CoA に基質特異性がある短鎖特異的 acyl-CoA oxidase であることが確認された。その最大活性は hexanoyl-CoA (C6) にあり、Km 値は 8.3μM であった。基質特異性及び Km 値はトウモロコシから単離された短鎖特異的 acyl-CoA oxidase とほぼ同じである(Km 値 6.0μM, Hooks et al. 1996)。また、高次構造、至適 pH もトウモロコシ短鎖特異的 acyl-CoA oxidase と共通であった。短鎖特異的 acyl-CoA oxidase は同一性の比較では acyl-CoA oxidase より acyl-CoA dehydrogenase により近い。しかし、短鎖特異的 acyl-CoA oxidase は acyl-CoA dehydrogenase 活性を保持しないことも明らかになった。

しかしながら、Hooks らの知見と異なる点もあり、トウモロコシ短鎖特異的 acyl-CoA oxidase のサブユニット分子量が 15,000 であるのに対し、47,000 と大きく異なっ

ていた。Hooks らの知見は中鎖特異的 acyl-CoA oxidase の精製は成功したが、短鎖特異的 acyl-CoA oxidase はカラム精製のある段階で大きく精製倍率が落ちており、部分精製に終わっている。このカラム精製中に部分的に分解されたタンパク質を、彼らは短鎖特異的 acyl-CoA oxidase としているのではないかと推測される。事実、彼らはゲル濾過を行った後、CBB 染色によりサブユニット分子量を決定しているが、この部分精製サンプルを次の精製カラムにかけると大きく精製倍率、比活性が落ちている。これらのことから、Hooks らが部分精製した短鎖特異的 acyl-CoA oxidase は活性は保持しているが、部分分解を受けているのではないかと思われる。

アミノ酸代謝

高等植物において、脂肪酸β酸化がマイクロボディのみで行われているのか、ミトコンドリアにも存在するかは未だに議論される問題である。しかし、いずれにせよマイクロボディに比べ、ミトコンドリアのβ酸化活性は非常に低いことは否めない。この活性の低さから考えて恒常的に行われる脂肪酸の分解はミトコンドリアでは行われていないのではないかと思われる。動物ではミトコンドリアの acyl-CoA dehydrogenase である isovaryl-CoA dehydrogenase, short/branched dehydrogenase, glutaryl-CoA dehydrogenase がロイシン、バリン、イソロイシン、リジンの代謝に関与していることが報告されている (Ikeda and Tanaka 1983a, Ikeda and Tanaka 1983b, Goodman and Frerman 1989)。高等植物においても、最近、ロイシン代謝系の一部分がミトコンドリアに局在することを示唆する報告がされている (Anderson et al. 1998)。しかし、マイクロボディ中にロイシン、バリン、イソロイシンの中間代謝産物が見られるとの知見もあり、まだ確定的なことは言えない (Gerbling and Gerhardt 1987)。

酵母ではマイクロボディのみで脂肪酸β酸化が行われている (Kawamoto 1978a)。

また、carnitine acetyltransferase がマイクロボディとミトコンドリアに局在することが判明していることから、マイクロボディで生成されたアセチルCoAはミトコンドリアに輸送されているのではないかと考えられている (Kawamoto 1978b, Elegersma et al. 1995)。短鎖特異的 acyl-CoA oxidase の酵素特性を解析した結果、短鎖特異的 acyl-CoA oxidase はイソブチル CoA に対して活性があった。これは、酵母の短鎖特異的 acyl-CoA oxidase と同じ結果である (Wang et al. 1998)。 Isobutyryl-CoA はバリン代謝の中間産物であることから、短鎖特異的 acyl-CoA oxidase はアミノ酸代謝に関与する可能性があるのではないだろうか。高等植物でも、今回、短鎖特異的 acyl-CoA oxidase が同定され、マイクロボディ内で完全に脂肪酸がアセチル CoA に分解されていることが示された。また、各器官によるイムノブロット解析によると、グリオキシル酸サイクルの isocitrate lyase がない器官においても短鎖特異的acyl-CoA oxidaseやthiolase は発現していた (Fig.20)。このことは、高等植物でも carnitine acetyltransferase がマイクロボディ、ミトコンドリアに存在し、脂肪酸やアミノ酸代謝産物のβ酸化により生じたアセチル CoA をミトコンドリアに輸送して TCA サイクルにより完全に酸化していることを示唆しているのではないだろうか。

<u>短鎖特異的 acyl-CoA oxidase と acyl-CoA dehydrogenase の同一性について</u>

分子量、TritonX-100 による活性阻害を受けないこと、長鎖特異的 acyl-CoA oxidase との同一性が 18% しかないこと、及び PS1,2 が完全に保存されていることなど、短鎖特異的 acyl-CoA oxidase は acyl-CoA dehydrogenase と非常に同一性が高い。また、進化系統樹を作製すると acyl-CoA dehydrogenase側に配置されることから acyl-CoA dehydrogenase と共通の祖先を持つのではないかと考えられる (Fig.16B)。ヒト肝の短鎖特異的 acyl-CoA dehydrogenase は適当な電子受容体が存在しないと電子を直接分子

状酸素（つまり acyl-CoA oxidase 活性を持つ）に渡すことが報告されている (Vanhove et al. 1993)。McFarland らの知見によると、ブタ肝 acyl-CoA dehydrogenase は pseudo substrate として β-(2-furyl)propionyl-CoA (FPCoA) を基質に用いた場合、ごく弱い反応ながら過酸化水素を発生させること、ブタ肝 acyl-CoA dehydrogenase と *Candida tropicalis* の短鎖特異的 acyl-CoA oxidase を FPCoA と反応させた場合、生成する中間反応物の charge-transfer complex の化学反応特性の違いにより ETF と反応するか、分子状酸素と反応するか決定していることを示した (McFarland et al. 1982, Rojas et al. 1985)。これらの知見は短鎖特異的 acyl-CoA oxidase と acyl-CoA dehydrogenase（特に短鎖特異的 acyl-CoA dehydrogenase）が共通の祖先を持つか、それ自身が短鎖特異的 acyl-CoA oxidase であるかを示唆している。植物では種子発芽時に脂肪酸をマイクロボディ中で完全に分解して糖新生の基質として利用する方が生存上有利に働いた結果、ミトコンドリアの短鎖特異的 acyl-CoA dehydrogenase がマイクロボディに移行してきたのかもしれない。そして、その結果、ミトコンドリアの脂肪酸 β 酸化の必要性が少なくなり、脂肪酸 β 酸化は主にマイクロボディにおいて行われるようになったのではないかと考えられる。

今回の解析により、短鎖特異的 acyl-CoA oxidase はこれまでに知られていない全く新規な acyl-CoA oxidase であることが明らかになった。この短鎖特異的 acyl-CoA oxidase がマイクロボディに局在することよりマイクロボディは脂肪酸をアセチル CoA に完全に分解する事ができる。動物のマイクロボディは短鎖特異的 acyl-CoA oxidase 活性が無いことから、この短鎖特異的 acyl-CoA oxidase が植物特有の生理機能に関与していることが示唆される。この短鎖特異的 acyl-CoA oxidase の器官特異的発現の解析により黄化子葉以外の器官にも発現が観察されることもこのことが裏付け

られる。今後、このタンパク質の黄化子葉以外での機能についての解析が期待される。

引用文献

Aebi, H. (1974) Methods of enzymatic analysis, 2: 673-684, Academic Press, New York

Altschul, S.F., Gish, W., Miller, W., Myers, E.W. and Lipman, D.J. (1990) J. Mol. Biol. 215:403-410

Anderson, M.D., Che, P., Song, J., Nikolau, B.J., Wurtele, E.S. (1998) Plant Physiol. 118:1127-1138

Bairoch, A., Bvcher, P. and Hofmann, K. (1995) Nucl. Acids Res. 25: 217-221

Battaile, K.P., Mohsen, A.W. and Vockley, J. (1996) Biochemistry 35: 15356-15363

Bross, P., Engst, S., Strauss, A.W., Kelly, D.P., Rasched, I. and Ghisla, S. (1990) J. Biol. Chem. 265: 7116-7119

Dommes, V. and Kunau, W.H. (1976) Anal. Biochem. 71:571-8

Elgersma, Y., van Roermund, W.T., Wanders, R.J. and Tabak, H.F. (1995) EMBO J. 14:3472-3479

Feinberg, A.P. and Vogelstein, B. (1984) Anal. Biochem. 139: 266-267

Furuta, S., Miyazawa, S. and Hashimoto, T. (1981) J. Biochem. (Tokyo) 90: 1739-1750

Gerbling, H. and Gerhardt, B. (1987) Planta 171: 386-391

Gerhardt, B. (1987) Methods Enzymol. 148: 516-525

Gerhardt, B. (1992) Prog. Lipid Res. 31:417-446

Goodman, T. and Frerman, T. (1989) In the Metabolic Basis of Inherited Disease, 845-853

Gould, S.J., Keller, G.A. and Subramani, S. (1987) J. Cell Biol. 105: 2923-2931

Hayashi, H., De Bellis, L., Yamaguchi, K., Kato, A., Hayashi, M. and Nishimura, M. (1998a) J. Biol. Chem. 273: 8301-8307

Hayashi, M., Toriyama, K., Kondo, M. and Nishimura, M. (1998b) Plant Cell 10: 183-195

Higgins, D.G., Bleasby, C.J. and Fuchs, R. (1992) Compt. Appl. Biosci. 8:189-191

Hodges, T.K. and Leonard, R.T. (1974) Methods Enzymol. 32: 392-406

Hooks, M.A., Bode, K. and Couée, I. (1996) Biochem. J. 320: 607-614

Ikeda, Y. and Tanaka, K. (1983a) J. Biol. Chem. 258:1077-1089

Ikeda, Y. and Tanaka, K. (1983b) J. Biol. Chem. 258:9477-9487

Kato, A., Hayashi, M., Takeuchi, Y. and Nishimura, M. (1996) Plant Mol. Biol. 22: 843-852

Kawamoto, S., Nozaki, C., Tanaka, A. and Fukui, S. (1978a) Eur. J. Biochem. 83: 609-613

Kawamoto, S., Ueda, M., Nozaki, C., Yamamura, M., Tanaka, A. and Fukui, S. (1978b) FEBS Lett. 96: 37-40

Kim, J.J., Wang, M. and Paschke, R. (1993) Proc. Natl. Acad. Sci. USA 90: 7523-7527

Kirsch, T., Löffler, H. -G. and Kindl, H. (1986) J. Biol. Chem. 261: 8570-8575

Laemmli, U.K. (1970) Nature 227:680-685

Lazarow, P.B. (1978) J. Biol. Chem. 253: 1522-1528

McFarland, J.T., Lee, M.Y., Reinsch, J. and Raven, W. (1982) Biochemistry 21:1224-1229

Nishimura, M., Takeuchi, Y., De Bellis, L. and Hara-Nishimura, I. (1993) Protoplasma 175: 131-137

Osumi, T. and Hashimoto, T. (1978) Biochem. Biophys. Res. Commun. 83: 479-485

Picataggio, S., Deanda, K. and Mielenz, J. (1991) Mol. Cell. Biol. 11:4333-4339

Rojas, C., Schmidt, J., Lee, M.Y., Gustafson, J. and McFarland J.T. (1985) Biochemistry 24:2947-2954

Sambrook, J., Fritsch, E.F. and Maniatis, T. (1989) Cold Spring Habour Laboratory Press, New York

Sanger, F., Nicklen, S. and Coulson, A.R. (1977) Proc. Natl. Acad. Sci. USA 74: 5463-5467

Schulz, H. (1991) Biochim. Biophys. Acta 1081:109-120

Srivastava, D.K. and Peterson, K.L. (1998) Biochemistry 37: 8446-8456

Towbin, H., Staehelin, T. and Gordon, J. (1979) Proc. Natl. Acad. Sci. USA. 76: 4350-4354

Vanhove, G., Van Veldhoven, P.P., Eyssen, H.J. and Mannaerts, G.P. (1993) Biochem. J. 292:23-30

Wang, H., Le Clainche, A., Le Dall, M.T., Wache, Y., Pagot, Y., Belin, J.M., Gaillardin, C. and Nicaud J.M. (1998) Yeast 14:1373-1386

総合討論

本研究で高等植物で初めて脂肪酸β酸化系の初発酵素である acyl-CoA oxidase の基質特異性の異なる 2 種類のアイソザイムについて cDNA をクローニングし、その一次構造を解析するとともに、マイクロボディ機能変換時における発現、及び器官特異的発現について解析を行った。

Acyl-CoA oxidase の発現調節機構

これまでに、マイクロボディの一部の酵素が光により制御を受けていることが示唆されていた。黄化子葉に光を照射すると緑化に伴いグリオキシソーム酵素である citrate synthase, thiolase が大きく減少し、緑葉パーオキシソーム酵素である glycolate oxidase, hydroxypyruvate reductase が著しく誘導される (Mori and Nishimura 1989, De Bellis and Nishimura 1991, Nishimura et al. 1993)。また、citrate synthase, thiolase の mRNA の転写量は暗所中で減少することから光以外の因子による調節もされていることが示唆された (Kato et al. 1995, Kato et al. 1996)。また、光以外の因子による調節として、遺伝子の発現制御が糖により行われていることを示唆する知見がグリオキシル酸サイクル酵素の malate synthase, isocitrate lyase について報告されている。 Malate synthase, isocitrate lyase の cis-acting element の解析から、malate synthase, isocitrate lyase には発芽と糖の 2 つの異なった cis-acting element があり、種間でこの 2 つの cis-acting element はよく似ていることが明らかになっている (Graham et al. 1994, Reynolds and Smith 1995a, 1995b, Sarah et al. 1996, De Bellis et al. 1997)。また、malate synthase の cis-acting element は酢酸やアセチル CoA にも応答することを示唆する結果が得られている (Graham et al. 1992)。今回の解析により、長鎖特

異的 acyl-CoA oxidase、短鎖特異的 acyl-CoA oxidase についても同じβ酸化系酵素の thiolase、グリオキシル酸サイクル酵素の citrate synthase と同様に転写レベルのみの調節だけでなくタンパク質レベルでの調節を受けていることが明らかになった。これらのことより、発芽段階においてグリオキシル酸サイクルと協調的に働く脂肪酸β酸化系の酵素群が同じ作用機乍で制御されていると考えられた。しかし、アラビドプシスの短鎖特異的 acyl-CoA oxidase の発現パターンを見ると短鎖特異的 acyl-CoA oxidase, thiolase と isocitrate lyase が異なった発現パターンを示している (Fig.19, 20)。また、これらのタンパク質の器官特異性では isocitrate lyase が黄化子葉のみに特異的に発現しているが、acyl-CoA oxidase, thiolase は様々な器官において発現していることが確認された。これらの結果は、脂肪酸β酸化系の酵素群とグリオキシル酸サイクルの酵素群が同じ制御機構により調節を受けているという説に疑問を投げかける。脂肪酸β酸化系では、遺伝子の発現制御が糖ではなく他の因子（脂肪酸、アシル CoA ）により行われているか、全く異なる発現制御機構により行われている可能性が考えられる。

その１つの候補として、パーオキシソーム増殖剤活性化受容体 (peroxisome proliferator-activator receptor: PPAR) による発現調節を考えている。動物細胞では、肝細胞増殖と脂肪酸代謝は、細胞内の脂肪量のホメオスタシスに適応して協調的に誘導されること、及び細胞内の脂肪の蓄積が主な要因となりパーオキシソームの増殖が誘導されることも確認されている (Bell and Elcombe 1993)。このように、脂肪酸代謝の制御にはパーオキシソームの増殖が中心的な役割を果たしていることが確認されている (Lee et al. 1995)。また、パーオキシソーム増殖剤の添加により、パーオキシソーム脂肪酸β酸化系の酵素群の発現が誘導されることが明らかになっている (Lazarow and de Duve 1976,

Hashimoto 1982, Latruffe et al. 1993)。このように、脂肪酸やPPARにより、パーオキシソーム脂肪酸β酸化系酵素が誘導されることは明らかになっている。興味深いことに、ラット、ヒトの acyl-CoA oxidase ではパーオキシソーム増殖剤応答エレメント (peroxisome proliferator-receptor element: PPRE) が同定されている (Isseman and Green 1990, Tugwood et al. 1992, Varanasi et al. 1996)。現在まで、特にラットなどの齧歯類でパーオキシソーム増殖剤により増殖が顕著なことから、PPAR は動物を中心に解析が進んでいる。しかし、大腸菌や酵母では脂肪酸を炭素源にするとマイクロボディ及び脂肪酸β酸化系酵素が誘導されてくることが確認されている。酵母ではβ酸化系酵素のプロモーター解析の結果より、オレイン酸 (C18:1) に応答する領域が同定されている (Sloots et al. 1991, Filipits et al. 1993, Wang et al. 1992)。 高等植物ではマイクロボディの誘導はまだ観察されていない。近年、工業的に重要な中鎖脂肪酸を植物により合成させる試みがされているが、中鎖脂肪酸の合成系に関与する酵素である lauroyl-acyl carrier protein thioesterase を過剰発現させた場合、 acyl-CoA oxidase の発現が誘導されることが報告がされている (Eccleston and Ohlrogge 1998)。この知見によれば、中鎖脂肪酸の合成系の過剰発現が確認されているにも関わらず、脂肪酸組成に大きな変化が見られなかった。このことは、細胞内に一定量の中鎖脂肪酸が蓄積すると脂肪酸β酸化を用いて脂肪酸量を調節していることを示唆している。このような、植物体内の脂肪酸組成をモニターする機構として PPAR ホモログが関与していないだろうか。これらの仮説を確認するために、今後、長鎖特異的 acyl-CoA oxidase、短鎖特異的 acyl-CoA oxidaseのcis-acting element の解析、及び PPAR ホモログの探索が行われることが期待される。

Acyl-CoA oxidase の役割

現在、データベースに登録されているのみの acyl-CoA oxidase も含めると、高等植物には分子量 60,000-70,000 のターゲティングシグナルの異なった acyl-CoA oxidase が 2 種類と分子量 47,000 と大きく異なる短鎖特異的 acyl-CoA oxidase が存在している。カボチャ長鎖特異的 acyl-CoA oxidase との同一性よりアラビドプシス (ACX2)、コチョウランの acyl-CoA oxidase ホモログは長鎖特異的 acyl-CoA oxidase ではないかと思われる。このコチョウラン acyl-CoA oxidase は花弁の老化時に発現する遺伝子として単離された (Do and Huang 1997)。先に、当研究室で行われた実験結果より、緑化子葉が老化すると thiolase の発現が、グリオキシル酸サイクルの酵素の発現と同時に誘導されることが明らかになっている (Kato et al. 1996)。老化時に発現が誘導される脂肪酸 β 酸化系は、他の組織に転流するために膜脂質を分解して糖に変えていると考えられている。コチョウラン acyl-CoA oxidase が花弁の老化時に発現することは、この推論を支持するものであり、長鎖特異的 acyl-CoA oxidase は黄化子葉のみではなく花の老化時においても発現することを示している。

一方、カボチャ長鎖特異的 acyl-CoA oxidase と同一性が低い PTS1 タイプのオオムギ acyl-CoA oxidase ホモログは乾燥ストレスにより発現が誘導される (Grossi et al. 1995)。また、傷害応答により acyl-CoA oxidase が誘導されるとの報告もある (Titarenko et al. 1997)。環境ストレスのシグナルの 1 つにジャスモン酸がある。ジャスモン酸の生成に β 酸化が関与していることから acyl-CoA oxidase の発現が誘導されたのではないだろうか？また、これら PTS1、PTS2 タイプの acyl-CoA oxidase はそれぞれが乾燥、老化に特異的に発現が誘導されるのだろうか？それとも、両方の acyl-CoA oxidase が発現し協調的に機能して

いるのであろうか？現在までの知見では、単独の acyl-CoA oxidase の発現を見たのみなのでこの点は不明である。すでに PTS1 タイプの acyl-CoA oxidase のアラビドプシス EST cDNA クローンが存在しており、カボチャ長鎖特異的 acyl-CoA oxidase と同様の解析を行い環境ストレスや老化時において acyl-CoA oxidase の発現を解析することが期待される。

他のβ酸化系酵素について

脂肪酸をアシル CoA に触媒する acyl-CoA synthetase はアイソザイムが多く存在し、局在性も様々であるが、高等植物では、マイクロボディ局在型 acyl-CoA synthetase はまだ同定されていない。最近、ナタネにおいて、動物の acyl-CoA synthetase の保存領域より作製した PCR クローニングにより 5 種類のアイソザイムがクローニングされた (Fulda et al. 1997)。このうち、2 種類については acyl-CoA synthetase 活性が確認されている。当研究室において、カボチャ黄化子葉の 76kDa のマイクロボディ膜タンパク質の解析したところ、活性がまだ未同定のナタネの acyl-CoA synthetase ホモログと同一性の高い N 末端アミノ酸配列を得られた。現在、この N 末端アミノ酸配列よりディジェネレイトプライマーを作製し、カボチャ cDNA ライブラリーを用いてスクリーニングを行っている。

また、今回、データは示さなかったが多機能酵素についてもカボチャ cDNA ライブラリーより cDNA をクローニングしている。すでに当研究室の加藤らにより thiolase のクローニングは終えているので脂肪酸β酸化系の全ての酵素がクローニングされたことになる (Kato et al. 1996)。これら脂肪酸β酸化系酵素群の変動を詳細に解析することにより、黄化子葉の緑化、及び老化

時においてマイクロボディ機能変換の分子機構の解明に寄与する事が期待される。

今後の展望

酵母の acyl-CoA oxidase 遺伝子破壊株の解析の結果、短鎖特異的 acyl-CoA oxidase の遺伝子破壊株では約 8 倍の長鎖特異的 acyl-CoA oxidase 活性の上昇が、また、長鎖特異的 acyl-CoA oxidase の遺伝子破壊株では約 20 倍の短鎖特異的 acyl-CoA oxidase 活性の上昇が観察された (Picataggio et al. 1991, Wang et al. 1998)。これらはアシル CoA もしくは脂肪酸の蓄積により acyl-CoA oxidase の発現が誘導されたのではないかと考えられている。また、ヒトの遺伝子疾患の解析より脂肪酸、アシル CoA、アセチル CoA の蓄積は細胞毒として働くことが明らかになっている (Schulz 1991)。高等植物、酵母、動物の acyl-CoA oxidase と動物の acyl-CoA dehydrogenase 間で進化系統樹を作製すると高等植物のacyl-CoA oxidaseは 3 つのパターンに分岐した (Fig.21)。短鎖特異的 acyl-CoA oxidaseはacyl-CoA dehydrogenase、PTS1 タイプの acyl-CoA oxidase は動物の acyl-CoA oxidase のブランチに配置された。また、PTS2 タイプの acyl-CoA oxidase は全く独自の系統を示した。このことは、PTS2 タイプの acyl-CoA oxidase が植物独自の生理機能に関与しているという仮説を支持する。このように、高等植物の acyl-CoA oxidase は動物、酵母による研究のみでは類推できない機能をもつことが予想される。これらの知見を鑑みて、acyl-CoA oxidase の機能欠損株を得ることは、今後、高等植物の脂肪酸 β 酸化系の解析に非常に有用であると考えている。当研究室では、これまでに β 酸化代謝基質になる 2,4-dichlorophenoxybutyric acid (2,4-DB) による選抜により β 酸化系酵素

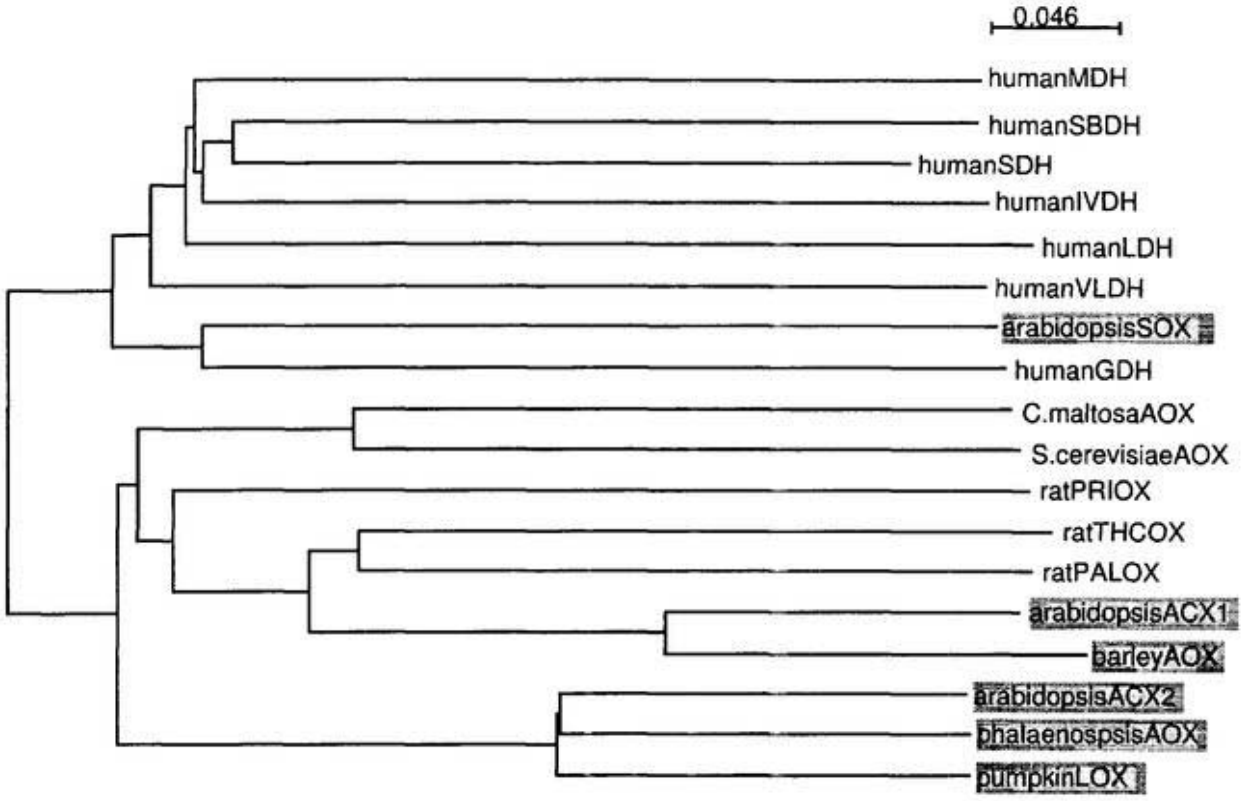

Fig. 21 Phylogenetic tree of acyl-CoA oxidases and acyl-CoA dehydrogenases.
Multiple sequence alignment of the protein sequences was performed using the CLUSTAL W program; the phylogenetic tree was constructed according to NJPLOT program. Known acyl-CoA oxidases and acyl-CoA dehydrogenases were aligned: pumpkin LOX, pumpkin long-chain acyl-CoA oxidase (GenBank accession No. AF002016); arabidopsis SOX,*Arabidopsis* short-chain acyl-CoA oxidase (AB017643); phalaenopsis ACOX, *Phalaenopsis* putative acyl-CoA oxidase (U66299); barley AOX, barley putative acyl-CoA oxidase (AJ001341); arabidopsis ACX 1, 2, *Arabidopsis* acyl-CoA oxidase homolog (AF057044, AF057043); rat PRIOX, rat pristanoyl-CoA oxidase (X95188); rat PALOX, rat palmitoyl-CoA oxidase (P07872); rat THCOX, rat trihydroxycoprostanoyl-CoA oxidase (X95189); S. cerevisiae AOX,*Saccharomyces cerevisiae* acyl-CoA oxidase (P13711); C. maltosa AOX,*Candida maltosa* acyl-CoA oxidase (P05335); Human VLDH, Human very long-chain acyl-CoA dehydrogenase (D43682); Human LDH, Human long-chain acyl-CoA dehydrogenase (M74096); Human MDH, Human medium-chain acyl-CoA dehydrogenase (M16827); Human SDH, Human short-chain acyl-CoA dehydrogenase (M26393); Human SBDH, Human short/branched-chain acyl-CoA dehydrogenase (U12778); human GDH, human glutaryl-CoA dehydrogenase (U69141); human IVDH, human isovaleryl-CoA dehydrogenase (M34192).
The proteins from higher plants are indicated background of shadowing.

thiolase 欠損アラビドプシスのスクリーニングに成功している (Hayashi et al.1998)。この thiolase 欠損株ではマイクロボディ内に電子密度の低い物質の蓄積が観察されている。これは脂肪酸β酸化の中間代謝産物ではないかと考えられている。同じスクリーニングの方法を用いて長鎖、短鎖特異的 acyl CoA oxidase 及び acyl CoA synthetase 欠損株のスクリーニング及びタグラインによるβ酸化系酵素の突然変異体のスクリーニングも試みることを検討している。また、長鎖特異的 acyl-CoA oxidase、短鎖特異的 acyl-CoA oxidase の *in vivo* での解析を行うために、アラビドプシスにおいてアンチセンス形質転換植物を作製中である。現在、T2 種子が得られた段階であるが、頂芽優勢の崩れている株、莢中の種子の数が極端に少ない株が見られる。長鎖特異的 acyl-CoA oxidase、短鎖特異的 acyl-CoA oxidase の発現が押さえられたホモ形質転換体が得られた場合、種子やその他の組織中での脂肪酸組成を分析する予定である。また、酵母の遺伝子破壊株のように、acyl-CoA oxidase 活性が変化していないか解析することを計画している。

これらの様々な解析を通じて得た知見が、脂肪酸β酸化系の高等植物における生理的機能及び黄化子葉の緑化、老化時のマイクロボディの機能変換の分子機構の解明に貢献することを期待している。

引用文献

Bell, D.R. and Elcombe, C.R. (1993) Peroxisome: biology and importance in toxicology and medicine 137-147

De Bellis, L and Nishimura, M. (1991) Plant Cell Physiol. 32:555-561

De Bellis, L., Ismail, I., Reynolds, S., Barrett, M.D. and Smith, S.M. (1997) Gene 197:375-378

Do, Y.Y. and Huang, P.L. (1997) Arch. Biochem. Biophys. 344: 295-300.

Eccleston, V.S. and Ohlrogge, J.B. (1998) Plant Cell 10: 613-622.

Filipits, M., Simon, M.M., Rapatz, W., Hamilton, B. and Ruis, H. (1993) Gene 132:49-55

Fulda, M., Heinz, E. and Wolter, F.P. (1997) Plant Mol. Biol. 33:911-922

Graham, I.A., Leaver, C.J. and Smith, S.M. (1992) Plant Cell 4:349-357

Graham, I.A., Baker, C.J. and Leaver, C.J. (1994) Plant Cell 6:761-772

Grossi, M., Gulli, M., Stanca, M. and Cattivelli, L. (1995) Plant Science 105:71-80

Hashimoto, T. (1982) Ann. NY Acad. Sci. 386:5-12

Hayashi, M., Toriyama, K., Kondo, M. and Nishimura, M. (1998) Plant Cell 2:183-195

Isseman, T. and Green, S. (1990) Nature 347:645-649

Kato, A., Hayashi, M., Mori, H. and Nishimura, M. (1995) Plant Mol. Biol. 22: 843-852

Kato, A., Hayashi, M., Takeuchi, Y. and Nishimura, M. (1996) Plant Mol. Biol. 27: 377-390

Lee, S.S., Pineau, T., Drago, J., Lee, E.J., Owens, J.W., Kroetz, D.L., Fernaudez-Salguero, P.M., Westphal, H. and Gonzalez, F.J. (1995) Mol. Cell. Biol. 15:3012-3022

Latruffe, N., Bugant, M., Bournot, P., Bentejac, M., Ramirez, I.C. and Maiki, M.C. (1993) Peroxisome: biology and importance in toxicology and medicine 173-203

Lazarow, P.B. and de Duve, C. (1976) Proc. Natl. Acad. Sci. USA 73:2043-2046

Mori, H. and Nishimura, M. (1989) FEBS Lett. 244: 163-166

Nishimura, M., Takeuchi, Y., De Bellis, L. and Hara-Nishimura, I. (1993) Protoplasma 175: 131-137.

Picataggio, S., Deanda, K. and Mielenz, J. (1991) Mol. Cell. Biol. 11:4333-4339

Reynolds, S.J. and Smith, S.M. (1995a) Plant Mol. Biol. 27:487-497

Reynolds, S.J. and Smith, S.M. (1995b) Plant Mol. Biol. 29:885-896

Sarah, C.J., Graham, I.A., Reynolds, S.J., Leaver, C.J., Smith, S.M. (1996) Mol. Gen. Genet. 250:153-161

Schulz, H. (1991) Biochim. Biophys. Acta 1081:109-120

Sloots, J.A., Aitchison, J.D. and Rachubinski, R.A. (1991) Gene 105:129-134

Titarenko, E., Rojo, E., Leon, J. and Sanchez-Serrano, J.J. (1997) Plant Physiol. 115:817-876

Tugwood, J.D., Isseman, I., Anderson, R.G., Bundell, K.R., McPheat ,W.L. and Green, S. (1992) EMBO J. 11:433-439

Varanasi, U., Chu, R., Huang, Q., Castellon, R., Yeldandi, A.V. and Reddy, J.K. (1996) J. Biol. Chem. 271:2147-2155

Wang, T.W., Lewin, A.S. and Small, G.M. (1992) Nucleic Acids Res. 20:3495-3500

謝辞

本研究を遂行するに当たり、終始ご指導とご鞭撻をいただきました西村幹夫教授には深く感謝いたします。また、終始適切なご助言、ご指導いただきました林誠助手に深く感謝いたします。近藤真紀氏、山口勝司氏には免疫電顕、N 末端アミノ酸解析をしていただき、感謝いたします。オルガネラ分画法のご指導とサンプルを分与していただきました加藤朗博士、また、生化学実験のご指導及び長鎖 acyl-CoA oxidase のカラム分析をしていただいた Luigi De Bellis 博士に感謝いたします。また、日常、ご助言をいただきました西村いくこ助教授、嶋田知生助手をはじめ研究室の職員、学生のみなさまに感謝いたします。総研大の同期生である山田健志博士には公私に渡り様々な相談にのって下さったことに深く感謝いたします。

最後に、常に物心両面から支えて下さった両親、兄弟に心から感謝いたします。

報文目録

Hiroshi Hayashi, Luigi De Bellis, Katsushi Yamaguchi, Akira Kato, Makoto Hayashi and Mikio Nishimura

Molecular Characterization of a Glyoxysomal Long-Chain Acyl-CoA Oxidase That Is Synthesized as a Precursor of Higher Molecular Mass in Pumpkin

J.Biol.Chem., 273: 8301-8307, 1998

Hiroshi Hayashi, Luigi De Bellis, Adriana Ciurli, Maki Kondo, Makoto Hayashi, and Mikio Nishimura

A Novel Acyl-CoA Oxidase That Can Oxidize Short-chain Acyl-CoA in Plant Peroxisomes

J.Biol.Chem., 274: 12715-12721, 1999

Printed in U.S.A.

Molecular Characterization of a Glyoxysomal Long Chain Acyl-CoA Oxidase That Is Synthesized as a Precursor of Higher Molecular Mass in Pumpkin*

(Received for publication, November 21, 1997, and in revised form, January 15, 1998)

Hiroshi Hayashi‡§, Luigi De Bellis‡¶, Katsushi Yamaguchi‡, Akira Kato‡, Makoto Hayashi‡§, and Mikio Nishimura‡§‖

From the ‡Department of Cell Biology, National Institute for Basic Biology, Okazaki, 444 Japan, §Department of Molecular Biomechanics, The Graduate University for Advanced Studies, Okazaki 444, Japan, and the ¶Dipartimento di Biologia delle Piante Agrarie, Sezione di Fisiologia Vegetale, via Mariscoglio 34, I-56124 Pisa, Italy

A cDNA clone for pumpkin acyl-CoA oxidase (EC 1.3.3.6; ACOX) was isolated from a λgt11 cDNA library constructed from poly(A)$^+$ RNA extracted from etiolated cotyledons. The inserted cDNA clone contains 2313 nucleotides and encodes a polypeptide of 690 amino acids. Analysis of the amino-terminal sequence of the protein indicates that the pumpkin acyl-CoA oxidase protein is synthesized as a larger precursor containing a cleavable amino-terminal presequence of 45 amino acids. This presequence shows high similarity to the typical peroxisomal targeting signal (PTS2). Western blot analysis following cell fractionation in a sucrose gradient revealed that ACOX is localized in glyoxysomes. A partial purification of ACOX from etiolated pumpkin cotyledons indicated that the ACOX cDNA codes for a long chain acyl-CoA oxidase. The amount of ACOX increased and reached to the maximum activity by day 5 of germination but decreased about 4-fold on the following days during the subsequent microbody transition from glyoxysomes to leaf peroxisomes. By contrast, the amount of mRNA was already high at day 1 of germination, increased by about 30% at day 3, and faded completely by day 7. These data indicated that the expression pattern of ACOX was very similar to that of the glyoxysomal enzyme 3-ketoacyl-CoA thiolase, another marker enzyme of the β-oxidation spiral, during germination and suggested that the expression of each enzyme of β-oxidation is coordinately regulated.

There are at least three types of microbodies in higher plants (glyoxysomes, leaf peroxisomes, and unspecialized microbodies) that are distinguishable by their enzyme complements (1, 2). During the postgerminative growth of pumpkin seedlings and upon exposure to light, etiolated cotyledons turn green; at the same time, a functional transition from glyoxysomes to leaf peroxisomes occurs (3, 4). In fat-storing seeds of plants such as pumpkin, lipid bodies are present in seed cells that store triacylglycerols, which are subsequently converted to fatty acids by lipase. Fatty acids represent the main energy and carbon sources for germinating seedlings. In glyoxysomes, fatty acids are degraded to acetyl-CoA via the β-oxidation pathway, and acetyl-CoA is metabolized by the glyoxylate cycle bypassing the decarboxylating steps of the Krebs cycle. We have shown previously that the expression of glyoxysomal enzymes and leaf peroxisomal enzymes are regulated not only at the transcriptional level but also at the posttranscriptional level during the microbody transition (5, 6). The gene expressions of the enzymes of the β-oxidation and glyoxylate cycles seem to be coordinately regulated. In a recent paper, we reported the nucleotide and deduced amino acid sequences of the cDNA for 3-ketoacyl-CoA thiolase (7). The time course for thiolase mRNA and thiolase levels during germination and postgerminative growth implied that the regulation of expression of this enzyme is similar to that of glyoxylate cycle enzymes, *e.g.* malate synthase (8) and citrate synthase (9). The glyoxysomal β-oxidation spiral consists of three different proteins: acyl-CoA oxidase (ACOX),[1] enoyl-CoA hydratase/3-hydroxy acyl-CoA dehydrogenase (bifunctional protein), and 3-ketoacyl-CoA thiolase (thiolase). ACOX converts acyl-CoA into *trans*-2-enoyl-CoA in the first step of the β-oxidation spiral and corresponds to the acyl-CoA dehydrogenase present in mitochondria of mammalian cells. Both enzymes are flavoproteins. Some plant ACOXs have been purified and characterized (10, 11) and have been shown to have different substrate specificities (for long, medium, and short chain acyl-CoAs, respectively). To further investigate the β-oxidation enzymes at the molecular level, we cloned a cDNA coding for a long chain ACOX, which is localized in glyoxysomes. Here, we report the nucleotide and deduced amino acid sequences of the cDNA. Developmental changes in the level of mRNA and protein were also determined in pumpkin cotyledons during seed germination and subsequent postgerminative growth.

EXPERIMENTAL PROCEDURES

Plant Materials—Pumpkin (*Cucurbita* sp. Kurokawa Amakuri) seeds were purchased from Aisan Seed Co. (Aichi, Japan). Seeds were soaked in running tap water overnight and germinated in Rock-Fiber soil (66R, Nitto Boseki, Chiba, Japan) at 25 °C in darkness. Some seedlings were transferred to light after 5 days.

Construction of the λgt11 cDNA Library—Total RNA was extracted from etiolated cotyledons of 4-day-old dark-grown seedlings by the SDS-phenol method. Poly(A)$^+$ RNA was prepared by column chromatography on oligo(dT) cellulose (Becton Dickinson). cDNA transcribed

* This work was supported by "Research for the Future" Program Grant JSPS-RFTF 96L00407, the Japan Society for the Promotion of Science and Grants-in-Aid for Scientific Research (09440271, 09274101, and 09274103), the Ministry of Education, Science and Culture, Japan, a grant from the Nissan Science Foundation (Tokyo), and the NIBB program for Molecular Mechanisms of Stress Response. The costs of publication of this article were defrayed in part by the payment of page charges. This article must therefore be hereby marked "*advertisement*" in accordance with 18 U.S.C. Section 1734 solely to indicate this fact.

The nucleotide sequence(s) reported in this paper has been submitted to the GenBank™/EBI Data Bank with accession number(s) AF002016.

‖ To whom correspondence should be addressed. Tel.: 81-564-55-7500; Fax: 81-564-55-7505; E-mail: mikosome@nibb.ac.jp.

[1] The abbreviations used are: ACOX, acyl-CoA oxidase; PTS, peroxisomal targeting signal; thiolase, 3-ketoacyl-CoA thiolase; PRISCOX, pristanoyl-CoA oxidase; MOPS, 3-(*N*-morpholino)propanesulfonic acid; PAGE, polyacrylamide gel electrophoresis.

from the poly(A)$^+$ RNA was constructed using the λgt11 system (Amersham, Tokyo, Japan).

Amino Acid Sequence Analysis—Determination of the amino-terminal sequence of glyoxysomal acyl-CoA oxidase was performed essentially as described by Matsudaira (12). Isolated glyoxysomes were subjected to SDS-PAGE and proteins were transferred to a polyvinylidene difluoride membrane (Problot, Applied Biosystems, Chiba, Japan). The membrane was stained with Coomassie Blue, and the band corresponding to acyl-CoA oxidase was cut out with a razor blade. Protein sequencing was performed by automated Edman degradation in a protein sequencer (model 473A, Applied Biosystems).

Screening and Sequencing of cDNA—A full sequence of pumpkin acyl-CoA oxidase was obtained by polymerase chain reaction employing 5′-CACAGGGAGATTCAAGA-3′ and 5′-TCGGATCGAATGTAGCT-3′ as the sense and antisense primers, respectively. The amplified DNA fragment was used as probe for the following experiment. Screening and plaque hybridization were performed by the standard techniques. The insert of the isolated phage clone was subcloned into the plasmid vector Bluescript II SK(−) (Stratagene). A series of unidirectional deletion clones was constructed with a deletion kit (Takara Shuzo, Kyoto, Japan), and DNA sequencing was performed by the method of Sanger *et al.* (13). DNA sequences were analyzed with GeneWorks Release 2.2 computer software (IntelliGenetics, Mountain View, CA). The BLAST server was utilized for the analysis of homologies among proteins. Alignment of several acyl-CoA oxidases was performed using Clustal W software (14).

Preparation of a Specific Antiserum—The pumpkin acyl-CoA oxidase cDNA was inserted into pET32b vector (Novagen, Madison, WI). A fusion protein between acyl-CoA oxidase and a histidine tag was synthesized in *Escherichia coli* cells and purified by column chromatography on Ni^{2+}-resin. The purified protein in 1 ml of sterilized water was emulsified with an equal volume of Freund's complete adjuvant (DIFCO, Detroit, MI). The emulsion was injected subcutaneously on the back of a rabbit. Four weeks later, a booster injection (about 0.25 mg of protein) was similarly given to the first injection. Blood was taken from a vein in the ear 7 days after the second booster injection. The serum was used for immunoblotting.

Hydrophobic Interaction Chromatography—Five-day-old etiolated pumpkin cotyledons were homogenized at 4 °C with 3 volumes of 150 mM Tris-HCl, pH 7.8, 10 mM KCl, 1 mM dithiothreitol, 10 μM FAD, 0.1 mM phenylmethylsulfonyl fluoride, and 10% glycerol. The homogenate was centrifuged at 15,000 × *g* for 20 min. To the resulting supernatant, an equal volume of 50 mM sodium phosphate, pH 7.0, containing 3.4 M $(NH_4)_2SO_4$ was added and loaded onto a 1-ml Pharmacia (Uppsala, Sweden) phenyl-Sepharose high performance HiTrap column. The column was washed with 50 mM sodium phosphate, pH 7.0, containing 1.7 M $(NH_4)_2SO_4$. Bound proteins were eluted by increasing the concentration of 50 mM sodium phosphate, pH 7.0, containing 60% ethylene glycol.

Subcellular Fractionation—Four-day-old etiolated cotyledons were homogenized in a Petri dish by chopping with a razor blade for 5 min in 10 ml of a medium that contained 150 mM Tricine-KOH, pH 7.5, 1 mM EDTA, and 0.5 M sucrose. The homogenate was passed through four layers of cheesecloth. 3 ml of the filtrate was layered onto a sucrose gradient that consisted of a 1-ml cushion of 60% (w/w) sucrose and 11 ml of a linear sucrose gradient from 60 to 30% without buffer. The gradient was centrifuged at 25,000 × *g* for 3 h in an SW 28–2 rotor in an ultracentrifuge (XL-90; Beckman, Fullerton, CA). After centrifugation, fractions (0.5 ml each) were collected with an automatic liquid fractionation (ALC-2L; Advantec, Tokyo). All procedures were carried out at 4 °C.

Enzyme Assay—Enzyme activities were measured at 25 °C in a 1-ml reaction mixture and monitored with a Hitachi (Tokyo) U-2000 spectrophotometer as follows: acyl-CoA oxidase (EC 1.3.3.6) according to Gerhardt (15), with the concentration of acyl-CoA substrates reduced to 25 μM; catalase (EC 1.11.1.6) according to Aebi (16); cytochrome *c* oxidase (EC 1.9.3.1) according to Hodges and Leonard (17).

Northern Blot Hybridization—10 μg of total RNA was extracted from etiolated pumpkin cotyledons and subjected to electrophoresis on an agarose gel that contained 0.66 M formaldehyde and 10 mM MOPS (pH 7.5). RNA was transferred onto a Hybond N$^+$ membrane (Amersham, Tokyo) in 50 mM NaOH and cross-linked by exposure to UV light (Funa-UV-Linker, FS-800; Funakoshi, Tokyo). The ACOX insert was excised by digestion with *Kpn*I and labeled with [α-^{32}P]dCTP (Amersham) using a Megaprime DNA labeling kit (Amersham). The membrane was hybridized in 0.5 M sodium phosphate (pH 7.2), 1 mM EDTA, 7% SDS, and 1% bovine serum albumin with 1.0×10^6 cpm ml^{-1} of radiolabeled DNA for 18 h at 42 °C. The membrane was washed in SSC buffer/0.1% SDS for 15 min, in 0.1× SSC/0.1% SDS for 15 min, and in SSC buffer at 60 °C twice for 15 min each. X-ray film was exposed to the washed membrane, and radioactivity was measured on the imaging plate of a BioImaging analyzer (FUJIX BAS 2000; Fuji Photo Film, Tokyo) after an 18-h exposure.

Western Blot Hybridization—Pumpkin cotyledons were homogenized in extraction buffer (0.1 M Tris-HCl, pH 8.0, 1 mM EDTA, 1 mM phenylmethylsulfonyl fluoride, 0.1% SDS), the homogenate was centrifuged at 15,000 × *g* for 20 min, and the supernatant was subjected to SDS-PAGE. Then, an immunoblot analysis was performed by the method of Towbin *et al.* (18). Immunologic reactions were detected by monitoring by activity of horseradish peroxidase (ECL system; Amersham) or of alkaline phosphatase (Organon Teknika, West Chester, PA). The intensity of the signal was quantitated with a densitometer. The antiserum against thiolase was prepared as described previously (5). Protein was quantitated with a protein assay kit (Nippon Bio-Rad Laboratories, Tokyo).

RESULTS

Cloning and Characterization of a cDNA for acyl-CoA Oxidase—Initially, we isolated glyoxysomal membranes from pumpkin cotyledons from seedlings grown in the dark for 5 days. The membranes were treated with 0.1 M $NaCO_3$. The soluble proteins were separated by SDS-PAGE and blotted electrophoretically onto a polyvinylidene difluoride membrane. Polypeptides were stained with Coomassie Brilliant Blue, and a protein band of approximately 73 kDa was cut out and subjected to protein sequencing by automated Edman degradation. The amino-terminal amino acid sequence (AAGKAKAKIEVDMGSLSLYMRGKHREIQERVFEYFN) was used to design degenerate primers; a 1.6-kilobase pair DNA fragment was obtained by polymerase chain reaction using a cDNA library produced from 5-day-old etiolated pumpkin cotyledons as a template. The DNA fragment showed a high similarity with ACOX from animals. Then, the fragment was used as a probe to screen a λgt11 cDNA library from 4-day-old etiolated pumpkin cotyledons. Several positive recombinant phages were recovered, including one containing the longest insert of approximately 2.4 kilobase pairs.

The nucleotide sequence for the putative pumpkin ACOX cDNA is presented in Fig. 1. The total length is 2313 base pairs, with an open reading frame of 2073 base pairs encoding a polypeptide of 690 amino acids and with a deduced molecular mass of 77,319 Da. Amino-terminal sequencing indicated that the molecular mass of the mature protein is 72,414 Da (Fig. 1). In the figure, the presequence is double underlined. Moreover, a putative flavin mononucleotide binding motif seems to be present from amino acid 447 to 462 (dotted line in Fig. 1) (19) and a putative cAMP/cGMP-dependent protein kinase phosphorylation site at amino acids 512–515 (20). The calculated amino acid composition of the mature protein is similar to that reported for the purified cucumber acyl-CoA oxidase (10) except for a few amino acids (data not shown).

Comparison of Pumpkin ACOX with Related Proteins—The polypeptide encoded by the pumpkin ACOX cDNA shows the highest sequence identity (76%), with a putative *Phalaenopsis* ACOX. The cDNA clone of *Phalaenopsis* was isolated as one of senescence-related genes in *Phalaenopsis* petals (21) and was not characterized in detail. The identity with ACOXs from animal sources is about 30%, *e.g.* 30% with rat pristanoyl-CoA oxidase, 29% with rat trihydroxycoprostanoyl-CoA oxidase, and 28% with rat palmitoyl-CoA oxidase. This led Do and Huang (21) to postulate that the *Phalaenopsis* cDNA codes for an ACOX.

The sequences of pumpkin ACOX, *Phalaenopsis* ACOX, and rat pristanoyl-CoA oxidase (PRISCOX) are aligned for comparison in Fig. 2. PRISCOX is a peroxisomal protein that oxidizes the CoA-esters of 2-methyl-branched fatty acids, *e.g.* pristanic acid, and straight long chain acyl-CoAs (22). Pumpkin ACOX

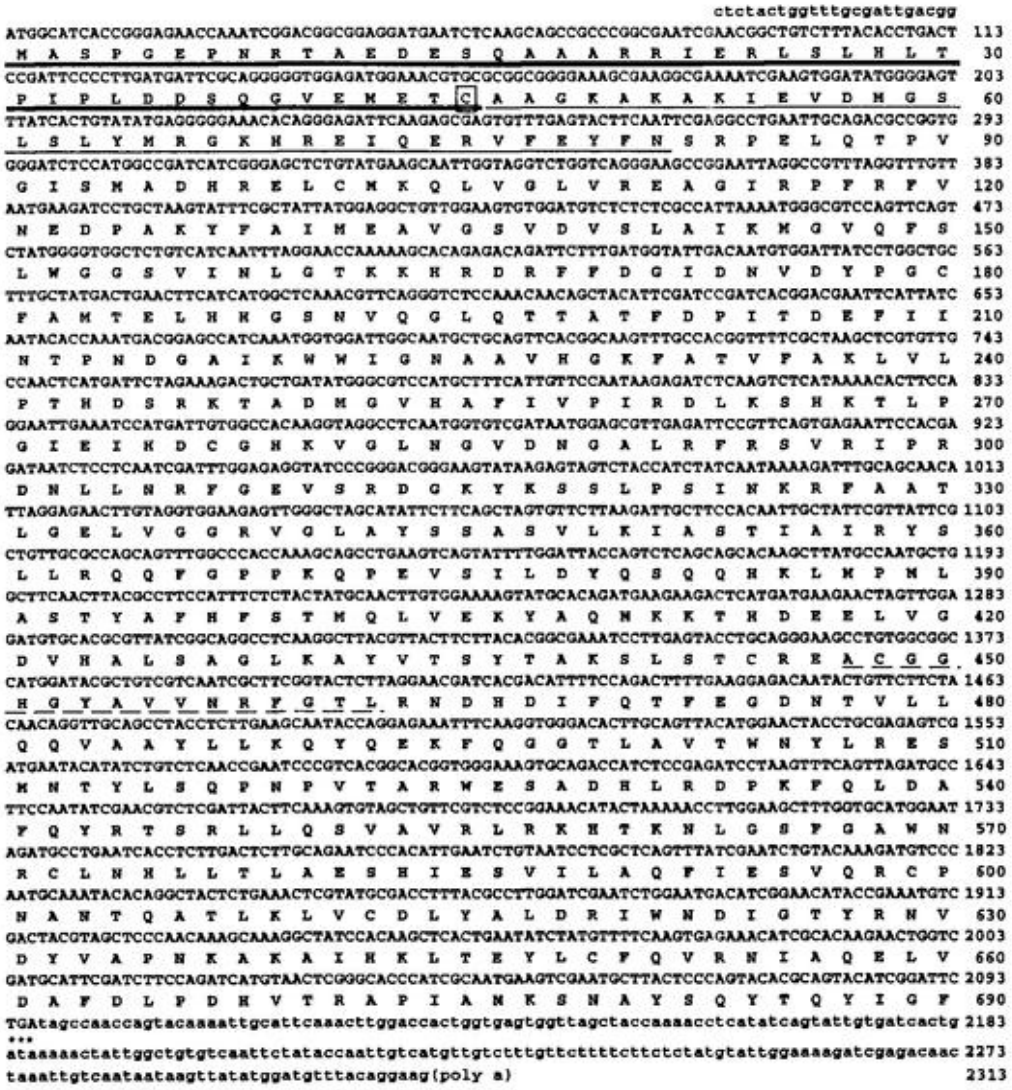

FIG. 1. **Nucleotide and deduced amino acid sequences of the pumpkin ACOX cDNA.** The amino-terminal amino acid sequence of the mature protein, as determined by Edman degradation, is *single underlined*, the putative presequence is *double underlined*, and the *dotted line* marks the putative flavin mononucleotide binding motif. The amino acid residue of the processing site is marked with an *open box*.

and *Phalaenopsis* ACOX are represented in their mature forms (putative for *Phalaenopsis* ACOX). The overall identity of the amino acid sequences looks low, but it is possible to recognize a stretch of identical amino acids from amino acids 444 to 488. This portion also shows high identity with the amino acid sequences of rat trihydroxycoprostanoyl-CoA oxidase, rat palmitoyl-CoA oxidase, and *Caenorhabditis elegans* acyl-CoA oxidase (data not shown). In addition, this region includes the putative flavin mononucleotide binding site (19) and six of the eight amino acids that represent the acyl-CoA dehydrogenase protein signature 2 (PS2: [QE]-x(2)-G-[GS]-x-G-[LIVMFY]-x(2)-[DEN]-x(4)-[KR]-x(3)-[DE]) (20). In respect to the acyl-CoA dehydrogenase protein signature 1 (PS1: [GAC]-[LIVM]-[ST]-E-x(2)-[GSAN]-G-S-D-x(2)-[GSA]) (20), it is possible to find seven of the nine amino acids in all three sequences of Fig. 2. This confirms the low homology between acyl-CoA oxidases and acyl-CoA dehydrogenases and suggests that the two protein stretches are involved in the FAD binding and/or in the binding with substrate.

Pumpkin ACOX Is Synthesized as a Larger Precursor—Some peroxisomal proteins are synthesized as larger precursors such as malate dehydrogenase (23, 24), thiolase (7, 25), and citrate synthase (9). These precursors are cleaved at a site near the amino-terminal end of the protein. An amino-terminal sequence comparison of the precursor protein with the mature protein, determined by protein sequencing following SDS-PAGE, indicates that pumpkin ACOX precursor protein is cleaved at the carboxyl side of amino acid 45 to give into the mature protein size. In recent studies, it was shown that the amino-terminal presequences of peroxisomal proteins also act as peroxisomal targeting signals (PTS2) (26, 27). Fig. 3 shows the alignment of the amino-terminal regions of pumpkin glyoxysomal ACOX, *Phalaenopsis* ACOX, and pumpkin glyoxysomal proteins that are synthesized as precursors of higher molecular mass (malate dehydrogenase (23, 24), citrate synthase (9), and thiolase (7, 25)). However, the cleavage site for the *Phalaenopsis* ACOX has not yet been confirmed. The targeting consensus sequence, R-[I/L/Q]-x5-H-L, is highly conserved. Thus, it is suggested that pumpkin ACOX and, by analogy, *Phalaenopsis* ACOX contain a PTS2-type targeting signal.

Activity of ACOX in Etiolated Pumpkin Cotyledons—To confirm that the ACOX cDNA actually codes for an ACOX, a crude extract from 5-day-old etiolated pumpkin cotyledons was subjected to hydrophobic interaction chromatography on a phenyl-Sepharose column (Fig. 4). Three peaks of ACOX activity were

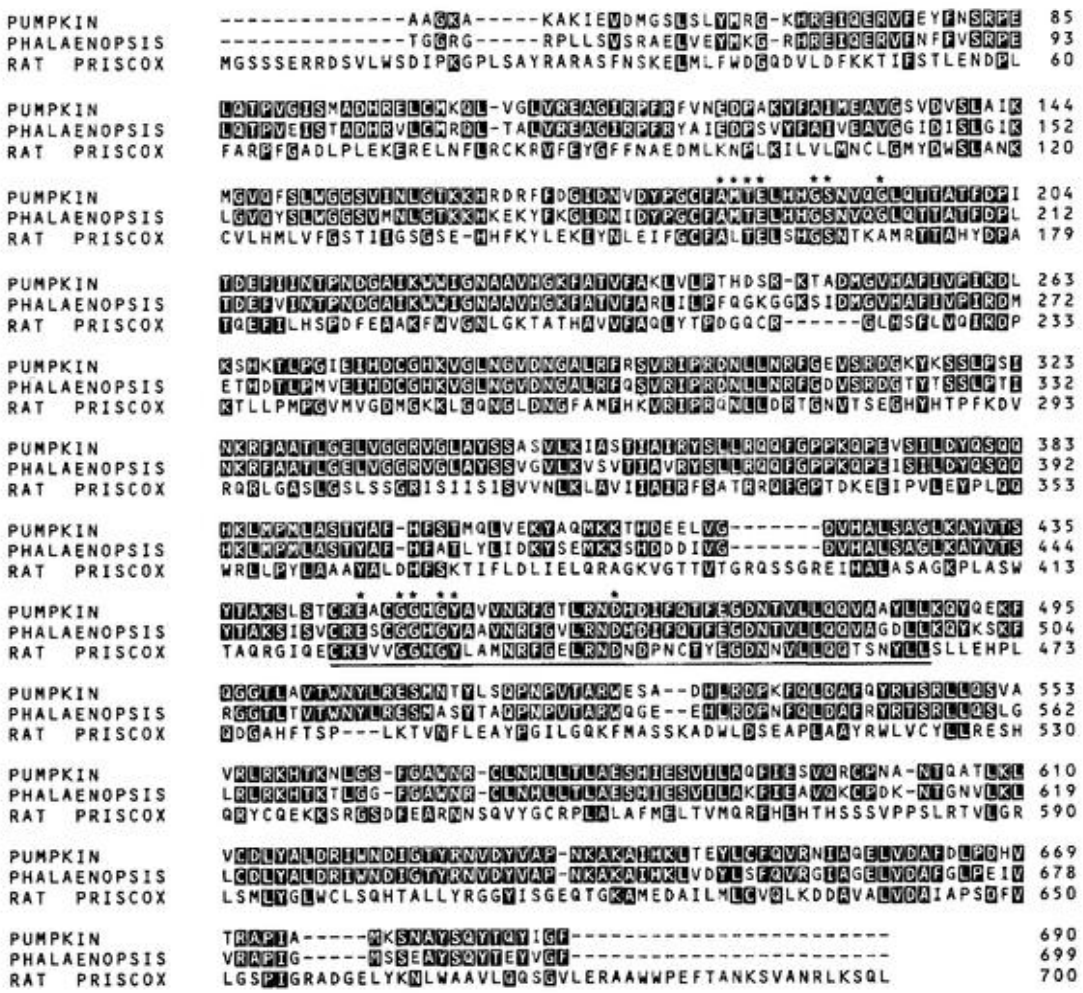

FIG. 2. **Alignment of amino acid sequences of pumpkin ACOX (pumpkin), *Phalaenopsis* ACOX (*Phalaenopsis*), and rat pristanoyl-CoA oxidase (rat PRISCOX).** The region of high homology is *underlined*, and *asterisks* mark amino acids common to the two protein signatures of acyl-CoA dehydrogenase (protein signature 1 and protein signature 2, respectively).

FIG. 3. **Alignment of the amino-terminal presequence of pumpkin ACOX with other presequences of microbody proteins that are synthesized as larger precursors.** pumACOX, pumpkin ACOX; phaACOX, *Phalaenopsis* ACOX (21); pumMDH, pumpkin glyoxysomal malate dehydrogenase (24); pumCS, pumpkin glyoxysomal citrate synthase (9); pumTHI, pumpkin glyoxysomal 3-keto-acyl-CoA thiolase (7). Conserved amino acids are shown in *bold*. Processing sites of presequences, determined by sequencing of the amino-terminal amino acids of mature proteins, are shown by *arrowheads*.

detected. The first peak (*circles*) was obtained using hexanoyl-CoA (C6) as a substrate and thus indicates the presence of a short chain ACOX. Two overlapping peaks were obtained with palmitoyl-CoA (C16) (*squares*) and decanoyl-CoA (C10) (*triangles*) as substrates and thus indicate a long/medium chain ACOX. Western blotting with polyclonal antiserum raised against the pumpkin ACOX expressed in *E. coli* (Fig. 4*B*) shows clearly that the antiserum recognizes a protein of approximately 73 kDa only in fractions showing long/medium chain ACOX activity. Because it was reported that plant long chain ACOX has a subunit molecular mass of approximately 72 kDa (10), and the medium chain ACOX has a subunit molecular mass of 62 kDa (11), we conclude that the isolated pumpkin cDNA encodes for a long chain ACOX.

Subcellular Localization of ACOX in Etiolated Pumpkin Cotyledons—To investigate the subcellular localization of the ACOX protein, enzyme activity and immunoblotting analyses were performed after fractionation by sucrose density gradient centrifugation of a pumpkin organelle homogenate (Fig. 5). Catalase and thiolase were used as glyoxysomal markers, and cytochrome *c* oxidase was used as a mitochondrial marker. ACOX activities were present in the supernatant and the glyoxysomal fractions. A small peak of activity was also detected in the mitochondrial fractions (namely fraction 11) but did not overlap with the activity of cytochrome *c* oxidase. As a small catalase activity was present in the fraction, these activities might be due to the contamination of glyoxysomes. The immunoblotting analysis confirmed that a protein of 73 kDa, corresponding to ACOX, is mainly present in the supernatant and in the glyoxysomal fractions (Fig. 5*B*). Interestingly, a similar pattern was also obtained for thiolase, another β-oxidation enzyme.

Time Course of mRNA and Protein Levels during Germination in Pumpkin Cotyledons—During greening of pumpkin cotyledons, the composition of matrix enzymes in microbodies changes dramatically, glyoxysomal enzymes decrease, and leaf peroxisomal enzymes are synthesized. Like thiolase, ACOX is a

part of the fatty acid β-oxidation spiral. Therefore, we followed the changes in the level of ACOX and thiolase mRNA and protein during the postgerminative growth of seedlings (Figs. 6 and 7). The relative levels of ACOX mRNA in dark-grown seedlings during the 9-day period after germination are indicated by Northern blot in Fig. 6*A* (*top panel*) and are quantified by densitometry (*bottom panel*). ACOX mRNA levels reached a maximum after 3 days and thereafter gradually disappeared. When some of the seedlings were transferred to light after 5 days (*middle panel*), the pattern did not change. Similar results were obtained for thiolase mRNA (Fig. 6*B*). Notably, the total amount of ACOX mRNA was much lower than that of thiolase mRNA. The ACOX protein levels are shown in Fig. 7*A*, in which the three panels correspond to the three mRNA panels in Fig. 6*A*. The curve for the dark-grown seedlings (*closed circles*, *bottom panel*) shows that the peak in the ACOX protein was delayed with respect to the mRNA peak, reaching a maximum level at day 5 after germination and subsequently decreasing. Similar results were obtained for thiolase (Fig. 7). Moreover, following illumination (*open circles*, *bottom panels*), ACOX disappeared more rapidly than thiolase. In general, however, the two patterns seem to be very similar.

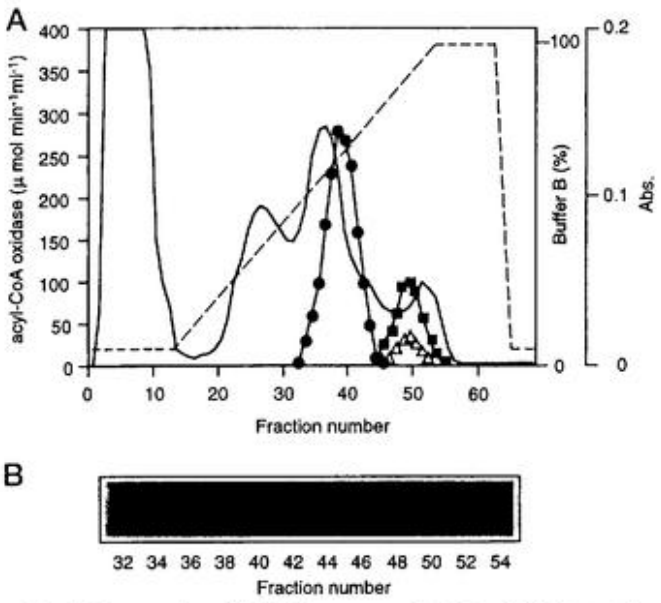

FIG. 4. *A*, separation of ACOX isoenzymes by hydrophobic interaction chromatography. A crude extract from 5-day-old dark-grown pumpkin cotyledons was loaded onto a phenyl-Sepharose high performance HiTrap column (1 ml), and proteins were eluted by increasing the concentration of buffer B (50 mM sodium phosphate, pH 7.0, containing 60% ethylene glycol) from 0 to 100%. Protein (*solid line*, A_{280}) and ACOX activities with different substrates (hexanoyl-CoA, ●; decanoyl-CoA, △; palmitoyl-CoA, ■) were determined. The *dashed line* represents the concentration (%) of buffer B. *B*, immunodetection of ACOX in fractions from the hydrophobic interaction chromatography. 25 μl of the fractions indicated were subjected to SDS-PAGE (10% acrylamide) and immunoblotted.

DISCUSSION

In the present study, we report the cDNA sequence of a pumpkin glyoxysomal long chain ACOX in addition to the cDNA sequence of a previously reported *Phalaenopsis* ACOX (21).

The present results clearly show that the protein encoded by this gene is a plant long chain ACOX. The deduced amino acid sequences of pumpkin and *Phalaenopsis* cDNA sequences have an identity of 76%, indicating that the *Phalaenopsis* cDNA also codes for a long chain ACOX. Comparing other ACOXs, the best identity (30%) is obtained for the rat pristanoyl-CoA oxidase, which acts on 2-methyl-branched CoA-esters and straight long chain acyl-CoAs (22). Mammalian peroxisomes contain three ACOX isozymes that are not capable of oxidizing acyl-chain CoA esters of less than 8 carbons. In mammalian cells, the β-oxidation of short chain fatty acids is accomplished in mitochondria, in which acyl-CoA dehydrogenases act instead of ACOXs. Three peroxisomal mammalian ACOXs have been identified: PRISCOX (30% identity), palmitoyl-CoA oxidase

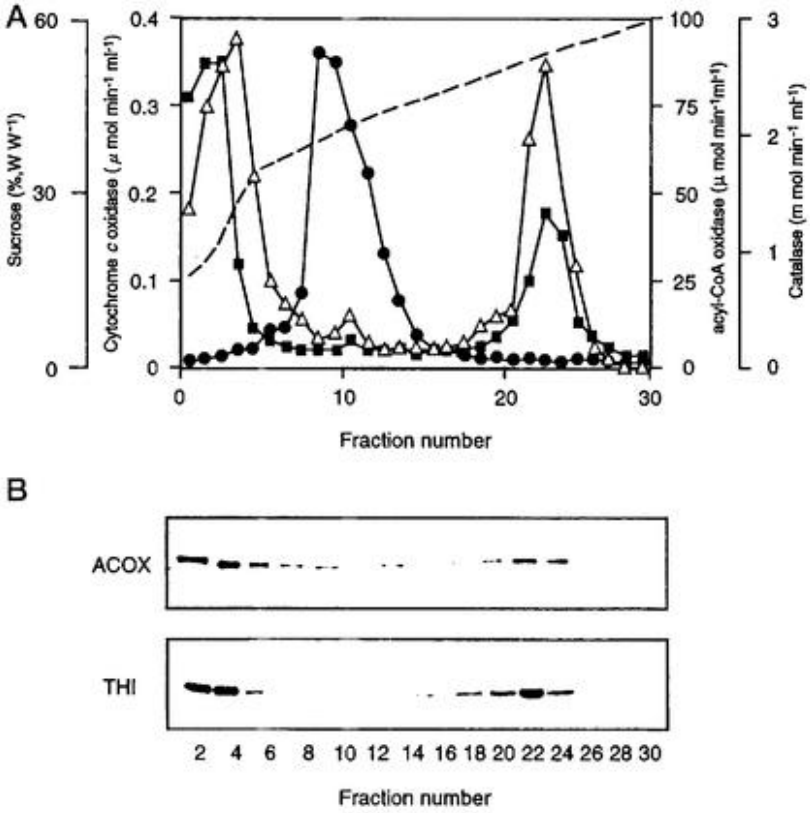

FIG. 5. **Subcellular localization of ACOX in etiolated pumpkin cotyledons.** An extract from 5-day-old etiolated cotyledons was fractionated by sucrose density gradient centrifugation. *A*, enzyme activities (cytochrome *c* oxidase, ●; catalase, ■, and ACOX, △). *Dashed line*, sucrose concentration (w/w). *B*, immunological detection of pumpkin ACOX. 5 μl from each odd-numbered fraction was subjected to SDS-PAGE (10% acrylamide) and immunoblotted.

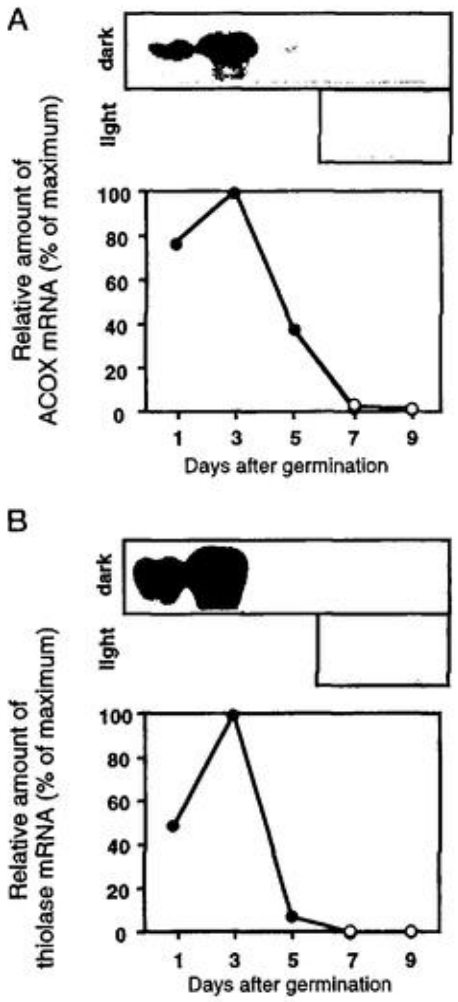

FIG. 6. **Developmental changes in the level of mRNAs for pumpkin ACOX (*A*) and thiolase (*B*).** *Top panels*, Northern blots of total RNA from one cotyledon of dark-grown seedlings. RNA was blotted on a nylon membrane, and then the membrane was allowed to hybridize with specific probes. *Middle panels*, Northern blots of RNA of seedlings after being transferred to continuous illumination 5 days after the onset of germination. *Bottom panels*, quantification of spot intensites of dark-grown (●) and light-grown (○) seedlings.

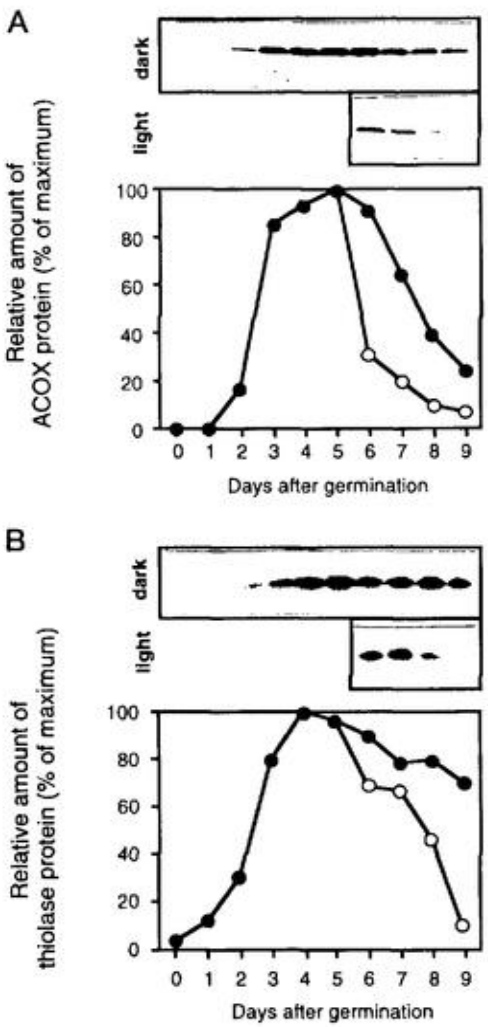

FIG. 7. **Developmental changes in the level of proteins for pumpkin ACOX (*A*) and thiolase (*B*).** *Top panels*, Western blots of 0.05% of total homogenate from 10 cotyledons of dark-grown seedlings. Total homogenate was blotted on a nylon membrane, and then the membrane was allowed to hybridize with specific probes. *Middle panels*, Western blots of total homogenate of seedlings after being transferred to continuous illumination 5 days after the onset of germination. *Bottom panels*, quantification of spot intensites of dark-grown (●) and light-grown (○) seedlings.

(28% identity), which reacts with CoA esters of very long, long, and medium chain fatty acids (28), and trihydroxycoprostanoyl-CoA oxidase (29% identity), which oxidizes the CoA esters of the bile acid intermediates dihydroxycoprostanic acid and trihydroxycoprostanic acid (29). On the contrary, plant peroxisomes seem to contain ACOXs that are active on short, medium, and long chain acyl-CoAs (11) and are able to perform a complete β-oxidation of fatty acids to acetyl-CoA (2). Three plant ACOX isozymes have previously been purified and characterized. One is from cucumber cotyledons that is active on long and medium chain acyl-CoAs and that is a homodimer with subunits of 72 kDa (10). The other two are from maize and are active on medium and short chain acyl-CoAs, respectively (11). The former is a monomeric enzyme of 62 kDa, and the latter is a homotetrameric enzyme of 15 kDa. Three different genes seem to code for the three ACOX isoforms, as they have different subunit molecular weights (11). The report by Hooks *et al.* (11) was the first to imply the presence of a short chain ACOX in eukaryotic cells. Mammalian ACOX isoforms, nevertheless, show slightly different substrate preferences and seem to have very similar subunit molecular weights of about 75 kDa. Therefore, only the plant long chain ACOX should share common ancestral genes with the mammalian ACOXs.

In the present study, we were able to correlate the sequence of the isolated ACOX clone with a long chain specific ACOX by applying an antiserum against the expressed ACOX/histidine-tagged fusion protein. This antiserum recognized only long chain and medium chain ACOX activity and not short chain ACOX activity when pumpkin enzymes were separated by hydrophobic interaction chromatography (Fig. 4). The immunoreactive band corresponded to a molecular mass of 73 kDa in accordance with the calculated molecular mass of mature pumpkin long chain ACOX (72,414 Da) and with the previous report of 72 kDa for the cucumber long chain ACOX (10).

The levels of ACOX mRNA do not seem to be greatly controlled by light. The ACOX protein that built up during the initial 5 days of germination disappeared during the transition from glyoxysomes to leaf peroxisomes upon exposure of the seedlings to light. Similar patterns have previously been observed for malate synthase (8) and citrate synthase (9). The appearance and disappearance of the mRNAs preceded the change in the ACOX protein during the microbody transition. Thus, the ACOX levels seem to be determined at both the

translational and posttranslational levels.

It is worth noting that pumpkin glyoxysomal long chain ACOX proteins are synthesized as larger precursors containing a cleavable amino-terminal presequence, namely PTS2 (27, 30), as in the case for some other plant peroxisomal proteins, such as malate dehydrogenase (23, 24), citrate synthase (9), and thiolase (7, 25). In all cloned mammalian ACOXs, a carboxyl-terminal signal (PTS1) is present, but there is no PTS2 signal (31). This indicates that the plant ACOX import mechanism differs from the mammalian one. It has been suggested that ACOX is a key enzyme of β-oxidation because it can control and regulate the flux of acyl-CoAs at the first step of the β-oxidation spiral (32). Particularly, the long chain acyl-CoA oxidase may represent a regulatory point considering the fact that most fatty acids of plant storage lipids are long chain molecules. In conclusion, this type of control mechanism could tightly regulate the long chain ACOX (as the first step of the β-oxidation cascade), or it could be involved in a coordinate or differential regulation of the expression of the three ACOX enzymes in plant tissues (11). To verify such a hypothesis, the cloning and an expression analysis of the two other ACOXs will be necessary.

Acknowledgments—We thank Prof. Dr. Claus Schnarrenberger (Free University of Berlin) for stimulating discussions and helpful comments on the manuscript.

REFERENCES

1. Beevers, H. (1979) *Annu. Rev. Plant Physiol.* **30,** 159–193
2. Huang, A. H. C., Trelease R. N., and Moore T. S. (1983) *Plant Peroxisome,* Academic Press, New York
3. Titus, D. E., and Becker, W. M. (1985) *J. Cell Biol.* **101,** 1288–1299
4. Nishimura, M., Yamaguchi, J., Mori, H., Akazawa, T., and Yokota, S. (1986) *Plant Physiol.* **81,** 313–316
5. Mori, H., Takeda-Yoshikawa, Y., Hara-Nishimura, I., and Nishimura, M. (1991) *Eur. J. Biochem.* **197,** 331–336
6. Tsugeki, R., Hara-Nishimura, I., Mori, H., and Nishimura, M. (1993) *Plant Cell Physiol.* **34,** 51–57
7. Kato, A., Hayashi, M., Takeuchi, Y., and Nishimura, M. (1996) *Plant Mol. Biol.* **22,** 843–852
8. Mori, H., and Nishimura, M. (1989) *FEBS Lett.* **244,** 163–166
9. Kato, A., Hayashi, M., Mori, H., and Nishimura, M. (1995) *Plant Mol. Biol.* **27,** 377–390
10. Kirsch, T., Löffler, H.-G., and Kindl, H. (1986) *J. Biol. Chem.* **261,** 8570–8575
11. Hooks, M. A., Bode, K., and Couée, I. (1996) *Biochem. J.* **320,** 607–614
12. Matsudaira, P. (1987) *J. Biol. Chem.* **262,** 10035–10038
13. Sanger, F., Nicklen, S., and Coulson, A. R. (1977) *Proc. Natl. Acad. Sci. U. S. A.* **74,** 5463–5467
14. Thompson, J. D., Higgins, D. G., and Gibson, T. J. (1994) *Nucleic Acids Res.* **8,** 4321–4325
15. Gerhardt, B. (1987) *Methods Enzymol.* **148,** 516–525
16. Aebi, H. (1974) in *Methods of Enzymatic Analysis* (Bergmeyer H. U., ed) Vol. 2, pp. 673–684, Academic Press, New York
17. Hodges, T. K., and Leonard, R. T. (1974) *Methods Enzymol.* **32,** 392–406
18. Towbin, H., Staehelin, T., and Gordon, J. (1979) *Proc. Natl. Acad. Sci. U. S. A.* **76,** 4350–4354
19. Debourdieu, M., and Fox, J. L. (1977) *J. Biol. Chem.* **252,** 1453–1463
20. Bairoch, A., Bucher, P., and Hofmann, K. (1995) *Nucleic Acids Res.* **24,** 189–196
21. Do, Y. Y., and Huang, P. L. (1997) *Arch. Biochem. Biophys.* **344,** 295–300
22. Van Veldhoven, P. P., Van Rompuy, J. C. T., Fransen, M., De Béthune, B., and Mannaerts, G. P. (1994) *Eur. J. Biochem.* **222,** 795–801
23. Gietl, C. (1990) *Proc. Natl. Acad. Sci. U. S. A.* **87,** 5773–5777
24. Kato, A., Takeda-Yoshikawa, Y., Hayashi, M., Kondo, M., Hara-Nishimura, I., and Nishimura, M. (1998) *Plant Cell Physiol.* **39,** 186–195
25. Preisig-Muller, R., and Kindle, H. (1993) *Plant Mol. Biol.* **22,** 59–66
26. Subramani, S. (1993) *Annu. Rev. Cell Biol.* **9,** 445–478
27. Kato, A., Hayashi, M., Kondo, M., and Nishimura, M. (1996) *Plant Cell* **8,** 1601–1611
28. Osumi, T., and Hashimoto, T. (1978) *Biochem. Biophys. Res. Commun.* **83,** 479–485
29. Van Veldhoven, P. P., Vanhove, G., Asselberghs, S., Eyssen, H. J., and Mannaerts, G. P. (1992) *J. Biol. Chem.* **267,** 20065–20074
30. Subramani, S. (1996) *J. Biol. Chem.* **271,** 32483–32486
31. Gould, S. J., Keller, G.-A. A., and Subramani, S. (1987) *J. Cell Biol.* **105,** 2923–2931
32. Kindl, H. (1987) in *The Biochemistry of Plants* (Stumpf, P. K., and Conn, E. E., eds) Vol. 9, pp. 31–52, Academic Press, New York

THE JOURNAL OF BIOLOGICAL CHEMISTRY
Vol. 274, No. 18, Issue of April 30, pp. 12715–12721, 1999
Printed in U.S.A.

A Novel Acyl-CoA Oxidase That Can Oxidize Short-chain Acyl-CoA in Plant Peroxisomes*

(Received for publication, December 30, 1998)

Hiroshi Hayashi‡§, Luigi De Bellis‡¶, Adriana Ciurli¶, Maki Kondo‡, Makoto Hayashi‡§, and Mikio Nishimura‡§‖

From the ‡Department of Cell Biology, National Institute for Basic Biology and the §Department of Molecular Biomechanics, Graduate University for Advanced Studies, Okazaki 444-8585, Japan and the ¶Dipartimento di Biologia delle Piante Agrarie, via Mariscoglio 34, 56124 Pisa, Italy

Short-chain acyl-CoA oxidases are β-oxidation enzymes that are active on short-chain acyl-CoAs and that appear to be present in higher plant peroxisomes and absent in mammalian peroxisomes. Therefore, plant peroxisomes are capable of performing complete β-oxidation of acyl-CoA chains, whereas mammalian peroxisomes can perform β-oxidation of only those acyl-CoA chains that are larger than octanoyl-CoA (C_8). In this report, we have shown that a novel acyl-CoA oxidase can oxidize short-chain acyl-CoA in plant peroxisomes. A peroxisomal short-chain acyl-CoA oxidase from *Arabidopsis* was purified following the expression of the *Arabidopsis* cDNA in a baculovirus expression system. The purified enzyme was active on butyryl-CoA (C_4), hexanoyl-CoA (C_6), and octanoyl-CoA (C_8). Cell fractionation and immunocytochemical analysis revealed that the short-chain acyl-CoA oxidase is localized in peroxisomes. The expression pattern of the short-chain acyl-CoA oxidase was similar to that of peroxisomal 3-ketoacyl-CoA thiolase, a marker enzyme of fatty acid β-oxidation, during post-germinative growth. Although the molecular structure and amino acid sequence of the enzyme are similar to those of mammalian mitochondrial acyl-CoA dehydrogenase, the purified enzyme has no activity as acyl-CoA dehydrogenase. These results indicate that the short-chain acyl-CoA oxidases function in fatty acid β-oxidation in plant peroxisomes, and that by the cooperative action of long- and short-chain acyl-CoA oxidases, plant peroxisomes are capable of performing the complete β-oxidation of acyl-CoA.

Oilseed plants convert reserve oil to sucrose after germination. This unique type of gluconeogenesis occurs in the storage tissues of oilseeds, such as endosperms or cotyledons (1). The metabolic pathway involves many enzymes in several subcellular compartments, including lipid bodies, glyoxysomes (a specialized peroxisome), mitochondria, and the cytosol. Within the entire gluconeogenic pathway, the conversion of a fatty acid to succinate takes place within the glyoxysomes, which contain enzymes for fatty acid β-oxidation and the glyoxylate cycle.

* This work was supported by Research for the Future Program Grant JSPS-RFTF 96L00407 from the Japan Society for the Promotion of Science; by Grants-in-aid for Scientific Research 09440271, 09274101, and 09274103 from the Ministry of Education, Science, and Culture of Japan; by a grant from the Nissan Science Foundation (Tokyo, Japan); and by the National Institute for Basic Biology Program for Molecular Mechanisms of Stress Response. The costs of publication of this article were defrayed in part by the payment of page charges. This article must therefore be hereby marked "*advertisement*" in accordance with 18 U.S.C. Section 1734 solely to indicate this fact.

‖ To whom correspondence should be addressed. Tel.: 81-564-55-7500; Fax: 81-564-55-7505; E-mail: mikosome@nibb.ac.jp.

Glyoxysomes and leaf peroxisomes are members of a group of organelles called peroxisomes (2). In glyoxysomes, fatty acids are first activated to fatty acyl-CoA by fatty acyl-CoA synthetase (3). Fatty acyl-CoA is the substrate for fatty acid β-oxidation, which consists of four enzymatic reactions (4). The first reaction is catalyzed by acyl-CoA oxidase. The second and third enzymatic reactions are catalyzed by a single enzyme that possesses enoyl-CoA hydratase and β-hydroxyacyl-CoA dehydrogenase activities (5). The fourth reaction is catalyzed by 3-ketoacyl-CoA thiolase (referred to as thiolase below) (6). Acetyl-CoA, an end product of fatty acid β-oxidation, is metabolized further to produce succinate by the glyoxylate cycle.

In mammalian cells, both peroxisomes and mitochondria contain a functional fatty acid β-oxidation system. In peroxisomes, the first enzyme of fatty acid β-oxidation, acyl-CoA oxidase, donates electrons to molecular oxygen, producing hydrogen peroxide (7). Mammalian peroxisomes oxidize long-chain fatty acids, but are inactive with fatty acids shorter than octanoic acid (C_8). This is mainly the consequence of the exclusive presence of long-chain acyl-CoA oxidases and the absence of acyl-CoA oxidases that are active on short-chain acyl-CoAs. In contrast, mammalian mitochondria are capable of complete oxidization of fatty acids to acetyl-CoA (8); the first step of fatty acid β-oxidation is accomplished by long-, medium-, and short-chain acyl-CoA dehydrogenases, and electrons generated by the dehydrogenases are transferred to the mitochondrial respiratory chain. By analogy, Thomas and co-workers (9–11) have postulated the existence of plant mitochondrial β-oxidation, but the presence of acyl-CoA dehydrogenase was not investigated or not detected (12). In contrast, data reported by Gerhardt and co-workers (13–15) have suggested that glyoxysomes in plants can completely metabolize fatty acids to acetyl-CoA.

We have previously reported the existence of an acyl-CoA oxidase that is active on long-chain acyl-CoA in glyoxysomes (16). In the present study, we report evidence that glyoxysomes contain another acyl-CoA oxidase that can metabolize short-chain acyl-CoA. We also discuss the unique features of fatty acid β-oxidation accomplished by these acyl-CoA oxidases in plant cells.

EXPERIMENTAL PROCEDURES

Plant Materials—Pumpkin seeds (*Cucurbita* sp. Kurokawa Amakuri) were purchased from Aisan Seed Co. (Aichi, Japan). Pumpkin seeds were soaked in running tap water overnight and germinated in Rock-Fiber soil (66R, Nitto Boseki, Chiba, Japan) at 25 °C in darkness. *Arabidopsis thaliana* ecotype Landsberg *erecta* seeds were surface-sterilized in 2% NaClO and 0.02% Triton X-100 and grown on growth medium (2.3 mg/ml Murashige-Skoog salts (Wako, Osaka, Japan), 1% sucrose, 100 μg/ml myoinositol, 1 μg/ml thiamine HCl, 0.5 μg/ml pyri-

doxine, 0.5 μg/ml nicotinic acid, 0.5 mg/ml Mes[1]-KOH, pH 5.7, and 0.2% Gellan gum (Wako)) in Petri dishes. *Arabidopsis* seeds were soaked in growth medium and germinated at 22 °C under continuous illumination or under darkness, and some of *Arabidopsis* seedlings were transferred to light after 4 days of growing in the dark. Some seedlings that were grown under continuous illumination for 2 weeks on growth medium were transferred to a 1:1 mixture of perlite and vermiculite. Plants were grown under continuous illumination at 22 °C.

Plasmids—The cDNA clone (GenBank™ accession number T46525) was obtained from the *Arabidopsis* Biological Resource Center (Ohio State University, Columbus, OH). DNA sequencing was performed by the method of Sanger *et al.* (17). DNA sequences were analyzed with GeneWorks Release 2.5 computer software (IntelliGenetics, Mountain View, CA). The BLAST server was utilized for the analysis of homologies among proteins. Alignment of several acyl-CoA oxidases and acyl-CoA dehydrogenases was performed using CLUSTAL W software (18).

Preparation of a Specific Antiserum—The *Arabidopsis* cDNA was inserted into pET32b vector (Novagen, Madison, WI). A fusion protein between short-chain acyl-CoA oxidase and a histidine tag was synthesized in *Escherichia coli* cells and purified by column chromatography on Ni^{2+} resin. The purified protein (~0.5 mg of protein) in 1 ml of sterilized water was emulsified with an equal volume of Freund's complete adjuvant (Difco). The emulsion was injected subcutaneously into the back of a rabbit. Four weeks later, a booster injection (~0.25 mg of protein) was given similarly to the first injection. Blood was taken from a vein in the ear 7 days after the second booster injection. The serum was used for immunoblotting.

Expression of Recombinant Short-chain Acyl-CoA Oxidase from Insect Cells—Short-chain acyl-CoA oxidase was produced employing the baculovirus expression system from Invitrogen (San Diego, CA) following the manufacturer's protocols. The system includes *Spodoptera frugiperda* (Sf9) as the insect cell line, pBlueBac 4.5 (19) as a transfer vector, and engineered baculoviral *Autographa californica* multiple polyhedrosis virus (Bac-N-Blue DNA) as an expression vector. In brief, the short-chain acyl-CoA oxidase cDNA was inserted into the pBlueBac 4.5 transfer vector and cotransfected together with linearized baculoviral Bac-N-Blue DNA in insect cells. Recombinant viruses were purified from the transfection supernatant by plaque assay on medium containing 5-bromo-4-chloro-3-indolyl β-D-galactopyranoside, and recombinant plaques were verified by polymerase chain reaction. Afterward, a high-titer recombinant viral stock was generated, and following a time course of expression experiment, the optimal expression time was determined. The recombinant protein expression levels were optimized, and a large-scale expression of recombinant protein was performed.

Purification of Recombinant Short-chain Acyl-CoA Oxidase from Insect Cells—Log-phase growing Sf9 cells in 20 75-cm^2 flasks were infected with recombinant viral stock at a multiplicity of infection of 10. Four days after infection, the cells were dislodged from the flask walls and centrifuged at 500 × *g* for 5 min at 4 °C. The cell pellets were washed with phosphate-buffered saline, gently suspended in buffer A (50 mM sodium phosphate, pH 6.7, 10 mM NaCl, 100 μg/mg phenylmethylsulfonyl fluoride, 10 μM FAD, and 10% glycerol), and lysed by three bursts of sonication (3 × 1 min at 30-min intervals on ice). After centrifugation of the sample at 15,000 × *g* for 30 min, the supernatant was dialyzed against buffer A and loaded on a HiTrap SP column (Amersham Pharmacia Biotech, Tokyo, Japan). Proteins were eluted with a gradient of 10–500 mM NaCl in buffer A, and fractions of 0.5 ml were collected. Fractions with high short-chain acyl-CoA oxidase activities were pooled and concentrated using Centricon 30 concentrators (Amicon Inc., Beverly, MA) and then loaded on a Superose 12 HR 10/30 column (Amersham Pharmacia Biotech) equilibrated with buffer B (10 mM sodium phosphate, pH 7.2, 250 mM NaCl, 10 μM FAD, and 10% glycerol). Proteins were eluted with buffer B, and fractions of 0.5 ml were collected and analyzed for the presence of acyl-CoA oxidase activity.

Subcellular Fractionation—Four-day-old pumpkin etiolated cotyledons (15 g, fresh weight) were homogenized in a Petri dish by chopping with a razor blade for 5 min in 10 ml of a medium that contained 150 mM Tricine-KOH, pH 7.5, 1 mM EDTA, and 0.5 M sucrose. The homogenate was passed through four layers of cheesecloth. Three ml of the filtrate was layered onto a sucrose gradient that consisted of a 1-ml cushion of 60% (w/w) sucrose and 11 ml of a linear sucrose gradient from 60 to 30% without buffer. The gradient was centrifuged at 21,000 rpm for 3 h in a Beckman SW 28.1 rotor in a Beckman Model XL-90 ultracentrifuge. After centrifugation, fractions of 0.5 ml were collected with a gradient fractionator (Model 185, Isco Inc., Lincoln, NE). All procedures were carried out at 4 °C. Subcellular fractionation of *Arabidopsis* etiolated cotyledons was performed as follows. One-hundred mg of seeds (~5000 seeds) was grown on growth medium for 5 days in darkness at 22 °C. Etiolated cotyledons were harvested and chopped with a razor blade in a Petri dish with 2 ml of chopping buffer (150 mM Tricine-KOH, pH 7.5, 1 mM EDTA, 0.5 M sucrose, and 1% bovine serum albumin). The extract was then filtered with a cell strainer (Becton Dickinson Labware, Franklin Lakes, NJ). Two ml of the homogenate was layered directly on top of a 16-ml linear sucrose density gradient (30–60%, w/w) that contained 1 mM EDTA. Centrifugation was performed in the SW 28.1 rotor at 25,000 rpm for 2.5 h at 4 °C. Fractions of 0.5 ml were collected with the gradient fractionator.

Immunoelectron Microscopy—*Arabidopsis* etiolated cotyledons were harvested after 3 days in darkness. The samples were fixed, dehydrated, and embedded in LR white resin (London Resin, Basingstoke, United Kingdom) as described previously (20, 21). Ultrathin sections were cut on a Reichert ultramicrotome (Leica, Heidelberg, Germany) with a diamond knife and mounted on uncoated nickel grids. The protein A-gold labeling procedure was essentially the same as that described (20, 21). Ultrathin sections were incubated at 4 °C overnight with a solution of catalase antiserum (diluted 1:1000) and then with a 30-fold diluted suspension of protein A-gold (10 nm for catalase; Amersham Pharmacia Biotech) at room temperature for 30 min. A solution of short-chain acyl-CoA oxidase antiserum (diluted 1:1000) was added to a 200-fold diluted biotinylated species-specific whole antibody and incubated at room temperature for 1 h and then with a 20-fold diluted suspension of streptavidin-gold (15 nm for short-chain acyl-CoA oxidase; Amersham Pharmacia Biotech) at room temperature for 30 min. The sections were examined with a transmission electron microscope (1200EX, Joel, Tokyo) at 80 kV.

Enzyme Assay and Isoelectric Focusing—Enzyme activities were measured at 25 °C in 1 ml of reaction mixture and monitored with a Beckman DU-7500 spectrophotometer. Acyl-CoA oxidase (EC 1.3.3.6) was assayed according to the method of Gerhardt (22), with the concentration of acyl-CoA substrates reduced to 25 μM. Acyl-CoA dehydrogenase (EC 1.3.99.3) was assayed according to Dommes and Kunau (23) and Furuta *et al.* (24). Catalase (EC 1.11.1.6) was assayed according to Aebi (25). Cytochrome *c* oxidase (EC 1.9.3.1) was assayed according to Hodges and Leonard (26). Isoelectric focusing was performed at 15 °C using a Multiphor II electrophoresis system and Immobiline Dry Strip gels (Amersham Pharmacia Biotech) according to the manufacturer's instructions.

Western Blot Hybridization—*Arabidopsis* and pumpkin cotyledons were homogenized in extraction buffer (0.1 M Tris-HCl, pH 8.0, 1 mM EDTA, 1 mM phenylmethylsulfonyl fluoride, and 0.1% SDS); the homogenate was centrifuged at 15,000 × *g* for 20 min; and the supernatant was subjected to SDS-polyacrylamide gel electrophoresis. Immunoblot analysis was then performed essentially following the method of Towbin *et al.* (27). Immunologic reactions were detected by monitoring horseradish peroxidase activity (ECL system, Amersham Pharmacia Biotech). Thiolase (28), castor bean isocitrate lyase (29), and pumpkin catalase (30) antisera were prepared as described previously. Protein was quantitated with a protein assay kit (Nippon Bio-Rad Laboratories, Tokyo).

RESULTS

Identification of a Short-chain Acyl-CoA Oxidase cDNA—As result of a similarity search with a long-chain acyl-CoA oxidase (16) in a DNA data base, we found a putative *Arabidopsis* acyl-CoA dehydrogenase cDNA[2] and the availability of another homologous cDNA clone (EBI/GenBank™ accession number T46525, AB017643) in the *Arabidopsis* Expressed Sequence Tag data base. We received the latter from the *Arabidopsis* Biological Resource Center and fully sequenced it. The expressed sequence tag clone contained an insert of 1.6 kilobases. The open reading frame encodes a polypeptide of 436 amino acids, which corresponds to a molecular mass of ~47 kDa (Fig. 1). Because mammalian acyl-CoA dehydrogenase is a mito-

[1] The abbreviations used are: Mes, 4-morpholineethanesulfonic acid; Tricine, *N*-[2-hydroxy-1,1-bis(hydroxymethyl)ethyl]glycine; PTS, peroxisomal targeting signal; PS, protein signature.

[2] Grellet, F., Gaubier, P., Wu, H.-J., Laudie, M., Berger, C., and Delseny, M. (1996) EBI/GenBank™ accession number U72505.

```
MAVLSSADRASNEKKVKSSYFDLPPMEMSV   30
AFPQATPASTFPPCTSDYYHFNDLLTPEEQ   60
AIRKKVRECMEKEVAPIMTEYWEKAEFPFH   90
ITPKLGAMGVAGGSIKGYGCPGLSITANAI  120
ATAEIARVDASCSTFILVHSSLGMLTIALC  150
GSEAQKEKYLPSLAQLNTVACWALTEPDNG  180
SDASGLGTTATKVEGGWKINGQKRWIGNST  210
FADLLIIFARNTTTNQINGFIVKKDAPGLK  240
ATKIPNKIGLRMVQNGDILLQNVFVPDEDR  270
LPGVNSFQDTSKVLAVSRVMVAWQPIGISM  300
GIYDMCHRYLKERKQFGAPLAAFQLNQQKL  330
VQMLGNVQAMFLMGWRLCKLYETGQMTPGQ  360
ASLGKAWISSKARETASLGRELLGGNGILA  390
DFLVAKAFCDLEPIYTYEGTYDINTLVTGR  420
EVTGIASFKPATRSRL                436
```

FIG. 1. **Deduced amino acid sequence of *Arabidopsis* short-chain acyl-CoA oxidase.** The peroxisomal targeting signal (PTS1) is *boxed*. The GenBank™ accession number for *Arabidopsis* short-chain acyl-CoA oxidase is AB017643.

chondrial enzyme, this putative acyl-CoA dehydrogenase was thought to be localized in plant mitochondria. However, we failed to find a mitochondrial targeting signal in the amino acid sequence. Instead, a typical peroxisomal targeting signal (PTS1) was present at the carboxyl terminus (SRL) (Fig. 1, *boxed*) (31). Therefore, we postulated that this cDNA encodes a second acyl-CoA oxidase with a substrate specificity that is different from that of a known plant acyl-CoA oxidase (16).

Expression, Purification, and Characterization of a Short-chain Acyl-CoA Oxidase—To confirm that the *Arabidopsis* cDNA actually encodes an acyl-CoA oxidase, we expressed the protein from the cDNA employing a baculovirus expression system. To ascertain whether this expression protein has short-chain acyl-CoA oxidase activity or not, we found that crude homogenates obtained from infected insect cells showed acyl-CoA oxidase activity on hexanoyl-CoA (C_6) (Table I). To purify the protein expressed by the cDNA, the crude homogenates were subjected to cation-exchange chromatography on a Hi-Trap SP column. Fractions containing high acyl-CoA oxidase activity were concentrated by ultrafiltration. The sample was then loaded on a Superose 12 column. The results of the purification are summarized in Table I. Analysis by SDS-polyacrylamide gel electrophoresis showed that the protein expressed in the insect cells and isolated by this purification scheme was pure (Fig. 2*A*). Fig. 2*B* shows an immunoblot analysis of the fractions from each purification step and of an extract prepared from *Arabidopsis* etiolated cotyledons using antibodies raised against this acyl-CoA oxidase. The immunoblot analysis revealed that the molecular mass (47 kDa; *arrowheads*) of the purified protein coincided with that of the immunoreactive protein in *Arabidopsis* etiolated cotyledons.

As shown in Fig. 3, the purified protein showed oxidase activity toward acyl-CoAs from butyryl-CoA (C_4) to octanoyl-CoA (C_8). The maximum activity was observed when hexanoyl-CoA (C_6) was used for the substrate. The K_m value for hexanoyl-CoA was estimated at 8.3 μM (Table II). No activity was observed employing crotonoyl-CoA ($C_{4:1}$, an unsaturated carboxylic ester) or glutaryl-CoA (a dicarboxylic ester). The enzyme was active on isobutyryl-CoA at a concentration of 67 μM (2.5 units/mg). Furthermore, we detected no acyl-CoA dehydrogenase activity when hexanoyl-CoA (C_6), decanoyl-CoA (C_{10}), and palmitoyl-CoA (C_{16}) were used as substrates. These data indicated that this *Arabidopsis* cDNA encodes a short-chain acyl-CoA oxidase.

Gel-filtration chromatography of the short-chain acyl-CoA oxidase on a Superose 12 HR 10/30 column indicated a native molecular mass of ~180 kDa (Table II). Because the subunit molecular mass of the short-chain acyl-CoA oxidase is 47 kDa,

TABLE I
Purification of recombinant Arabidopsis short-chain acyl-CoA oxidase expressed employing the baculovirus expression system

Short-chain acyl-CoA oxidase activities were tested with hexanoyl-CoA as a substrate.

Step	Activity	Protein	Specific activity	Yield	Purification
	units	*mg*	*units/mg*	*%*	*-fold*
15,000 × g supernatant	23.5	3.3	7.1	100	1.0
Hi Trap SP	16.1	0.58	27.8	68.5	3.9
Superose 12	3.4	0.031	109.8	14.5	15.5

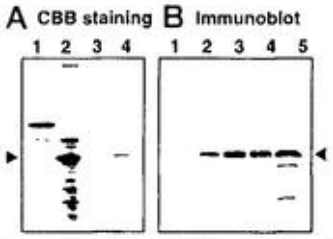

FIG. 2. **SDS-polyacrylamide gel electrophoresis and immunoblot analysis of samples taken at various steps during the purification of *Arabidopsis* short-chain acyl-CoA oxidase produced in the baculovirus expression system.** *A*, SDS-polyacrylamide gel stained with Coomassie Brilliant Blue dye; *B*, immunoblot analysis of polyclonal antibodies raised against recombinant *Arabidopsis* short-chain acyl-CoA oxidase. The *arrowheads* indicate the bands corresponding to the *Arabidopsis* short-chain acyl-CoA oxidase. *Lane 1*, homogenate (15,000 × *g* supernatant) from insect cells infected with the wild-type baculovirus; *lane 2*, homogenate (15,000 × *g* supernatant) from insect cells infected with the recombinant baculovirus (harboring the *Arabidopsis* short-chain acyl-CoA oxidase cDNA); *lane 3*, HiTrap SP column fraction showing short-chain acyl-CoA oxidase activity; *lane 4*, gel-filtration fraction showing short-chain acyl-CoA oxidase activity; *lane 5*, homogenate (15,000 × *g* supernatant) from 5-day-old dark-grown *Arabidopsis* etiolated cotyledons.

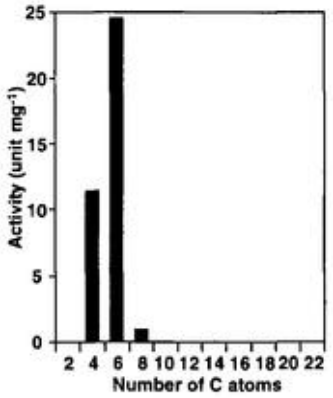

FIG. 3. **Substrate specificity of *Arabidopsis* short-chain acyl-CoA oxidase produced in a baculovirus expression system.** The activity was monitored employing various acyl-CoAs as substrates at a concentration of 25 μM.

TABLE II
Properties of Arabidopsis short-chain acyl-CoA oxidase

K_m and optimal pH values were determined employing hexanoyl-CoA as a substrate. Acyl-CoA dehydrogenase activity was tested with hexanoyl-CoA, decanoyl-CoA, and palmitoyl-CoA as substrates.

Subunit molecular mass	47 kDa
Native molecular mass	180 kDa
pI	9.5
K_m	8.3 μM
Optimal pH	8.5–9.0
Acyl-CoA dehydrogenase activity	None
Subcellular localization	Peroxisomes

the purified enzyme must be a homotetramer. The highest activity was observed between pH 8.5 and 9.0. Table II summarizes the characteristics of the short-chain acyl-CoA oxidase.

Interestingly, the alignment of the conserved regions of acyl-CoA oxidases and acyl-CoA dehydrogenases revealed that the short- and long-chain acyl-CoA oxidases have conserved signatures for mammalian acyl-CoA dehydrogenase (PS1, (G/A/C)-(L/I/V/M)(S/T)EX_2(G/S/A/N)GSDX_2(G/S/A); and PS2, (Q/E)X_2G(G/S)XG(L/I/V/M/F/Y)X_2(D/E/N)X_4(K/R)X_3(D/E)) (Fig. 4) (32). It is possible that these regions are important for the interaction with the substrates. X-ray crystallography and mutational analyses indicated that the glutamic acid residues of mammalian medium-chain (Glu-376) and short-chain (Glu-368) acyl-CoA dehydrogenases serve as the α-proton-abstracting base (33–36). Both the *Arabidopsis* short-chain and pumpkin long-chain acyl-CoA oxidases contain a glutamic acid residue in a corresponding position (Fig. 4*A*, *asterisk*). To analyze the similarity between acyl-CoA oxidases and acyl-CoA dehydrogenases, we compared amino acid sequences of plant acyl-CoA oxidases with human acyl-CoA oxidases and acyl-CoA dehydrogenases. A phylogenetic tree indicates that the plant short-chain acyl-CoA oxidase is clustered together with mitochondrial acyl-CoA dehydrogenases, whereas it is relatively far from other peroxisomal acyl-CoA oxidases (Fig. 4*B*).

Subcellular Localization of Short-chain Acyl-CoA Oxidase—To investigate the subcellular localization of the short-chain acyl-CoA oxidase, homogenates from 5-day-old *Arabidopsis* etiolated cotyledons were subjected to sucrose density gradient centrifugation. Fractions thus obtained were analyzed using an immunoblot technique with antibodies raised against the short-chain acyl-CoA oxidase and catalase. Catalase was used as a glyoxysomal marker enzyme. As shown in Fig. 5*A*, short-chain acyl-CoA oxidase and catalase were present together in fractions 21–23.

Although these enzymes were detected in the first few fractions (top of the gradient), this may be due to disruption of the glyoxysomes during homogenization and subsequent cell fractionation. We confirmed this result using 5-day-old pumpkin etiolated cotyledons. As is the case with *Arabidopsis*, a short-chain acyl-CoA oxidase was detected in fractions 21–23 by the immunoblot technique (Fig. 5*B*). These fractions had short-chain acyl-CoA oxidase as well as catalase activities. In contrast, no short-chain acyl-CoA oxidase activity was detected in fractions 8–13, which correspond to the activity of a mitochondrial marker enzyme, cytochrome *c* oxidase.

Fig. 6 shows an immunoelectron microscopic observation of short-chain acyl-CoA oxidase and catalase in cotyledon cells of *Arabidopsis* etiolated seedlings. Double staining by polyclonal antibodies against *Arabidopsis* short-chain acyl-CoA oxidase (*arrow*) and pumpkin catalase (*arrowhead*) revealed that both enzymes are co-localized in glyoxysomes. No signal was detected on other organelles. These results clearly indicated that the short-chain acyl-CoA oxidase is exclusively localized in glyoxysomes.

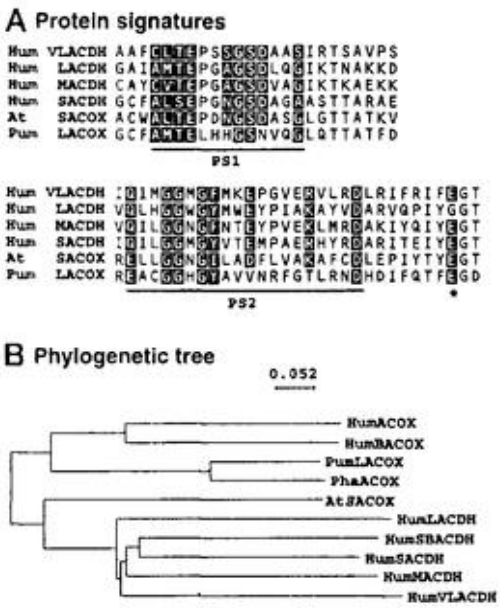

FIG. 4. **Partial alignment of acyl-CoA oxidases and acyl-CoA dehydrogenases (*A*) and phylogenetic tree of acyl-CoA oxidases and acyl-CoA dehydrogenases (*B*).** *White letters* indicate corresponding PS1 and PS2 amino acids. The PS1 and PS2 regions are *underlined*. PS1 has the form (G/A/C)(L/I/V/M)(S/T)EX_2(G/S/A/N)GSDX_2(G/S/A), and PS2 has the form (Q/E)X_2G(G/S)XG(L/I/V/M/F/Y)X_2(D/E/N)X_4(K/R)X_3(D/E) (32). Multiple sequence alignments of the protein sequences were performed using the CLUSTAL W program. The phylogenetic tree was constructed according to the NJPLOT program. *AtSACOX*, *Arabidopsis* short-chain acyl-CoA oxidase (GenBank™ accession number AB017643); *PumLACOX*, pumpkin long-chain acyl-CoA oxidase (accession number AF002016); *PhaACOX*, *Phalaenopsis* acyl-CoA oxidase (accession number U66299); *HumACOX*, human acyl-CoA oxidase (accession number S69189); *HumBACOX*, human branched-chain acyl-CoA oxidase (accession number X95190); *HumVLACDH*, human very long-chain acyl-CoA dehydrogenase (accession number D43682); *HumLACDH*, human long-chain acyl-CoA dehydrogenase (accession number M74096); *HumMACDH*, human medium-chain acyl-CoA dehydrogenase (accession number M16827); *HumSACDH*, human short-chain acyl-CoA dehydrogenase (accession number M26393); *HumSBACDH*, human short/branched-chain acyl-CoA dehydrogenase (accession number U12778).

Developmental Changes in the Level of Short-chain Acyl-CoA Oxidase—Fig. 7 shows changes in the levels of short-chain acyl-CoA oxidase during the post-germinative growth of the *Arabidopsis* seedlings. An immunoblot analysis of *Arabidopsis* seedlings grown in the dark showed that short-chain acyl-CoA oxidase as well as thiolase, another enzyme for fatty acid β-oxidation, reached a maximum level after 5–7 days of growth. These enzymes were still present in the seedlings after 9 days of growth in the dark. After illumination of the seedlings was started, the amount of these enzymes decreased, but faint bands were still detectable after 5 days of illumination (Fig. 7, *4D5L*). Instead, isocitrate lyase, an enzyme of the glyoxylate cycle, reached a maximum level earlier than short-chain acyl-CoA oxidase (3 days after germination) and completely disappeared after 9 days in the dark.

Presence of Short-chain Acyl-CoA Oxidase in Various Organs—Short-chain acyl-CoA oxidase was particularly abundant in 5-day-old *Arabidopsis* etiolated cotyledons (Fig. 8, *upper panel, lane 1*). This enzyme was also present in flowers, roots, and siliques (*lanes 4*, *5*, and *7*), whereas it was present at very low levels or not at all in 7-day-old green cotyledons, rosette leaves, and stems (*lanes 2*, *3*, and *6*). The expression pattern of the thiolase was essentially similar to that of short-chain acyl-CoA oxidase, except that a band was detected at certain levels in 7-day-old green cotyledons, rosette leaves, and

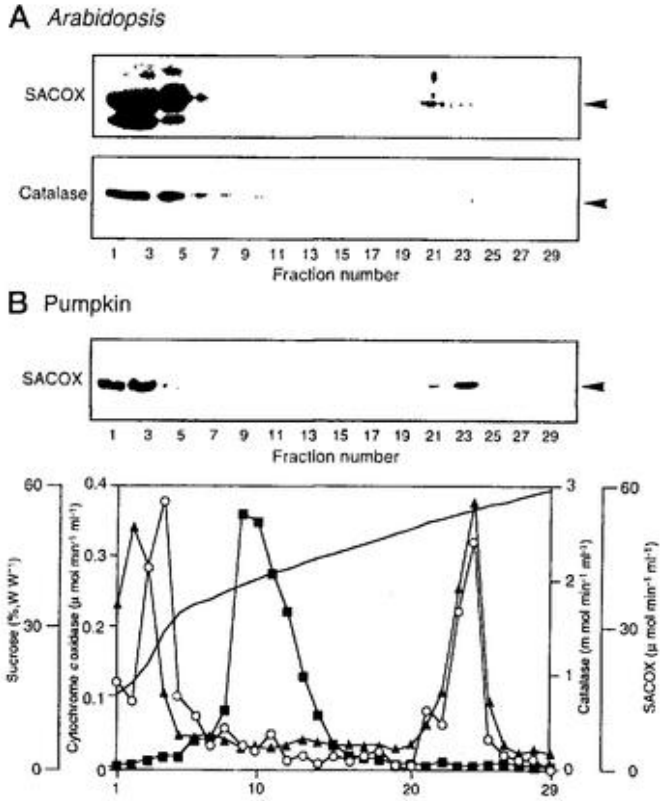

FIG. 5. **Subcellular localization of short-chain acyl-CoA oxidase in *Arabidopsis* (*A*) and pumpkin (*B*) etiolated cotyledons.** Both extracts from 5-day-old etiolated cotyledons were fractionated by sucrose density gradient centrifugation. The *arrowheads* indicate the bands corresponding to the short-chain acyl-CoA oxidase. *A*, immunological detection of *Arabidopsis* short-chain acyl-CoA oxidase (*SACOX*) and catalase; *B*, immunological detection of pumpkin short-chain acyl-CoA oxidase and enzyme activities. ○, short-chain acyl-CoA oxidase; ▲, catalase; ■, cytochrome *c* oxidase; ——, sucrose concentration (w/w). Twenty μl (*Arabidopsis* short-chain acyl-CoA oxidase) and 5 μl (pumpkin short-chain acyl-CoA oxidase and catalase) of samples from each odd-numbered fraction were subjected to SDS-polyacrylamide gel electrophoresis (10% acrylamide) and immunoblotting.

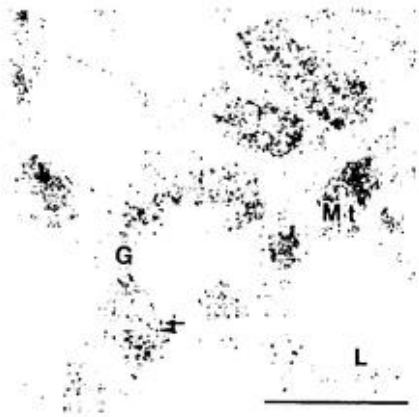

FIG. 6. **Immunoelectron microscopic analysis of the localization of *Arabidopsis* cotyledons of 3-day-old dark-grown seedlings using polyclonal antibodies against *Arabidopsis* short-chain acyl-CoA oxidase and pumpkin catalase.** *Mt*, mitochondria; *G*, glyoxysome; *L*, lipid body. The *arrow* indicates short-chain acyl-CoA oxidase (15-nm gold particles), and the *arrowhead* indicates catalase (10-nm gold particles). *Bar* = 1 μm.

stems (Fig. 8, *center panel*). In contrast, isocitrate lyase was detected only in extracts from etiolated cotyledons (Fig. 8, *lower panel*).

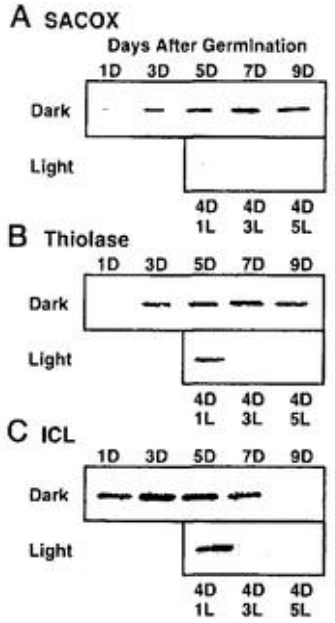

FIG. 7. **Developmental changes in the levels of short-chain acyl-CoA oxidase, thiolase, and isocitrate lyase in *Arabidopsis* cotyledons.** *D* indicates the days of growth in the dark. *L* indicates the days of continuous illumination following 4 days in the dark. Each lane was loaded with 10 μg (short-chain acyl-CoA oxidase) or 5 μg (thiolase, isocitrate lyase) of total proteins extracted from *Arabidopsis* cotyledons. Electrophoresed proteins were blotted on a nylon membrane, and then the membrane was allowed to hybridize with polyclonal antibodies raised against recombinant *Arabidopsis* short-chain acyl-CoA oxidase (*SACOX*; *A*), pumpkin thiolase (*B*), and castor bean isocitrate lyase (*ICL*; *C*).

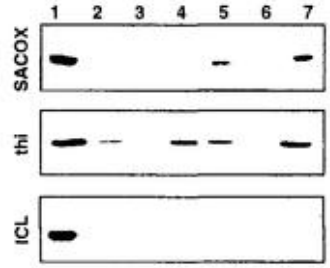

FIG. 8. **Short-chain acyl-CoA oxidase, thiolase, and isocitrate lyase expression in various *Arabidopsis* tissues.** Each lane was loaded with 10 μg of total proteins. The tissues indicated below were excised from 5-week-old plants, except cotyledons, which were excised 5 or 7 days after sowing. *SACOX*, short-chain acyl-CoA oxidase; *thi*, thiolase; *ICL*, isocitrate lyase. *Lane 1*, *Arabidopsis* etiolated cotyledons from plants grown in the dark for 5 days; *lane 2*, green *Arabidopsis* cotyledons from plants grown in the dark for 4 days, followed by 3 days in the light; *lane 3*, rosette leaves; *lane 4*, flowers; *lane 5*, roots; *lane 6*, stems; *lane 7*, siliques.

DISCUSSION

In higher plants with fatty seeds such as pumpkin, the triacylglycerols are stored in lipid bodies. During germination, the fatty acids are liberated by lipase and then degraded by the β-oxidation system in the glyoxysomes, and the resulting acetyl-CoA is further metabolized by the glyoxylate cycle. Thus, fatty acids serve as the main source for energy and carbon compounds. Therefore, fatty acid β-oxidation plays an important role in metabolism until the etiolated cotyledons turn green during late germination. To use storage lipids efficiently, fatty acids need to be completely converted from acyl-CoA to acetyl-CoA by fatty acid β-oxidation. Because most storage lipids are long-chain molecules (C_{16}–C_{18}) in higher plants, the first step in fatty acid β-oxidation begins with long-chain acyl-CoA oxidase, and for the shorter acyl-CoAs, short-chain acyl-

CoA oxidase takes the place of long-chain acyl-CoA oxidase. Thus, higher plants make efficient use of storage lipids to produce carbon and energy sources. In this study, we characterized an *Arabidopsis* peroxisomal short-chain acyl-CoA oxidase and its cDNA. The presence of a peroxisomal short-chain acyl-CoA oxidase explains how higher plant peroxisomes are able to completely oxidize fatty acids by a β-oxidation system.

In mammalian cells, fatty acid β-oxidation is localized both in peroxisomes and in mitochondria. The presence of a short-chain acyl-CoA oxidase distinguishes the peroxisomal β-oxidation of higher plants from that of mammals. In fact, mammalian peroxisomes contain three acyl-CoA oxidase isoforms that act on CoA derivatives of fatty acids with chain lengths from C_8 to C_{18} and that are inactive in oxidizing acyl-CoA esters with carbon chains shorter than 8 carbons. Short-chain fatty acids (C_4–C_8) that could not be oxidized by these peroxisomal acyl-CoA oxidases are transported to mitochondria (7). The mitochondrial β-oxidation system is able to completely degrade fatty acids from long- to short-chain fatty acids (37).

Common features of the amino acid sequences of the *Arabidopsis* short-chain acyl-CoA oxidase and the mammalian mitochondrial acyl-CoA dehydrogenase are shown in Fig. 4 and can be summarized as follow: (*a*) the presence of the two acyl-CoA dehydrogenase protein signatures (PS1 and PS2) in both enzymes; (*b*) a 35% identity between acyl-CoA oxidase and acyl-CoA dehydrogenase; and (*c*) similar subunit molecular masses. However, the short-chain acyl-CoA oxidase differs from pumpkin long-chain acyl-CoA oxidase (16), not considering the substrate specificity, as follows: (*a*) a subunit molecular mass of 47 *versus* 77 kDa (precursor subunit), (*b*) the presence of a C-terminal peroxisomal targeting signal (PTS1) *versus* an N-terminal cleavable targeting signal (PTS2), (*c*) a total identity of only ~18%, and (*d*) a tetrameric structure *versus* a dimeric one. A phylogenetic tree (Fig. 4*B*) including some representative acyl-CoA dehydrogenases and acyl-CoA oxidases from mammals and higher plants clearly summarizes the data presented above: the short-chain acyl-CoA oxidase of *Arabidopsis* is relatively unrelated to the other peroxisomal acyl-CoA oxidases, whereas it is clustered together with mitochondrial acyl-CoA dehydrogenases. The low homology to other acyl-CoA oxidases might suggest that the short-chain acyl-CoA oxidase shares a common ancestor with acyl-CoA dehydrogenases. Short-chain acyl-CoA oxidase could have arisen from a mitochondrial acyl-CoA dehydrogenase that acquired the peroxisomal targeting signal and the new intracellular location during evolution. That allowed plant peroxisomes to host a novel acyl-CoA oxidase ability that distinguishes plant organelles from mammalian peroxisomes.

At least five isoforms of acyl-CoA dehydrogenase are present in mammalian mitochondria: very long-, long-, medium-, short-, and short/branched-chain acyl-CoA dehydrogenases. Except for the very long-chain acyl-CoA dehydrogenase, all the other isoforms are tetrameric enzymes with a subunit of ~45 kDa. Very long-chain acyl-CoA dehydrogenase appears to be a dimer of ~75 kDa (8). In conclusion, both acyl-CoA dehydrogenases and acyl-CoA oxidases are tetramers or dimers of ~45 or 75 kDa. Our analysis revealed the presence of a short-chain acyl-CoA oxidase in plant peroxisomes that shares high homology with mitochondrial acyl-CoA dehydrogenases in mammals. The alignment of the conserved regions of acyl-CoA oxidases and acyl-CoA dehydrogenases (Fig. 4*A*) revealed that the short- as well as long-chain acyl-CoA oxidases contain amino acids of the typical mammalian acyl-CoA dehydrogenase protein signatures (PS1 and PS2). PS1 has the form (G/A/C)(L/I/V/M)(S/T)EX_2(G/S/A/N)GSDX_2(G/S/A), and PS2 has the form (Q/E)X_2G(G/S)XG(L/I/V/M/F/Y)X_2(D/E/N)X_4(K/R)X_3(D/E) (32). The amino acid sequence of pumpkin long-chain acyl-CoA oxidase also contains 7 of the 9 amino acids of PS1 and 6 of the 8 amino acids of PS2 (Fig. 4*A*). Therefore, PS1 and PS2 might be unrelated to the functions of the dehydrogenase and the oxidase.

The purified short-chain acyl-CoA oxidase was active exclusively against short-chain acyl-CoA (C_4–C_8) substrates and had a reduced affinity for octanoyl-CoA (C_8) and a very low activity for branched-chain substrates. This substrate specificity resembles the characteristics of the maize short-chain acyl-CoA oxidase as indicated by Hooks *et al.* (38). The K_m value of 8.3 μM is close to the value reported for the maize enzyme (6 μM). The optimum pH of 8.5–9.0 is similar to that of the maize enzyme (pH 8.3–8.5). Hooks *et al.* have reported the purification of medium- and short-chain acyl-CoA oxidases from maize. The former was a monomeric enzyme of 62 kDa, and the latter was a homotetrameric enzyme of 15-kDa subunits. The 15-kDa subunit has one-third of the subunit mass (47 kDa) of the *Arabidopsis* short-chain acyl-CoA oxidase. Since the maize short-chain acyl-CoA oxidase was not yet cloned, the discrepancy in the subunit molecular mass needs to be further investigated to determine whether there are different families of acyl-CoA oxidases.

Regulation of the expression of short-chain acyl-CoA oxidase seems to be similar to that of other β-oxidation enzymes such as thiolase (Figs. 7 and 8). A similar regulatory mechanism was reported for the expression of pumpkin long-chain acyl-CoA oxidase (16). On the contrary, isocitrate lyase, a marker enzyme of the glyoxylate cycle, is differently regulated. This enzyme disappeared very quickly compared with short-chain acyl-CoA oxidase and thiolase. Additionally, the organ-specific expression of short-chain acyl-CoA oxidase and thiolase does not appear to be coordinated with the expression of isocitrate lyase. These results suggest that β-oxidation enzymes are present in a wider range of organs than enzymes of the glyoxylate cycle such as isocitrate lyase. Particularly, it seems that β-oxidation enzymes are present in significant amounts in flowers, roots, and siliques (Fig. 8, *lanes 4*, *5*, and *7*). Our data further support the hypothesis that the β-oxidation pathway plays an important role not only during the degradation of stored lipids, but also in normal lipid turnover and senescence (28) and in jasmonic acid synthesis (39). This hypothesis is also supported by the finding that the cDNA of an acyl-CoA oxidase of *Phalaenopsis* (which is probably a long-chain acyl-CoA oxidase) was isolated by a search for flower senescence-related genes (40). Recent additional evidence has indicated that the expression of a gene for medium-chain acyl-CoA oxidase was induced when a lauroylacyl carrier protein thioesterase was overexpressed in *Brassica* (41), indicating that expression of the acyl-CoA oxidase gene is regulated by fatty acid biosynthesis or by the amount of fatty acids that are present in the cells. Thus, acyl-CoA oxidase isoforms might have a fundamental role in the control of fatty acid homeostasis in higher plants.

Acknowledgments—We are most grateful to Dr. Masayoshi Maeshima (Nagoya University) for kindly providing the antibody against castor bean isocitrate lyase and Dr. Roland R. Theimer (Institute for Physiological Chemistry of Plants, Bergische University, Wuppertal, Germany) for stimulating discussions and helpful comments on the manuscript.

REFERENCES

1. Beevers, H. (1982) *Ann. N. Y. Acad. Sci.* **386**, 243–251
2. Beevers, H. (1979) *Annu. Rev. Plant Physiol.* **30**, 159–193
3. Huang, A. H. C., Trelease, R. N., and Moore, T. S. (1983) *Plant Peroxisome*, Academic Press, New York
4. Kindl, H. (1993) *Biochimie (Paris)* **75**, 225–230
5. Preisig-Muller, R., Guhnemann-Schafer, K., and Kindl, H. (1994) *J. Biol. Chem.* **269**, 20475–20481
6. Preisig-Muller, R., and Kindle, H. (1993) *Plant Mol. Biol.* **22**, 59–66
7. Hashimoto, T. (1996) *Ann. N. Y. Acad. Sci.* **804**, 86–98

8. Eaton, S., Bartlett, K., and Pourfarzam, M. (1996) *Biochem. J.* **320,** 345–357
9. Wood, C., Burgess, N., and Thomas, D. R. (1986) *Planta (Heidelb.)* **167,** 54–57
10. Masterson, C., Wood, C., and Thomas, D. R. (1990) *Planta (Heidelb.)* **182,** 129–135
11. Miernyk, J. A., Thomas D. R., and Wood, C. (1991) *Plant Physiol. (Bethesda)* **95,** 564–569
12. Hoppe, A., and Theimer, R. R. (1997) *Planta (Heidelb.)* **202,** 227–234
13. Gerhardt, B. (1983) *Planta (Heidelb.)* **159,** 238–246
14. Gerbling, H., and Gerhardt, B. (1987) *Planta (Heidelb.)* **171,** 386–391
15. Kleiter, A. E., and Gerhardt, B. (1998) *Planta (Heidelb.)* **206,** 125–130
16. Hayashi, H., De Bellis, L., Yamaguchi, K., Kato, A., Hayashi, M., and Nishimura, M. (1998) *J. Biol. Chem.* **273,** 8301–8307
17. Sanger, F., Nicklen, S., and Coulson, A. R. (1977) *Proc. Natl. Acad. Sci. U. S. A.* **74,** 5463–5467
18. Thompson, J. D., Higgins, D. G., and Gibson, T. J. (1994) *Nucleic Acids Res.* **8,** 4321–4325
19. Luckow, V. A., and Summers, M. D. (1988) *Virology* **167,** 56–71
20. Nishimura, M., Takeuchi, Y., De Bellis, L., and Hara-Nishimura, I. (1993) *Protoplasma* **175,** 131–137
21. Hayashi, M., Toriyama, K., Kondo, M., and Nishimura, M. (1998) *Plant Cell* **2,** 183–195
22. Gerhardt, B. (1987) *Methods Enzymol.* **148,** 516–525
23. Dommes, V., and Kunau, W. H. (1976) *Anal. Biochem.* **71,** 571–578
24. Furuta, S., Miyazawa, S., and Hashimoto, T. (1981) *J. Biochem. (Tokyo)* **90,** 1739–1750
25. Aebi, H. (1974) in *Methods of Enzymatic Analysis* (Bergmeyer H. U., ed) Vol. 2, pp. 673–684, Academic Press, New York
26. Hodges, T. K., and Leonard, R. T. (1974) *Methods Enzymol.* **32,** 392–406
27. Towbin, H., Staehelin, T., and Gordon, J. (1979) *Proc. Natl. Acad. Sci. U. S. A.* **76,** 4350–4354
28. Kato, A., Hayashi, M., Takeuchi, Y., and Nishimura, M. (1996) *Plant Mol. Biol.* **22,** 843–852
29. Maeshima, M., Yokoi, H., and Asahi, T. (1988) *Plant Cell Physiol.* **29,** 381–384
30. Yamaguchi, J., and Nishimura, M. (1984) *Plant Physiol. (Bethesda)* **74,** 261–267
31. Gould, S. J., Keller, G.-A. A., and Subramani, S. (1987) *J. Cell Biol.* **105,** 2923–2931
32. Bairoch, A., Bvcher, P., and Hofmann, K. (1997) *Nucleic Acids Res.* **25,** 217–221
33. Bross, P., Engst, S., Strauss, A. W., Kelly, D. P., Rasched, I., and Ghisla, S. (1990) *J. Biol. Chem.* **265,** 7116–7119
34. Kim, J. J., Wang, M., and Paschke, R. (1993) *Proc. Natl. Acad. Sci. U. S. A.* **35,** 7523–7527
35. Battaile, K. P., Mohsen, A. W., and Vockley, J. (1996) *Biochemistry* **35,** 15356–15363
36. Srivastava, D. K., and Peterson, K. L. (1998) *Biochemistry* **37,** 8446–8456
37. Lazarow, P. B. (1978) *J. Biol. Chem.* **253,** 1522–1528
38. Hooks, M. A., Bode, K., and Couée, I. (1996) *Biochem. J.* **320,** 607–614
39. Wasternack, C., and Parthier, B. (1997) *Trends Plant Sci.* **2,** 302–307
40. Do, Y. Y., and Huang, P. L. (1997) *Arch. Biochem. Biophys.* **344,** 295–300
41. Eccleston, V. S., and Ohlrogge, J. B. (1998) *Plant Cell* **10,** 613–622

JPR Symposium

Microbody Defective Mutants of Arabidopsis*

Mikio Nishimura**, Makoto Hayashi, Kanako Toriyama, Akira Kato, Shoji Mano, Katsushi Yamaguchi, Maki Kondo and Hiroshi Hayashi

Department of Cell Biology, National Institute for Basic Biology, Okazaki, 444 Japan

In germinating fatty seedlings, microbodies are differentiated to leaf peroxisomes from glyoxysomes during greening, and then transformed to glyoxysomes from leaf peroxisomes during senescence. These transformations of microbodies are regulated at various level, such as gene expression, splicing of the mRNA and degradation of microbody proteins. In order to clarify the regulatory mechanisms underlying these transformations of microbodies, we tried to obtain glyoxysome-deficient mutants of Arabidopsis. We screened 2, 4-dichlorophenoxybutyric acid (2, 4-DB) mutants of Arabidopsis which have defects in glyoxysomal fatty acid β-oxidation. Four mutants can be classified as carrying alleles at three independent loci, which we designated *ped1*, *ped2*, and *ped3*, respectively (where *ped* stands for peroxisome defective). The characteristics of these *ped* mutants are described.

Key words: Arabidopsis — Fatty acid β-oxidation — Glyoxysomes — Leaf peroxisomes — Mutant — Transformation of microbodies

Transformation of Microbodies between Glyoxysomes and Leaf Peroxisomes

Dramatic metabolic changes which underlie the shift from heterotrophic to autotrophic growth occur in greening of seed germination. Accompanying these metabolic changes, many constitutive organelles are also functionally transformed. For example, etioplasts differentiate into chloroplasts and mitochondria acquire the ability to oxidize glycine. Glyoxysomes which are microbodies engaged in the degradation of reserve oil via β-oxidation and the glyoxylate cycle, are transformed into leaf peroxisomes that function in several crucial steps of photorespiration (Nishimura *et al.* 1986, Titus and Becker 1985). After the functional transition of glyoxysomes to leaf peroxisomes during the greening of pumpkin cotyledons, the reverse microbody transition of leaf peroxisomes to glyoxysomes occurs during senescence (De Bellis and Nishimura 1991, De Bellis *et al.* 1991, Nishimura *et al.* 1993). Microbody enzymes function after their transport to microbodies. Since the enzyme compositions and functions of glyoxysomes and leaf peroxisomes differ from each other, it was likely that the two types of microbodies possess different machineries for protein import.

Microbody proteins are synthesized in the cytosol on free polysomes and are transported post-translationally into microbodies (Nishimura *et al.* 1996). Two types of targeting signals to microbodies have been reported. One type of targeting signal is part of the mature protein. One such signal, the tripeptide Ser-Lys-Leu, occurs at the C-terminal end has been identified as a targeting signal (Gould *et al.* 1987). Ser-Lys-Leu and related amino acid sequences commonly function in mammals, insects, fungi, and plants (Keller *et al.* 1991). Glyoxysomal enzymes, such as tetrafunctional enzyme (Preisig-Muller *et al.* 1994), malate synthase (Comai *et al.* 1989, Graham *et al.* 1989, Mori *et al.* 1991, Rodriguez *et al.* 1990, Turley *et al.* 1990a) and isocitrate lyase (Beeching and Northcote 1987, Mano *et al.* 1996, Turley *et al.* 1990b, Zhang *et al.* 1993), and leaf peroxisomal enzymes, such as glycolate oxidase (Tsugeki *et al.* 1993, Volokita and Somerville 1987) and hydroxypyruvate reductase (Greenler *et al.* 1989, Hayashi *et al.* 1996b), contain the targeting signal at their C-terminal ends.

To characterize the targeting signal, we have examined an ability of 24 carboxy-terminal amino acid sequences to facilitate the transport of a bacterial protein, β-glucuronidase (GUS) into microbodies in green cotyledonary cells of transgenic Arabidopsis (Hayashi *et al.* 1996a, Hayashi *et al.* 1997). Immunocytochemical analysis of the transgenic plants revealed that carboxy-terminal tripeptide sequences of the form [C/A/S/P]-[K/R]-[I/L/M] function as a microbody-targeting signal, although tripeptides with proline at the first amino acid position and isoleucine at the carboxyl terminus show weak targeting efficiencies. All known microbody enzymes that are synthesized in a form similar in size to the mature molecule, except catalase, contain one of these tripeptide sequences at their carboxyl terminus. These carboxyl tripeptides function as a targeting signal to the microbodies, not only to glyoxysomes but also to leaf peroxisomes.

A second type of targeting signal involved a cleavable N-terminal sequence. A small group of microbody proteins, such as 3-ketoacyl-coenzyme A (CoA) thiolase (Kato *et al.*

* The extended abstract of a paper presented at the 13th International Symposium in Conjugation with Award of the International Prize for Biology "Frontier of Plant Biology"

** Correspondence: Fax +81-564-55-7505, E-mail mikosome@nibb.ac.jp

1996b, Preisig-Muller and Kindl 1993), malate dehydrogenase (Gietl 1990, Kato *et al.* 1998), glyoxysomal citrate synthase (gCS) (Kato *et al.* 1995) are synthesized as precursor proteins with larger molecular masses than those of the mature proteins. Recently, we have found that pumpkin long chain acyl-CoA oxidase is synthesized as a larger molecular mass precursor (Hayashi *et al.* 1998a). Each of these proteins has a cleavable presequence at its N-terminal end. To investigate the role of the presequence in the transport of the protein to the microbodies, we generated transgenic Arabidopsis plants that expressed GUS with the N-terminal presequence of the precursor to gCS (Kato *et al.* 1996a). Immunogold labeling and cell fractionation studies showed that the chimeric protein was transported into microbodies and subsequently was processed. The chimeric protein was transported to functionally different microbodies, such as glyoxysomes, leaf peroxisomes and nonspecialized microbodies. These observations indicated that the transport of gCS is mediated by its amino-terminal presequence and that the transport system is functional in all plant microbodies. Therefore, it is unlikely that glyoxysomes and leaf peroxisomes possess different targeting machineries.

The microbody transition has been shown to be regulated at various levels, such as gene expression and protein degradation (Nishimura *et al.* 1996). Recently, we have shown that two different forms of hydroxypyruvate reductase which are localized in leaf peroxisomes and in the cytosol, are produced by alternative splicing (Hayashi *et al.* 1996b). The alternative splicing is regulated by light, suggesting that the microbody transition is also regulated at the level of splicing for mRNA.

Arabidopsis Mutants Have Defects in Glyoxysomal Fatty Acid β-Oxidation

A genetic approach may be an effective strategy toward understanding the regulatory mechanism(s) underlying the microbody transition at the level of gene expression, protein translocation, and protein degradation. We screened 2, 4-dichlorophenoxybutyric acid (2, 4-DB)-resistant mutants that have defects in glyoxysomal fatty acid β-oxidation (Fig. 1) (Hayashi *et al.* 1998b). It has been previously demonstrated that 2, 4-DB is metabolized to produce a herbicide, 2, 4-D, by the action of fatty acid β-oxidation in higher plants (Wain and Wightman 1954). In order to isolate mutants that have defects in glyoxysomal fatty acid β-oxidation, mutant lines of *Arabidopsis* seedlings were screened for growth in the presence of toxic levels of 2, 4-DB (Fig. 2A). We isolated 12 Arabidopsis mutants (LR11, LR24, LR27, LR40, LR43, LR47, LR53, LR77, LR81, LR91, LR92, and LR98: LR; long root in the presence of 2, 4-DB) that showed resistance specifically to 2, 4-DB, not to 2, 4-D (Fig. 2B).

Most of the 2, 4-DB-resistant mutants grew on the growth medium without sucrose as well as the wild-type plants did. But four of the mutants, namely LR40, LR43, LR47, and LR81, could expand their green cotyledons and leaves only when sucrose was supplied to the growth medium, suggesting that these mutants have defects in glyoxysomal fatty acid β-oxidation, since glyoxysomal fatty acid β-oxidation has an important role in converting sucrose from storage lipids during germination. Genetic analysis revealed that LR40, LR43, and LR47 are nonallelic mutations, whereas LR43 and LR 81 are allelic. We designated *ped1* as LR40, *ped2* as LR47, *ped3-1* as LR43, and *ped3-2* as LR81.

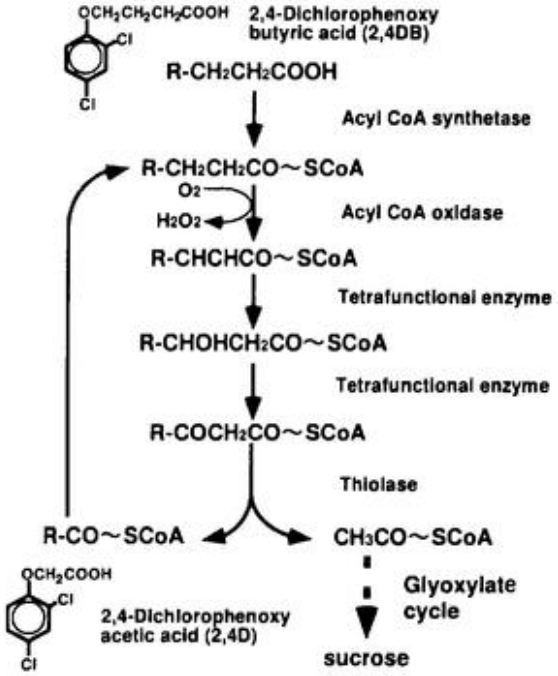

Fig. 1. Schematic representation of fatty acid metabolism in glyoxysomes. In the glyoxysomes, fatty acids ($R\text{-}CH_2CH_2COOH$) are first activated to fatty acyl CoA by fatty acyl CoA synthetase. Fatty acyl CoA is the substrate for fatty acid β-oxidation, which consists of four enzymatic reactions. The first reaction is catalyzed by acyl CoA oxidase. The second and third enzymatic reactions are catalyzed by a single enzyme so called tetrafunctional enzyme that possesses enoyl CoA hydratase and β-hydroxyacyl CoA dehydrogenase activities. The fourth reaction is catalyzed by 3-ketoacyl CoA thiolase. Acetyl CoA, an end product of fatty acid β-oxidation, is metabolized further to produce succinate by the action of glyoxylate cycle. Succinate is finally converted to sucrose. 2, 4-dichlorophenoxybutyric acid is known to produce 2, 4-dichlorophenoxyacetic acid by the action of fatty acid β-oxidation.

To characterize the phenotypes of the mutants, glyoxysomal enzymes in 5-day-old etiolated cotyledons were analyzed by an immunoblot technique using antibody against thiolase which is involved in glyoxysomal fatty acid β-oxidation. Two mutants showed different thiolase patterns from that of the wild-type plant. In the cotyledons of *ped1* mutant, no accumulation of thiolase was observed at any stage of postgerminative growth regardless of the light conditions. In cotyledons of *ped2* mutant, two types of thiolase were detected. One of these had the same molecular mass (45 kD) as that found in the wild-type plant, whereas the other was an additional protein with a higher

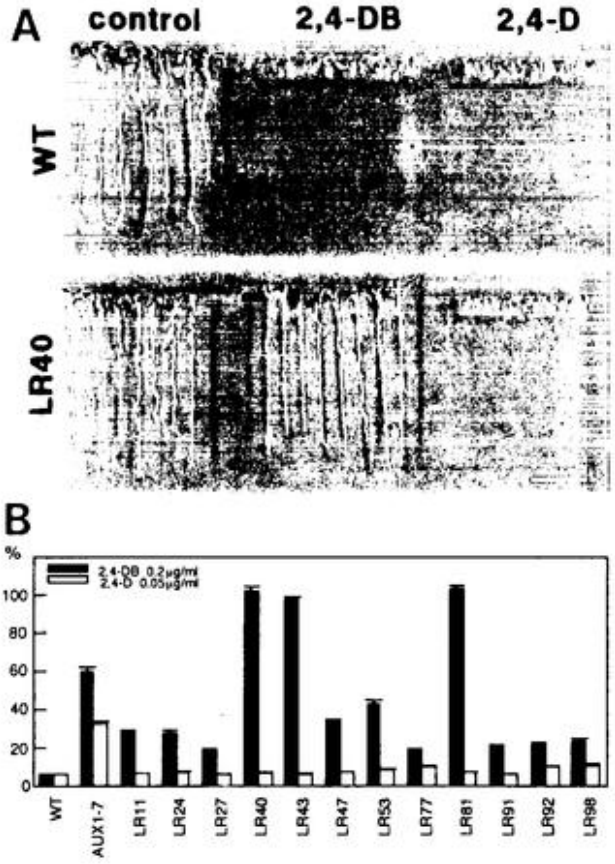

Fig. 2. Effects of 2, 4-DB and 2, 4-D on the growth of mutants and wild-type seedlings. (A) Phenotypes of wild-type Arabidopsis (WT) and 2, 4-DB-resistant mutant (LR40) grown for 7 days on growth medium (control), growth medium containing 0.2 μg/mL of 2, 4-DB (2, 4-DB) or 0.05 μg/mL 2, 4-D (2, 4-D) under constant illumination. Photographs were taken after the seedlings were removed from the media and rearranged on agar plates. Bar=1 cm.
(B) The effect of 2, 4-DB and 2, 4-D on root elongation is expressed relative to the mean root elongation of the same genotype on growth medium. Each value represents the mean of measurements of at least 10 seedlings±SE. Name of each mutant is indicated at the bottom. AUX1-7 represents the 2, 4-D-resistant mutant.

molecular mass (48 kD), a precursor to the protein.

Etiolated cotyledons of both mutants have glyoxysomes with abnormal morphology. Glyoxysomes in *ped1* mutant were two or three times greater in diameter than those in the wild-type plant and contained vesicle-like structures. By contrast, most of the glyoxysomes found in the cells of *ped2* mutant were shrunken and not round. Further analysis is necessary to clarify the formation of these abnormal glyoxysomes.

Comparison of thiolase genes for wild-type plant and *ped1* mutant revealed that ATT codon for ^{100}Ile at 4th exon of wild-type thiolase gene (accession No. AB008855) is changed to ATGG in thiolase gene of *ped1* mutant (accession No. AB008856). Nucleotide substitution of T to GG causes frame shift, and produces stop codon within the 4th exon. Therefore thiolase gene in *ped1* mutant encodes a smaller protein composed of 114 amino acids, and first 99 amino acids of the protein are identical to wild-type thiolase. Identification of the genes of other *ped* mutants are now in progress. The functional transformation from glyoxysomes to leaf peroxisomes is also characterized in these mutants. These *ped* mutants provides us useful clues for understanding regulatory mechanisms underlying the reversible transformation between glyoxysomes and leaf peroxisomes.

This work was supported in part by a grant from the Research for the Future Program of the Japanese Society for the Promotion of Science (No. JSPS-RFTE96L00407), by grants-in-aid for scientific resarch from the Ministry of Education, Science, and Culture of Japan (No. 09274101, No. 09274103, No. 09440271, and No. 10874123 to M.N. and No. 09740606 to M.H.). and by grant from the Nissan Science Foundation (Tokyo, Japan) to M.H.

References

Beeching, J.R. and Northcote, D.H. 1987. Nucleic acid (cDNA) and amino acid sequences of isocitrate lyase from castor bean. Plant Mol. Biol. **8**: 471-475.

Comai, L., Baden, C.S. and Harada, J.J. 1989. Deduced sequence of a malate synthase polypeptide encoded by a subclass of the gene family. J. Biol. Chem. **264**: 2778-2782.

De Bellis, L. and Nishimura, M. 1991. Development of enzymes of the glyoxylate cycle during senescence of pumpkin cotyledons. Plant Cell Physiol. **32**: 555-561.

De Bellis, L., Tsugeki, R. and Nishimura, M. 1991. Glyoxylate cycle enzymes in peroxisomes isolated from petals of pumpkin (*Cucurbita* sp.) during senescence. Plant Cell Physiol. **32**: 1227-1235.

Gietl, C. 1990. Glyoxysomal malate dehydrogenase from watermelon is synthesized with an amino-terminal transit peptide. Proc. Natl. Acad. Sci. USA **87**: 5773-5777.

Gould, S.J., Keller, G.-A.A. and Subramani, S. 1987. Identification of a peroxisomal targeting signal at the carboxy terminus of firefly luciferase. J. Cell. Biol. **105**: 2923-2931.

Graham, I.A., Smith, L.M., Brown, J.W., Leaver, C.J. and Smith, S.M. 1989. The malate synthase gene of cucumber. Plant Mol. Biol. **13**: 673-684.

Greenler, J.M., Sloan, J.S., Schwartz, B.W. and Becker, W.M. 1989. Isolation, characterization and sequence analysis of a full-length cDNA clone encoding NADH-dependent hydroxypyruvate reductase from cucumber. Plant Mol. Biol. **13**: 139-150.

Hayashi, H., De Bellis, L., Yamaguchi, K., Kato, A., Mano, S., Hayashi, M. and Nishimura, M. 1998a. Molecular characterization of a glyoxysomal long-chain acyl-CoA oxidase that is synthesized as a precursor of higher molecular mass in pumpkin. J. Biol. Chem. **273**: 8301-8307.

Hayashi, M., Aoki, M., Kato, A., Kondo, M. and Nishimura, M.

1996a. Transport of chimeric proteins that contain a carboxy-terminal targeting signal into plant microbodies. Plant J. **10**: 225-234.

Hayashi, M., Aoki, M., Kondo, M. and Nishimura, M. 1997. Changes in targeting efficiencies of proteins to plant microbodies caused by amino acid substitutions in the carboxy-terminal tripeptide. Plant Cell Physiol. **38**: 759-768.

Hayashi, M., Toriyama, K., Kondo, M. and Nishimura, M. 1998b. 2, 4-Dicholorophenoxybutyric acid-resistant mutants of Arabidopsis have defects on glyoxysomal fatty acid β-oxidation. Plant Cell **10**: 183-195.

Hayashi, M., Tsugeki, R., Kondo, M., Mori, H. and Nishimura, M. 1996b. Pumpkin hydroxypyruvate reductases with and without a putative C-terminal signal for targeting to microbodies may be produced by alternative splicing. Plant Mol. Biol. **30**: 183-189.

Kato, A., Hayashi, M., Kondo, M. and Nishimura, M. 1996a. Targeting and processing of a chimeric protein with the N-terminal presequence of the precursor to glyoxysomal citrate synthase. Plant Cell **8**: 1601-1611.

Kato, A., Hayashi, M., Mori, H. and Nishimura, M. 1995. Molecular characterization of a glyoxysomal citrate synthase that is synthesized as a precursor of higher molecular mass in pumpkin. Plant Mol. Biol. **27**: 377-390.

Kato, A., Hayashi, M., Takeuchi, Y. and Nishimura, M. 1996b. cDNA cloning and expression of a gene for 3-ketoacyl-CoA thiolase in pumpkin cotyledons. Plant Mol. Biol. **31**: 843-852.

Kato, A., Takeda-Yoshikawa, Y., Hayashi, M., Kondo, M., Hara-Nishimura, I. and Nishimura, M. 1998. Glyoxysomal malate dehydrogenase in pumpkin: cloning of a cDNA and functional analysis of its prosequence. Plant Cell Physiol. **39**: 186-195.

Keller, G.A., Krisans, S., Gould, S.J., Sommer, J.M., Wang, C. C., Schliebs, W., Kunau, W., Brody, S. and Subramani, S. 1991. Evolutionary conservation of a microbody targeting signal that targets proteins to peroxisomes, glyoxysomes, and glycosomes. J. Cell Biol. **114**: 893-904.

Mano, S., Hayashi, M., Kondo, M. and Nishimura, M. 1996. cDNA cloning and expression of a gene for isocitrate lyase in pumpkin cotyledons. Plant Cell Physiol. **37**: 941-948.

Mori, H., Takeda-Yoshikawa, Y., Hara-Nishimura, I. and Nishimura, M. 1991. Pumpkin malate synthase: Cloning and sequencing of the cDNA and Northern blot analysis. Eur. J. Biochem. **197**: 331-336.

Nishimura, M., Hayashi, M., Kato, A., Yamaguchi, K. and Mano, S. 1996. Functional transformation of microbodies in higher plant cells. Cell Struct. Funct. **21**: 387-393.

Nishimura, M., Takeuchi, Y., De Bellis, L. and Hara-Nishimura, I. 1993. Leaf peroxisomes are directly transformed to glyoxysomes during senescence of pumpkin cotyledons. Protoplasma **175**: 131-137.

Nishimura, M., Yamaguchi, J., Mori, H., Akazawa, T. and Yokota, S. 1986. Immunocytochemical analysis shows that glyoxysomes are directly transformed to leaf peroxisomes during greening of pumpkin cotyledons. Plant Physiol. **80**: 313-316.

Preisig-Muller, R., Guhnemann-Schafer, K. and Kindl, H. 1994. Domains of the tetrafunctional protein acting in glyoxysomal fatty acid beta-oxidation. Demonstration of epimerase and isomerase activities on a peptide lacking hydratase activity. J. Biol. Chem. **269**: 20475-20481.

Preisig-Muller, R. and Kindl, H. 1993. Thiolase mRNA translated *in vitro* yields a peptide with a putative N-terminal presequence. Plant Mol. Biol. **22**: 59-66.

Rodriguez, D., Ginger, R.S., Baker, A. and Northcote, D.H. 1990. Nucleotide sequence analysis of a cDNA clone encoding malate synthase of castor bean (*Ricinus communis*) reveals homology to DAL7, a gene involved in allantoin degradation in *Saccharomyces cerevisiae*. Plant Mol. Biol. **15**: 501-504.

Titus, D.E. and Becker, W.M. 1985. Investigation of the glyoxysome-peroxisome transition in germinating cucumber cotyledons using double-label immunoelectron microscopy. J. Cell. Biol. **101**: 1288-1299.

Tsugeki, R., Hara-Nishimura, I., Mori, H. and Nishimura, M. 1993. Cloning and sequencing of cDNA for glycolate oxidase from pumpkin cotyledons and Northern blot analysis. Plant Cell Physiol. **34**: 51-57.

Turley, R.B., Choe, S.M., Ni, W. and Trelease, R.N. 1990a. Nucleotide sequence of cottonseed malate synthase. Nucleic Acids Res. **18**: 3643.

Turley, R.B., Choe, S.M. and Trelease, R.N. 1990b. Characterization of a cDNA clone encoding the complete amino acid sequence of cotton isocitrate lyase. Biochim. Biophys. Acta **1049**: 223-226.

Volokita, M. and Somerville, C.R. 1987. The primary structure of spinach glycolate oxidase deduced from the DNA sequence of a cDNA clone. J. Biol. Chem. **262**: 15825-15828.

Wain, R.L. and Wightman, F. 1954. The growth-regulating activity of certain ω-substituted alkyl carboxylic acids in relation to their β-oxidation within the plant. Proc. Roy. Soc. Lond. Biol. Sci. **142**: 525-536.

Zhang, J.Z., Gomez, P.M., Baden, C.S. and Harada, J.J. 1993. Two classes of isocitrate lyase genes are expressed during late embryogeny and postgermination in *Brassica napus* L. Mol. Gen. Genet. **238**: 177-184.

(Received March 30, 1998; Accepted April 13, 1998)

参考論文目録

Mikio Nishimura, Makoto Hayashi, Kanako Toriyama, Akira Kato, Shoji Mano, Katsushi Yamaguchi, Maki Kondo and Hiroshi Hayashi

Microbody Defective Mutants of Arabidopsis

J. Plant Res., 111: 329-332, 1998

Luigi De Bellis, Pietro Giuntini, Hiroshi Hayashi, Makoto Hayashi and Mikio Nishimura

Purification and Characterization of Pumpkin Long-chain Acyl-CoA Oxidase

Physiol. Plant., in press, 1999

Makoto Hayashi, Kanako Toriyama, Akira Kato, Shoji Mano, Luigi De Bellis, Yasuko Hayashi-Ishimaru, Katsushi Yamaguchi, Maki Kondo, Hiroshi Hayashi and Mikio Nishimura

Functional Transformation of Plant Peroxisomes

Cell Biochem. Biophys., in press, 1999

Purification and characterization of pumpkin long-chain acyl-CoA oxidase

Luigi De Bellis, Pietro Giuntini, Hiroshi Hayashi, Makoto Hayashi and Mikio Nishimura

De Bellis L., Giuntini P., Hayashi H., Hayashi M. and Nishimura M. 1999. Purification and characterization of pumpkin long-chain acyl-CoA oxidase. - Physiol. Plant. XX: YY-ZZ.

Abstract

Pumpkin (*Cucurbita* sp.) long-chain acyl-CoA oxidase (EC 1.3.3.6) was purified to homogeneity by hydrophobic interaction, hydroxyapatite, affinity and anion exchange chromatographies. The purified isoenzyme is a dimeric protein, consisting of two apparently identical 72 kDa subunits. The protein is exclusively localized in glyoxysomes. The enzyme catalyzes selectively the oxidation of CoA esters fatty acids with 12 to 18 C atoms and exhibits highest activity on C-14 fatty acids but no activity on isobutyryl-CoA and isovaleryl-CoA (branched chain) or glutaryl-CoA (dicarboxylic). The enzyme is strongly inhibited by high concentrations of palmitoyl-CoA and a minor inhibition by high concentration of myristoyl-CoA was observed. It is also inhibited by Triton X-100 at concentrations above 0.02%. The consequences of the substrate inhibition for the evaluation of long-chain acyl-CoA oxidase activity in plant tissues are discussed.

Key words - acyl-CoA oxidase, β-oxidation, *Cucurbita*, pumpkin.

L. De Bellis (*corresponding author, e-mail ldebelli@agr.unipi.it*) and Pietro Giuntini, Dipartimento di Biologia, via Prov.le Lecce-Monteroni, 73100 Lecce and Dipartimento di Biologia delle Piante Agrarie, via Mariscoglio 34, 56124 Pisa, Italy; Hiroshi Hayashi, Makoto Hayashi and Mikio Nishimura, Department of Cell Biology, National Institute for Basic Biology, Okazaki 444-8585, Japan.

Introduction

Acyl-CoA oxidases (ACOXs, EC 1.3.3.6) are flavoproteins which catalyze the initial step in each cycle of the peroxisomal β-oxidation, the conversion of acyl-CoA to *trans*-2-enoyl-CoA, transferring electrons to molecular oxygen to produce hydrogen peroxide.

In mammalian cells both mitochondria and peroxisomes host the enzymes of the β-oxidation pathway. In mitochondria the first step of the pathway is catalyzed by acyl-CoA dehydrogenases which transfer electrons to an electron transfer flavoprotein and then to the mitochondrial respiratory chain. Four acyl-CoA dehydrogenases which vary in their specificity for acyl-chain length are present allowing mammalian mitochondria to perform the β-oxidation of the entire acyl-CoA esters (Eaton et al. 1996). On the contrary, peroxisomal β-oxidation can metabolize long-chain acyl-CoA esters only partly because the three peroxisomal acyl-CoA oxidases (palmitoyl-CoA oxidase, pristanoyl-CoA oxidase and trihydroxycoprostanoyl-CoA oxidase) show a very low affinity to short-chain acyl-CoAs (Van Veldhoven et al. 1992).

In contrast, the affinity of the plant peroxisomal ACOXs to both long- and short-chain acyl-CoAs (Gerhardt 1985, Hook et al. 1995) permits the plant peroxisomes other than the mammalian peroxisomes to degrade the fatty acids completely. In addition, plant peroxisomes are capable of β-oxidizing a variety of substrates: CoA

esters of straight-chain and unsaturated fatty acids, esters of uncommon fatty acids such as ricinoleic acid and branched-chain 2-oxo acids (Gerhardt 1992).

Some plant ACOXs were purified to apparent homogeneity: long-chain ACOX from cucumber cotyledons (Kirsh et al. 1986) and medium- and short-chain ACOX from maize plantlets (Hook et al. 1996). They are characterized by different molecular masses (from 15 kDa of short-chain to 72 kDa of long-chain ACOX) of the subunits. So far, the activity on branched-chain or dicarboxylic acyl-CoAs was not analyzed.

Since similar subunit molecular masses were reported for peroxisomal ACOXs from mammals (Hashimoto 1996) and both the two published cDNAs that code for *Phalaenopsis* (Do and Huang 1997) and pumpkin (Hayashi et al. 1998) ACOX indicate a molecular mass of 72 kDa for the mature protein subunit we decided to engage in the purification of all the ACOXs present in pumpkin cotyledons. The aim is to shed light on the above mentioned apparent discrepancy and to eventually determine which ACOX isoforms acts on branched-chain 2-oxo acids formed by transamination of leucine, isoleucine and valine which are catabolized by plant peroxisomes (Gerbling and Gerhardt 1989).

We report here the purification and the characterization of pumpkin long-chain ACOX and the comparison with the characteristics of other plant and mammalian ACOXs.

Abbreviations – ACOX, acyl-CoA oxidase; FAD, flavin adenine dinucleotide; NEM, N-ethylmaleimide; PMSF, phenylmethylsulfonyl fluoride; SHAM, salicylhydroxamate.

Materials and Methods

Plant material and chemicals

Pumpkin seeds (*Cucurbita* sp., var. Amakuri Nankin) were soaked overnight and germinated in the dark in a growth chamber for 5 days at 25°C. The CoA esters of various fatty acids were purchased from Sigma (St. Louis, Missouri, USA). Econo-Pac CHT-II Cartridge 5 ml and Econo-Pac 10DG columns were purchased from Bio Rad Laboratories (Hercules, CA, USA), Phenyl Sepharose High Performance, Hi Trap Blue 1 ml, Mono S HR5/5 and other gels for chromatography were obtained from Pharmacia (Uppsala, Sweden).

ACOX purification

Five-day-old etiolated pumpkin cotyledons were homogenized in 3 ml of grinding medium per g fresh weight consisting of 150 m*M* Tris pH 7.6, 10 m*M* KCl, 1 m*M* EDTA, 1m*M* DTT, 10 μ*M* FAD, 1 m*M* PMSF, 10% glycerol. The homogenate was centrifuged for 20 min at 12,000g and 4 °C. The supernatant, deprived of the top layer of lipids, was mixed with an equal amount of 3.4 *M* ammonium sulfate in 50 m*M* K-phosphate buffer, pH 7.2. It was then applied directly to a column (16 x 150 mm) with Phenyl Sepharose High Performance equilibrated with buffer A (1.7 *M* ammonium sulfate, 20 m*M* Na-phosphate, 10 μ*M* FAD, 10% glycerol, pH 7.2). The column was washed with buffer A and eluted with a linear ethylene glycol gradient (0-60%). Long-chain ACOX and short-chain ACOX were efficiently separated by this

chromatographic step. Fractions with higher short-chain ACOX activity were pooled and desalted using Econo-Pac 10DG columns equilibrated with buffer B (10 m*M* Na-phosphate, 10 μ*M* FAD, 10% glycerol, pH 7.2). The sample was loaded on a Econo-Pac CHT-II Cartridge 5 ml (ceramic hydroxyapatite) equilibrated with buffer B, and the proteins were eluted by increasing the concentration of Na-phosphate to 0.5 *M*. Enzymatically active fractions were dialyzed against buffer B and loaded on a HiTrap Blue 1 ml column. Proteins were eluted with a linear NaCl gradient (0-3 *M*) in buffer B. Finally, enzymatically active fractions were dialyzed against buffer C (50 m*M* Na-phosphate, 10 μ*M* FAD, 10% glycerol, pH 6.7) and loaded on a MonoS HR 5/5 column. Proteins were eluted with a linear NaCl gradient (0-0.2 *M*) in buffer C. Gel filtration was performed with a Superdex 200 16/60 column (Pharmacia) equilibrated with a buffer composed of 50 m*M* Tris, pH 8.0, 150 m*M* NaCl, 10 μ*M* FAD and 10% glycerol.

Electrophoresis and western blotting

SDS-PAGE and IEF were performed at 15 °C using a Phast System apparatus with PhastGel gradient 4-15 or IEF 3-9 gels (Pharmacia). Gels were silver-stained in the developer unit of the Phast System according to the instructions of the manufacturer. Western blottings were performed as indicated in Hayashi et al. (1998) employing ACOX specific antiserum prepared against an ACOX fusion protein synthesized in *Escherichia coli* (Hayashi et al. 1998). Subcellular fractionation was performed following the procedure indicated by Hayashi et al. (1998).

Enzyme assays

ACOX assays were performed by following the H_2O_2 formation coupled with a peroxidatic reaction (Gerhardt, 1987). The assay mixture consisted of 175 m*M* Tris pH 8.5, 50 μ*M* FAD, 13 m*M* p-hydroxybenzoic acid, 1 m*M* 4-aminoantipyrine, 1 m*M* NaN_3, 5 units horseradish peroxidase and 25 μ*M* acyl-CoA substrate. This assay was also used to determine K_m values and inhibition by substrates and by different chemicals. Bis-tris-propane 175 m*M* in the range 6.5-9.5 and Tris 175 m*M* in the range 7.5-8.8 were used to determine the pH optimum of the purified enzyme. Acyl-CoA dehydrogenase assays were performed following two slightly different methods (Dommes and Kunau 1976, Furuta et al. 1981).

Results

A long-chain ACOX was purified about 710-fold from 5-day-old etiolated pumpkin cotyledons and a specific activity of 13.5 nmol (mg protein)$^{-1}$ min $^{-1}$ (with 25 μM palmitoyl-CoA as substrate) was obtained. Although the overall yield was rather low, about 1.8 % of the activity in the crude homogenate, the procedure was reproducible for the purification. The results of a typical purification experiment are summarized in Table 1. After homogenization, the ammonium sulfate concentration in the homogenate was brought to 1.7 *M* and the solution was loaded onto a Phenyl Sepharose column. Two peaks of ACOX activity were eluted when the ionic strength of the buffer was reduced, the first peak identified by the enzymatic assay employing hexanoyl-CoA (C6) as substrate, the second peak by using decanoyl-CoA (C10) and palmitoyl-CoA (C16) (data not shown; cf. Hayashi et al., 1998). This indicates a good separation of short-chain and long-chain ACOX. Fractions of the second peak were collected and pooled for further purification. After desalting the sample was loaded on a ceramic hydroxyapatite column and a single peak of acyl-CoA activity (employing esters of C10 and C16 fatty acids) was eluted after increasing the concentration of Na-phosphate in the buffer. No short-chain ACOX activity (C6 as substrate) was detected following the hydroxyapatite chromatography. The latter step was still very effective, yielding an enrichment of 4.5-fold. With subsequent affinity chromatography and cation exchange chromatography a further relative enrichment of 2.4-fold and 1.9-fold was achieved, respectively, both showing a single peak of ACOX activity.

When the peak fractions from the various purification steps were subjected to SDS-PAGE, only one single polypeptide band with a molecular mass of approximately 72 kDa was detected in the lanes corresponding to cation exchange chromatography (Fig. 1A). This indicates that the long-chain ACOX had been purified to homogeneity. Also, the subunit molecular mass is similar to that reported by Kirsh et al. (1986). To determine the molecular mass of the native protein the purified enzyme was loaded on a calibrated Superdex 200 16/60 column. The ACOX activity eluted from the column at a position corresponding to a molecular mass of approximately 140 kDa. This data together with the results from the SDS-PAGE analysis (Fig. 1) indicate that in pumpkin cotyledons the long-chain ACOX is a dimeric protein. When purified preparations of ACOX were subjected to IEF (Fig. 1B) on a PhastGel IEF 3-9 only one protein band was observed whose pI value was estimated to be 8.6. In the course of purification the long-chain ACOX proved to be stable when keeping the enzyme in solution contained 5-10 μM FAD and 10% glycerol. Also, freezing and thawing of the purified protein caused a minimal loss of activity after several weeks if stored in presence of FAD and glycerol.

In our study of the specificity for the fatty acid chain length of the purified ACOX we tested various acyl-CoA esters using the same concentration (25 μM) as Kirsh et al. (1986) in order to facilitate a comparison with these previous data (Fig. 2). The purified enzyme showed the highest activity with myristoyl-CoA, a C14 fatty acid chain, and the activity was 20% lower with palmitoyl-CoA as substrate. The enzyme was active on esters of fatty acids from C8 to C22 and inactive on C4-C6 chains. These results are summarized in Figure 2A. They illustrate that the pumpkin ACOX

shows activity with a rather broad spectrum of fatty acyl-CoAs. The effect of double bonds in the acyl moiety of the substrate is demonstrated for C18 fatty acid esters in Figure 2B: the purified enzyme reveals higher activity on C18 mono- and diunsaturated fatty acids than on C18 saturated fatty acids.

Figure 3 shows the effects of albumin (0.06% w/v) on enzyme activity with different concentrations of myristoyl-CoA and palmitoyl-CoA. Without albumin the purified enzyme displayed a marked substrate inhibition at concentrations of palmitoyl-CoA above 40 μM while similar concentrations of myristoyl-CoA had no or little inhibitory effect. With albumin in test solution the enzyme reaches its maximum activity at concentrations of palmitoyl-CoA that are 3-4 times higher than in the absence of albumin. Also, the inhibitory effect of high substrate concentrations is less dramatic.

Further biochemical properties of the long-chain ACOX from pumpkin are summarized in Table II. Optimum activity of the enzyme was observed at pH 8.3-8.5 and activities of over 80% of the maximum were found between 7.8 and 8.8 for both palmitoyl-CoA and myristoyl-CoA as substrates. The apparent K_m values (in absence of albumin) for C_{14}-CoA and C_{16}-CoA were 1.4 and 6.6 μM, respectively. The purified enzyme exhibited no activity with branched-chain fatty acids (tested with isobutyryl-CoA and isovaleryl-CoA as substrates) nor with glutaryl-CoA (a dicarboxylic acyl-CoA) and it was not active as acyl-CoA dehydrogenase. Sucrose density gradient fractionation confirmed that in etiolated pumpkin cotyledons the long-chain ACOX is localized in peroxisomes (data not shown; cf. Hayashi et al. 1998).

Furthermore, we have tested the effects of various possible inhibitors on the activity of long-chain ACOX employing myristoyl-CoA as substrate. Among the compounds tested EDTA and NaN_3 (both at 10 m*M*) showed no effect whereas PMSF (1 m*M*) reduced the enzyme activity by less than 20%, NEM (1 m*M*) and SHAM (2 m*M*) reduced the enzyme activity by 25-30%. Triton X-100 was found to inhibit the ACOX activity at concentrations above 0.02% with both palmitoyl-CoA and myristoyl-CoA as substrates as illustrated in Figure 4.

Discussion

Subunit and native molecular masses

ACOX, the first enzyme in the β-oxidation pathway for fatty acids, is considered to be peroxisomal enzyme. Recently, for higher plants the existence of three distinct ACOX varieties each specific for short-, medium- or long-chain acyl-CoAs, respectively, has been demonstrated in higher plants (Hook et al. 1996) and cDNAs for long-chain ACOX from *Phalaenopsis* and pumpkin have already been cloned (Do and Huang 1997, Hayashi et al. 1998). The Hook's paper indicated three different subunit molecular masses and multimeric structure for the three plant ACOXs (Hook et al. 1996) whereas mammalian short-, medium- and long-chain ACOXs have a similar subunit molecular mass and dimeric structure (Hashimoto 1996). In order to clarify the protein structure of the plant ACOXs we tried to purify and characterize these proteins and screen their corresponding cDNAs (Hayashi et al. 1988). In this paper we present data about the purification and characterization of the corresponding native enzyme. We assume that the published pumpkin long-chain ACOX cDNA (Hayashi et al. 1998) encode for the purified pumpkin long-chain ACOX because: 1) the antibodies raised against the fusion protein expressed in *Escherichia coli* recognize exclusively long- / medium-chain ACOX activity when pumpkin ACOX isoforms were separated by hydrophobic interaction chromatography (Hayashi et al. 1998); 2) the same antibodies showed high affinity and specificity for the purified enzyme; 3) western blotting experiments both following preliminary purification attempts not reported here and following the four chromatography steps indicated in Table I clearly

revealed a 72 kDa immunoreactive band exclusively in fractions showing long- / medium-chain ACOX activity (data not shown).

The enzyme was purified to apparent homogeneity and although the protein was obtained in relatively low yield the specific activity of 13.5 µmol min^{-1} mg^{-1} is within the range of activity (27 µmol min^{-1} mg^{-1}) reported by Kirsh et al. (1986) for the long-chain ACOX from cucumber. The subunit molecular mass of 72 kDa is identical to that reported by Kirsh et al. (1986) and matches perfectly the subunit size of the mature protein deduced from the cDNA (Hayashi et al. 1998). By size exclusion chromatography the native enzyme was identified as a dimeric protein which also confirms previous results (Kirsh et al., 1986). Also, its molecular mass (140 kDa) is similar to that of the native mammalian ACOXs (Hashimoto 1996).

Biochemical properties

Comparison of the biochemical properties of ACOXs from pumpkin and cucumber (Kirsh et al. 1986) reveals only few differences. The pI of 8.6 for the pumpkin enzyme is higher than the value of 7.8 reported by Kirsh et al. (1986) but much closer to the value of 9.1 that had been calculated from the deduced amino acid sequence of the mature protein (Hayashi et al. 1998). The cucumber enzymes is more active (at a substrate concentration of 25 µ*M*) with C16-C18 fatty acid chains as substrates (C14 fatty acid substrate had apparently not been tested) and some residual activity on C6 and C4 substrates had also been found. The enzyme from pumpkin cotyledons exhibits higher activity with C14 fatty acid as substrate and it is not active with short-

chain fatty acid as substrates. The reported K_m values are 6.6 and 20 μM for the pumpkin and the cucumber enzyme, respectively. The preference towards unsaturated C18 fatty acids was also observed in cucumber ACOX (Kirsh et al. 1986). The data presented in this report as well as in the paper by Kirsh et al. (1986) clearly indicate the existence of an ACOX isoform specific for esters of long-chain fatty acids. Such findings and the level of identity (about 30%) of the polypeptide encoded by the pumpkin ACOX cDNA with rat pristanoyl-CoA oxidase, trihydroxycoprostanoyl-CoA oxidase and palmitoyl-CoA oxidase (Hayashi et al. 1988) provide good evidence that the enzymes from both pumpkin and cucumber are the plant counterparts of the mammalian ACOXs. We propose to use the name of long-chain ACOX for both enzymes. As suggested by the data of Hook et. al (1996) the other two plant ACOXs which are specific for short- and medium-chain acyl-CoAs are less related proteins which is indicated by both the different subunit molecular masses and different secondary structures.

The high activity of pumpkin ACOX on esters of C14 –chain fatty acids is of particular interest. As mentioned above, Kirsh et al. (1986) did not test myristoyl-CoA in the course of the characterization of the purified cucumber ACOX. Hook et al. (1986) reported that the maize long-chain ACOX prefers palmitoyl-CoA. On the contrary, Gerhardt (1985) analyzing the substrate specificity of peroxisomal ACOX from spinach leaves and mung bean hypocotyls reported an higher V_{max} and a lower K_m with myristoyl-CoA than with palmitoyl-CoA. Olsen and Huang (1988) examined the ability of glyoxysomes isolated from germinating seed of elm, rape and maize to metabolize fatty acids. With the exception of elm, whose seeds contain high levels of

C10-fatty acids, glyoxysomes obtained from both maize and rape, showed a strong preference for myristoyl-CoA (higher V_{max}). Concluding, in plant tissues the initial enzymes of the β-oxidation system look to be particularly active on C14 chains nevertheless plant seeds generally contain fatty acids with chain length ≥ 18C. Of course, this does not exclude the presence of of other ACOXs active on longer (> 18C) acyl-CoAs.

Substrate inhibition

The substrate inhibition and the effect of albumin presented in Figure 3 are features common among rat liver ACOXs (Van Veldoven et al. 1992). In fact, partially purified rat pristanoyl-CoA oxidase displayed a marked substrate inhibition at concentration above 50 μM of palmitoyl-CoA or lignoceroyl-CoA in the absence of albumin. The enzyme activity was stimulated at higher substrate concentrations by the presence of albumin (0.06% w/v). Albumin was stimulatory, moderately or strongly, for all three rat ACOXs (Van Veldoven et al. 1992). Furthermore, Hashimoto (1982) reported K_m values of 12 μ*M* and K_i values of 20 μ*M* employing palmitoyl-CoA as substrate. Although for the enzyme from pumpkin the stimulatory effect was very low for the pumpkin enzyme, albumin at least clearly reduced the negative effect of high concentrations of palmitoyl-CoA (Fig. 3). As suggested by Van Veldoven et al. (1992) the effect of albumin could be due to several factors: stabilization or protection from inactivation, release of substrate inhibition by binding excess of substrate, enhancement of product dissociation from the enzyme by product binding, or preference by the

enzyme for the bound over the unbound substrate. A marked substrate inhibition by palmitoyl-CoA was not observed in crude homogenates or relatively unpurified ACOX preparations which contain a high concentration of soluble proteins. Therefore, 50 μM palmitoyl-CoA could be inhibitory for the assay of purified plant peroxisomes because of the low protein content, whereas a concentration of 100 μM as recently employed by Hoppe and Theimer (1997) or Eccleston and Ohlrogge (1998) should represent a good compromise considering the data shown in Figure 3. Because palmitoyl-CoA is a standard substrate for the assay of ACOX and β-oxidation (Gerhardt 1987) further investigations designed to establish the optimum concentration of palmitoyl-CoA for the assay of ACOX in different preparations such as crude homogenates or peroxisomal fractions from different plant tissues are needed. Probably V_{max} values could be the best parameter to compare the activity of ACOX with long-chain fatty acids as substrates.

Inhibition by chemicals

Other aspects of this study concern the inhibition by Triton X-100, NEM and SHAM. As previously indicated by Gerhardt (1987) it was shown that Triton X-100 inhibits the purified enzyme at concentrations higher than 0.02% (Fig. 4). Such substance should therefore be omitted from the assay mixture. The effect of NEM was tested because Furuta et al. (1981) suggested the addition of the compound in the assay for acyl-CoA dehydrogenases to trap free sulfhydryl groups. SHAM, a respiratory chain inhibitor, was employed in order to discriminate between

mitochondrial and peroxisomal β-oxidation in plants (e.g. Dideuaide et al. 1993). However, we registered a low inhibitory effect of SHAM on ACOX activity. Therefore, a careful investigation of the effects of SHAM on short- and medium-chain ACOX is needed to assess if SHAM is an appropriate inhibitor to study the subcellular localization of the β-oxidation pathway in plants.

Acknowledgments - This work was supported in part by a grant from the Research of the Future Program of the Japanese Society for the Promotion of Science (JSPS-RFTF96L00407), by grants-in-aid for scientific research from the Ministry of Education, Science and Culture of Japan (09274101, 09274103, 09440271 to M.N. and 09740606 to M.H.) and by a grant from the Nissan science foundation (Tokyo, Japan) to M.H.; L.D.B was supported as a COE fellow by a Monbusho scholarship. We acknowledge Dr. Roland R. Theimer (Bergische University, Germany) for critical reading of the manuscript and stimulating discussion.

References:

Dieuaide, M., Couée, I., Pradet; A. & Raymond, P. 1993. Effects of glucose starvation on the oxidation of fatty acids by maize root tip mitochondria and peroxisomes: evidence for mitochondrial fatty acid β-oxidation and acyl-CoA dehydrogenase activity in a higher plant. - Biochem. J. 296: 199-207.

Do, Y. -Y. & Huang, P.- L. 1997. Characterization of a pollination-related cDNA from *Phalaenopsis* encoding a protein which is homologous to human peroxisomal acyl-CoA oxidase. - Arch. Biochem. Biophys. 344: 295-300.

Dommes, V. & Kunau, W. H. 1976. A convenient assay for acyl-CoA-dehydrogenase. - Anal. Biochem. 71: 571-578.

Eaton, S., Bartlett, K. & Pourfarzam, M. 1996. Mammalian mitochondrial β-oxidation. - Biochem. J. 320: 345-357.

Eccleston, V. S. & Ohlrogge, J. B. 1998. Expression of lauroyl-acyl carrier protein thioesterase in *Brassica napus* seeds induces pathways for both fatty acid oxidation and biosynthesis and implies a set point for triacylglycerol accumulation. - Plant Cell 10: 613-621.

Furuta, S., Miyazawa, S. & Hashimoto, T. 1981. Purification and properties of rat liver acyl-CoA dehydrogenase and electron transfer flavoprotein. - J. Biochem. 90: 1739-1750.

Gerbling, H. & Gerhardt, B. 1989. Peroxisomal degradation of branched-chain 2-oxo acids. - Plant Physiol. 91: 1387-1392.

Gerhardt, B. 1983. Localization of β-oxidation enzymes in peroxisomes isolated from nonfatty plant tissues. - Planta 159: 238-246.

Gerhardt, B. 1985. Substrate specificity of peroxisomal acyl-CoA oxidase. - Phytochem. 24: 351-252.

Gerhardt, B. 1987. Peroxisomes and fatty acid degradation. - Methods Enzymol. 148: 516-525.

Gerhardt, B. 1992. Fatty acid degradation in plants. - Prog. Lipid Res. 31: 417-446

Hashimoto, T. 1982. Individual peroxisomal β-oxidation enzymes. - Ann. N.Y. Acad. Sci. 386: 5-12.

Hashimoto, T. 1996. Pèroxisomal β-oxidation: enzymology and molecular biology. - Ann. N.Y. Acad. Sci. 804: 86-98.

Hayashi, H., De Bellis, L., Hayashi, M., Yamaguchi, K., Kato, A. & Nishimura, M. 1998. Molecular characterization of a glyoxysomal long-chain acyl-CoA oxidase that is synthesized as a precursor of higher molecular mass in pumpkin. - J. Biol. Chem. 273: 8301-8307.

Hoppe, A. & Theimer, R. R. 1997. Enzymes for lipolysis and fatty acid metabolism in different organelle fractions from rape seed cotyledons. - Planta 202: 227-234.

Hook, M. A., Bode, K. & Couće, I. 1995. Regulation of acyl-CoA oxidases in maize seedlings. - Phytochem. 40: 657-660.

Hook, M. A., Bode, K. & Couée, I. 1996. Higher-plant medium- and short-chain acyl-CoA oxidases: identification, purification and characterization of two novel enzymes of eukaryotic peroxisomal b-oxidation. - Biochem. J. 320: 607-614.

Kirsh, T., Loffler, H. G. & Kindl, H. 1986. Plant acyl-CoA oxidase. Purification, characterization, and monomeric apoprotein. - J. Biol. Chem. 261: 8570-8575.

Olsen, J. A. & Huang A. H. C. 1988. Glyoxysomal acyl-CoA synthetase and oxidase from germinating elm, rape and maize seed. - Phytochem. 27: 1601-1603.

Van Veldhoven, P. P., Vanhove, G., Assselberghs, S., Eyssen, H. J. & Manaerts, G. P. 1992. Substrate specificities of rat liver peroxisomal acyl-CoA oxidase: palmitoyl-CoA oxidase (inducible acyl-CoA oxidase), pristanoyl-CoA oxidase (non-inducible acyl-CoA oxidase), and trihydroxycoprostanoyl-CoA oxidase. - J. Biol. Chem. 267: 20065-20074.

Figure legends:

Figure 1. A, SDS-PAGE analysis of long-chain ACOX on PhastGel gradient 10-15% during purification. Peak fractions from Phenyl Supherose, Hydroxyapatite, HiTrap Blue and Mono S (fractions no. 21-23) columns were subjected to SDS-PAGE. Approximately similar amounts of activity were loaded per lane. Lane M represents molecular mass markers whose values are indicated on the left. B, Isoelectric focusing in the range pH 3 to pH 9 of the purified long-chain ACOX. 1 µl from peak fraction (no. 23) after the Mono S chromatography step was loaded. Lane M represent pI markers whose pH values are indicated on the left. The gels were silver-stained.

Figure 2. Substrate specificity profiles of purified pumpkin ACOX. A. Selectivity for the chain length of the fatty acids acyl-CoA as substrate. B. Selectivity for C18 fatty acids with an increasing number of double bonds. All activities were determined using 25 µ*M* acyl-CoA as substrates. The highest activity between the data of the two panels was arbitrarily set at 100.

Figure 3. Activity of the purified long-chain ACOX as a function of substrate concentration in presence or absence of albumin (0.06% w/v). A. Activity measured with increasing concentration of palmitoyl-CoA with (#) and without (!) albumin. B. Activity measured at increasing concentration of myristoyl-CoA with (□) or without (■) of albumin. In each diagram the highest activity was arbitrarily set at 100.

Figure 4. The effect of increasing concentrations of Triton X-100 on the activity of the purified pumpkin ACOX. Myristoyl-CoA (25 μM) was used in the standard assay mix. The activity in absence of Triton X-100 was arbitrarily set at 100.

Table I. Purification of long-chain acyl-CoA oxidase from pumpkin cotyledons

Purification step	Total protein	Total activity	Recovery	Specific activity	Purificati
	mg	*μmol min^{-1}*	*%*	*μmol min^{-1} mg^{-1}*	*-fold*
Crude extract	1500	28.4	100	0.019	-
Phenyl Supherose	16.8	11.2	39.4	0.67	35
Hydroxyapatite	2.1	6.3	22.2	3.0	158
Hi Trap Blue	0.210	1.5	5.3	7.1	374
Mono S	0.037	0.5	1.8	13.5	710

Table II. Properties of pumpkin long-chain acyl-CoA oxidase

Native molecular mass	140 kD
Subunit molecular mass	72 kD
Isoelectric point	8.6
K_m (palmitoyl-CoA)	6.6
K_m (myristoyl-CoA)	1.4
pH optimum (palmitoyl-CoA)	8.3-8.5
pH optimum (myristoyl-CoA)	8.3-8.5
Activity on branched-chain acyl-CoAs (isobutyryl-CoA and isovaleryl-CoA)	None
Activity on glutaryl-CoA (dicarboxylic)	None
Acyl-CoA dehydrogenase activity	None
Subcellular localization	Peroxisomes

To: Prof. Mikio Nishimura

FAX 0081 564 55 7505

4 pages FAX

Hi! Physiol Plant. figs

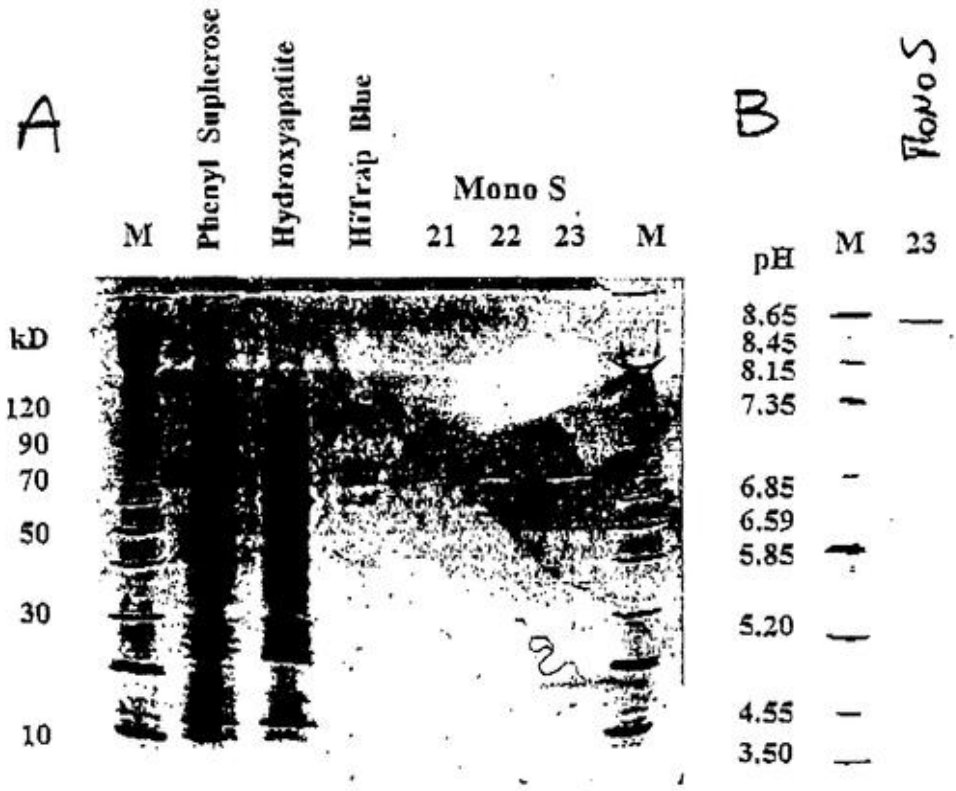

Fig 1

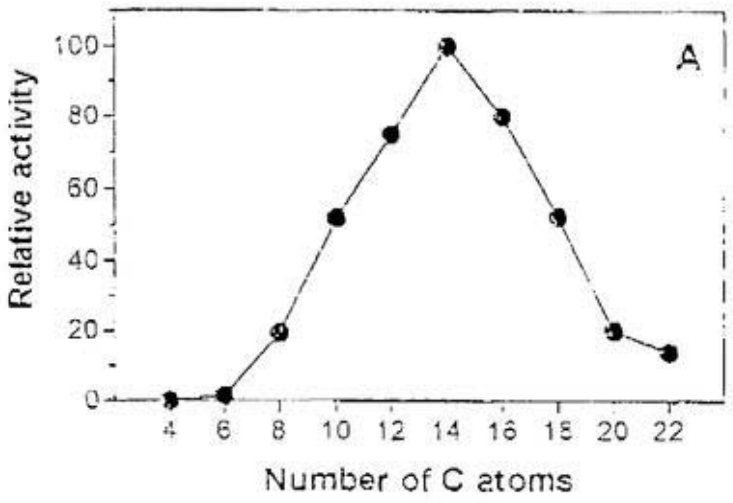
A
Relative activity
100
80
60
40
20
0
4
6
8
10
12
14
16
18
20
22
Number of C atoms

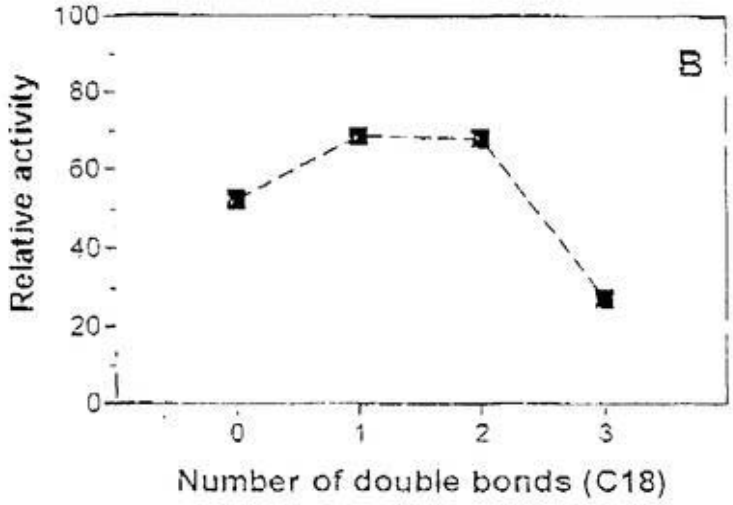
B
Relative activity
100
80
60
40
20
0
0
1
2
3
Number of double bonds (C18)

FIG 2

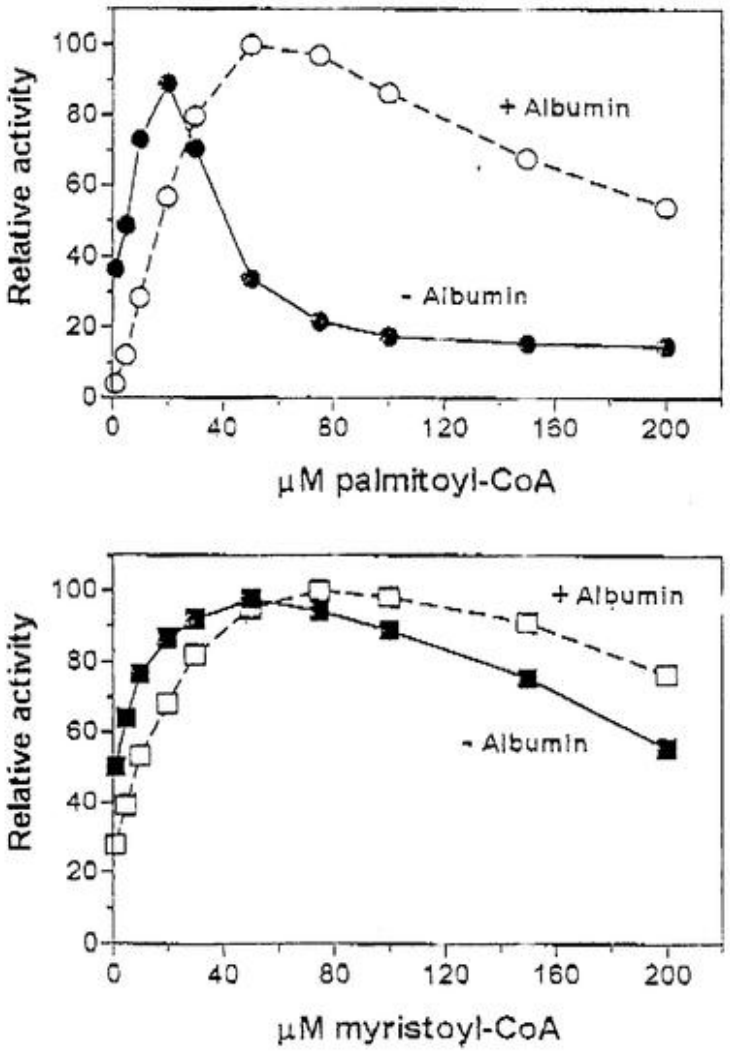
Relative activity
100
80
60
40
20
0
+ Albumin
- Albumin
0
40
80
120
160
200
µM palmitoyl-CoA
Relative activity
100
80
60
40
20
0
+ Albumin
- Albumin
0
40
80
120
160
200
µM myristoyl-CoA

FIG 3

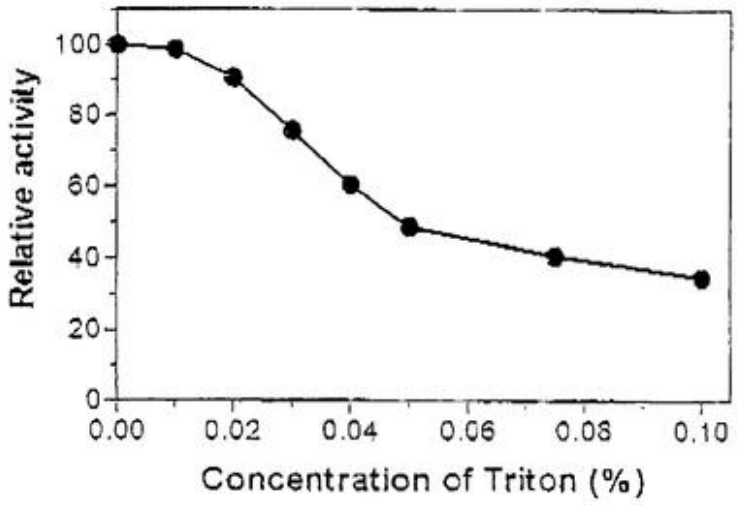
Relative activity
100
80
60
40
20
0
0.00
0.02
0.04
0.06
0.08
0.10
Concentration of Triton (%)

Fig 4

Functional Transformation of Plant Peroxisomes

Makoto Hayashi, Kanako Toriyama, Maki Kondo, Akira Kato, Shoji Mano, Luigi De Bellis, Yasuko Ishimaru, Katsushi Yamaguchi, Hiroshi Hayashi and Mikio Nishimura***

Department of Cell Biology, National Institute for Basic Biology, Okazaki 444, Japan

Running title: Plant peroxisomes

Corresponding author:

Mikio Nishimura

Department of Cell Biology

National Institute for Basic Biology, Okazaki 444, Japan

Phone number; 81-564-55-7500

Fax number; 81-564-55-7505

E-mail; mikosome@nibb.ac.jp

Footnote: *Permanent address: Dipartimento di Biologia delle Piante Agrarie, Sezione di Fisiologia Vegetale, Via Mariscoglio 34, 56124 Pisa, Italy. **Author to whom all correspondence and reprint requests should be addressed. E-mail mikosome@nibb.ac.jp.

ABSTRACT

Peroxisomes in higher plant cells are known to differentiate into at least three different classes, namely glyoxysomes, leaf peroxisomes and unspecialized peroxisomes, depending on the cell types. In germinating fatty seedlings, glyoxysomes that first appear in the etiolated cotyledonary cells are functionally transformed into leaf peroxisomes during greening. Subsequently, the organelles are transformed back into glyoxysomes during senescence of the cotyledons. Flexibility of function is a distinct feature of plant peroxisomes. This review briefly describes recent studies on the regulatory mechanisms involved in the changes of the function of plant peroxisomes.

Index Entries: Glyoxysomes; leaf peroxisomes; fatty acid β-oxidation; glyoxylate cycle; photorespiration; Arabidopsis

CLASSIFICATION AND FUNCTION OF PLANT PEROXISOMES

In higher plants, peroxisomes can be classified into at least three classes in terms of function, *i.e.* glyoxysomes, leaf peroxisomes, and unspecialized peroxisomes (*1*). Each class of plant peroxisomes contains a special set of enzymes that is related to a distinct metabolic role, although all plant peroxisomes have common features that are characteristic of peroxisomes.

Numerous studies on glyoxysomes in storage organs of oil seeds, such as endosperm and cotyledons, have revealed that glyoxysomes play an important role in lipid metabolism (*2*). During the postgerminative growth of the seedlings, the stored fats are metabolized to produce sucrose. Sucrose is then transferred to the shoot and root apical meristems, and provides a carbon source that is necessary for division and growth of the cells before the plants are able to start photosynthesis. This unique type of gluconeogenesis involves many enzymes localized in several subcellular compartments, including lipid bodies, glyoxysomes, mitochondria, and the cytosol. Within this gluconeogenic pathway, the conversion of fatty acids to succinate takes place only in the glyoxysomes.

In the glyoxysomes, the fatty acids are first activated to fatty acyl coenzyme A (CoA) by a fatty acyl CoA synthetase (*3*). Subsequently fatty acyl CoA is the substrate for fatty acid β-oxidation which consists of four enzymatic reactions (*4*), the first reaction being catalyzed by acyl CoA oxidase. Three isozymes of acyl CoA oxidase each with a distinct substrate specificity for long, medium or short chain acyl CoAs have been discovered (*5, 6*). The cooperative action of these isozymes permits glyoxysomes to completely metabolize fatty acids producing acetyl CoA within the organelles. From this point of view, glyoxysomes in plant cells are different from mammalian peroxisomes. Acyl CoA oxidase in mammalian peroxisomes can metabolize only long and medium chain fatty acids (*7*), whereas mammalian

mitochondria have four isozymes of an acyl CoA dehydrogenease that are responsible for complete fatty acid β-oxidation in mammalian cells (*8*). In this context, it is noteworthy that plant mitochondria are believed to lack fatty acid β-oxidation (*9, 10*), although this is still a matter of controversy (*11*). The second and third enzymatic reactions are catalyzed by a single enzyme, a so-called multifunctional enzyme, that is comprised of enoyl CoA hydratase and β-hydroxyacyl CoA dehydrogenase activities (*12*). The fourth reaction is catalyzed by 3-ketoacyl CoA thiolase (referred to simply as thiolase in this paper.) (*13, 14*). Acetyl CoA, an end product of fatty acid β-oxidation, is metabolized further to produce succinate by the action of five enzymes of the glyoxylate cycle involving malate synthase (*15-19*), isocitrate lyase (*20-23*), malate dehydrogenase (*24, 25*), citrate synthase (*26*) and aconitase (*27, 28*). Except aconitase which appears to be cytosolic (*29, 30*), these enzymes were all shown to be localized in the glyoxysomes. By the combination of fatty acid β-oxidation and the glyoxylate cycle, fat-storing plant tissues can efficiently convert lipids into a transportable sugar (sucrose) that can be transferred through the vascular system.

Leaf peroxisomes are widely found in cells of photosynthetic plant tissues, such as green cotyledons or leaves (*31*). In C3 plants, these cells exhibit a light-dependent O_2 uptake and CO_2 release that is called photorespiration. This physiological phenomenon is initiated by the oxygenase reaction of ribulose bisphosphate carboxylase/oxygenase (RuBisCO; the key enzyme for CO_2 fixation in photosynthesis) that depends on the O_2 concentration and on light intensity. Two phosphoglycolates, byproducts of the oxygenase reaction, are converted to produce one phosphoglycerate, an intermediate of the Calvin-Benson cycle, along with CO_2 and ammonia by the photorespiration. The metabolic pathway involves many enzymatic reactions located in leaf peroxisomes, chloroplasts and mitochondria. Leaf peroxisomes possess some of the enzymes, such as glycolate oxidase (*32, 33*), hydroxypyruvate reductase (*34, 35*) and some aminotransferases *(31)*. By a combination of these enzymes, leaf peroxisomes convert glycolate to glycine, and metabolize serine to glycerate.

Unspecialized peroxisomes are found in other plant organs, such as roots and stems, that contain neither glyoxysomes nor leaf peroxisomes. However, the main metabolic function of the unspecialized peroxisomes is not defined.

FUNCTIONAL TRANSFORMATION OF PLANT PEROXISOMES

Plant peroxisomes are known to interconvert in function between glyoxysomes and leaf peroxisomes during certain cellular developmental processes, such as greening and senescence (*36*). The functional transformation of plant peroxisomes has been most extensively studied in cotyledonary cells of oil seed plants. When the seeds germinate, seedlings start mobilizing the seed reserve substances in the etiolated cotyledons. During subsequent development in the light, the etiolated cotyledons turn green and begin photosynthesis. In order to support this drastic metabolic changes that occur as a result of illumination, the glyoxysomes of the cotyledonary cells are transformed directly into leaf peroxisomes during the greening process (*37, 38*). Once the young plants expand their leaves, the green cotyledons undergo senescence. Along with this process, a reverse transformation of leaf peroxisomes to glyoxysomes has been demonstrated in cotyledonary cells (*39*). The glyoxysomes that appear in the senescent organs seem to be responsible for the recovery of carbon from membrane lipids before the senescing cells die. Induction of glyoxysomes was also found in cells of other senescent organs, such as leaves or petals (*40*). It has been also demonstrated that peroxisomes in anise (*Pimpinella anisum*) suspension-cultured cells interconvert in function between glyoxysomes and unspecialized peroxisomes when the source of carbon in the growth medium was changed (*41*).

Since the enzyme composition of glyoxysomes differs from that of leaf peroxisomes, the functional transformation requires the replacement of distinct sets of enzymes necessary for either peroxisomal function. The enzymes localized in plant

peroxisomes can be divided into three categories: One is the glyoxysome-specific enzymes, such as malate synthase and isocitrate lyase, which are members of the glyoxylate cycle. The second category consists of leaf peroxisome-specific enzymes such as hydroxypyruvate reductase and glycolate oxidase, which participate in photorespiration. The third category contains the enzymes that are mainly present in glyoxysomes but still remain in leaf peroxisomes, such as catalase, malate dehydrogenase and the enzymes for fatty acid β-oxidation. Therefore, the transformation of glyoxysomes to leaf peroxisomes occurring during post-germinative growth is accompanied by [1] the disappearance of glyoxysome-specific enzymes, [2] the appearance and accumulation of leaf peroxisome-specific enzymes, and [3] the decrease of enzymes present in both glyoxysomes and leaf peroxisomes. The reverse process takes place when leaf peroxisomes are transformed back into glyoxysomes during senescence. Both the appearance and the disappearance of the peroxisomal enzymes are regulated at the transcriptional level (*36, 42*), and by a specific protein degradation that eliminates the pre-existing enzymes (*43*).

PROTEIN TARGETING TO PLANT PEROXISOMES

Enzymes localized in plant peroxisomes are synthesized in the cytosol, and become functional after their post-translational transport into peroxisomes (*36, 44*). Two types of targeting signals to plant peroxisomes have been elucidated. One type of targeting signal is a unique tripeptide sequence found in the carboxyl terminus of the mature proteins that is similar to animal and yeast PTS1 (PTS stands for peroxisomal targeting signal) (*45, 46*). In order to characterize the targeting signal, we have examined the ability of 24 carboxy-terminal amino acid sequences to facilitate the transport of a bacterial protein, β-glucuronidase (GUS) into peroxisomes of cells of transgenic Arabidopsis plants (*47, 48*). Immunocytochemical analysis of the transgenic plants revealed that permissible combinations of amino acids for PTS1 in plant cells are

[C/A/S/P]-[K/R]-[I/L/M], although tripeptides with proline at the first amino acid position and isoleucine at the carboxyl terminus show weak targeting efficiencies (*48*). As shown in Table 1, the plant PTS1 is similar but not completely identical to animal and yeast PTS1. At present, a multifunctional enzyme (*12*), malate synthase (*15-19*), isocitrate lyase (*20-23*), glycolate oxidase (*32, 33*), hydroxypyruvate reductase (*34, 35*), and uricase (*49*) are known to contain the plant PTS1 at their carboxyl terminus. In the case of hydroxypyruvate reductase, alternative splicing of mRNA also participates in determining the localization of leaf peroxisomal and cytosolic hydroxypyruvate reductase (*35*). In contrast to our studies, other studies using tobacco BY-2 suspension-cultured cells suggest that a wider range of amino acid residues may function as the plant PTS1 (*50*).

Another type of targeting signal is included in a cleavable amino terminal presequence. In higher plant cells, long chain acyl CoA oxidase (*5*), thiolase (*13, 14*), malate dehydrogenase (*24, 25*) and citrate synthase (*26*) are known to be synthesized as precursor proteins which shows a higher molecular mass due to the amino-terminal presequence. The amino terminal presequences of these proteins contain a consensus sequence [R]-[L/Q/I]-X5-[H]-[L] (X stands for any amino acid) that is similar to the animal and yeast PTS2 signal *(5, 44)*. We generated transgenic Arabidopsis plants that express fusion proteins containing GUS with the amino terminal presequence of either citrate synthase or malate dehydrogenase (*25, 51*). In both cases, the fusion proteins were correctly transported and the amino terminal presequences were removed to produce mature proteins within the peroxisomes. When an amino acid substitution was introduced into the PTS2, the fusion proteins were no longer transported into peroxisomes. On the other hand, when a cysteine residue at the processing site was changed to another amino acid, the fusion protein was transported to peroxisomes, but accumulated in the precursor form with a higher molecular mass. These results indicate that the plant PTS2 functions as a targeting signal for plant peroxisomes, and the intracellular transport of the PTS2-proteins does not require the processing of the

presequence (*52*).

Glyoxysomal enzymes have been shown to be transported into both leaf peroxisomes and unspecialized peroxisomes by an *in vitro* protein transport experiments using isolated peroxisomes (*43*) and by *in vivo* experiments using transgenic plants expressing glyoxysomal enzymes in ectopic organs (*53, 54*). Further analyses employing transgenic plants revealed that fusion proteins containing either PTS1 or PTS2 were also incorporated into all types of plant peroxisomes, *i.e.* glyoxysomes, leaf peroxisomes, and unspecialized peroxisomes (*47, 51*). These results indicate both that all plant peroxisomes have common protein transport machineries, and that the protein transport machineries are not changed by the functional transformation of plant peroxisomes.

GENETIC ANALYSIS OF PLANT PEROXISOMES

A genetic approach may be an effective strategy toward understanding the regulatory mechanism(s) leading to the functional transformation of plant peroxisomes. In order to identify the genes involved in the regulation of the peroxisomal function, we used 2,4-dichlorophenoxybutyric acid (2,4-DB) as a compound for the identification of plant mutants that have defective peroxisomes (*55*). It has been demonstrated that two methylene groups of the butyric side chain in 2,4-DB are removed by the action of peroxisomal fatty acid β-oxidation resulting in the formation of the herbicide, 2,4-dichlorophenoxyacetic acid (2,4-D) (*56*). Therefore, we expected that 2,4-DB would inhibit the growth of wild-type plants because of its conversion to 2,4-D (Fig. 1, upper panel), whereas mutants that have defects in peroxisomal fatty acid β-oxidation would become resistant to 2,4-DB. On the basis of this hypothesis, we isolated four *Arabidopsis thaliana* mutants (obtained from ethyl methanesulfonate-mutagenized M2 seeds) that show specifically resistance to 2,4-DB but not to 2,4-D during the early stage of post-germinative growth (Fig. 1, upper panel). Genetic analyses revealed that

these mutants can be classified as carrying alleles at three independent loci, which we designated *ped1*, *ped2*, and *ped3* (where *ped* stands for peroxisome defective).

To determine the correct function of the glyoxysomes in these mutants, we first examined the effect of sucrose on their growth because defects in glyoxysomal fatty acid β-oxidation may inhibit the conversion of seed storage lipids into sucrose that is required for the early stages of post-germinative growth. As shown in Fig. 1 (lower panel), a wild-type plants can grow well and expand green leaves in the absence of sucrose but the growth of the mutants on sucrose-free growth medium is strongly inhibited. However, when these mutants were germinated on growth medium supplied with sucrose, they correctly expanded both green cotyledons and leaves. After onset of photosynthesis, they no longer require sucrose for growth. The requirement for sucrose only at the early stage of seedling growth was taken as an indication that the activity of glyoxysomal fatty acid β-oxidation in these mutants is blocked.

Indeed, immunoblot analyses revealed that the *ped1* mutant lacks detectable amounts of thiolase, an enzyme of the fatty acid β-oxidation complex in the glyoxysomes (Fig. 2, *ped1*). Further analyses indicated that the *PED1* locus encodes for thiolase, and that *ped1* shows a frame-shift mutation at the fourth exon of the gene. Evidently, the lack of thiolase in the glyoxysomes of the *ped1* mutant may be the reason for the inhibition of fatty acid β-oxidation. This loss of fatty acid β-oxidation activity then prevents both the production of sucrose from seed storage lipids as well as that of 2,4-D from 2,4-DB. Furthermore, the glyoxysomes in the *ped1* mutant are two or three times larger in diameter than those in the wild-type plant and exhibit vesicle-like structures within the matrix (Fig. 3, B). Since leaf peroxisomes and unspecialized peroxisomes in the *ped1* mutant have normal size and structure, such morphological changes of the glyoxysomes may be due to the accumulation of one or more metabolic intermediates of the fatty acid β-oxidation.

In contrast, etiolated cotyledons of the *ped2* mutant were demonstrated to contain two types of thiolase (Fig. 2, *ped2*). One of them has the mature form of the

thiolase protein (45 kD), whereas the other form obviously is the precursor of the protein with a somewhat higher molecular mass (48 kD) (*13, 14*). Precursors to other PTS2-containing proteins were also accumulated in the *ped2* mutant, indicating that the *ped2* mutant has a defect in the import of PTS2-containing proteins into glyoxysomes. The missing of these proteins causes a reduction of the glyoxysomal matrix. This is indicated by the observation that the density of *ped2* glyoxysomes in sucrose density gradients is reduced to 1.19 g/cm^3 as opposed to wild-type glyoxysomes (1.25 g/cm^3). In electron micrographs of etiolated cotyledons of the *ped2* mutant, the glyoxysomes appear small and shrunken (Fig. 3, C).

Analyses of yeast mutants in which protein import to peroxisomes or biogenesis of peroxisomes is defective succeeded in identifying many peroxins (*57, 58*). Peroxins are proteins that are involved in peroxisome biogenesis including peroxisomal matrix protein import, membrane biogenesis, peroxisome proliferation, and peroxisome inheritance. In addition, these studies cloned and characterized the corresponding *PEX* genes. Among these *PEX* genes, *PEX7* has been shown to encode the PTS2 receptor and peroxisomes in the *pex7* mutant fail to import thiolase, but can import PTS1-containing proteins (*59, 60*). Most of the other *PEX* mutants, except *PEX5*, which encodes the PTS1 receptor, are unable to import both PTS1-containing proteins and PTS2-containing proteins (*61*). It was suggested that *PEX13* and *PEX14* encode peroxisomal membrane proteins that bind to Pex5p and/or Pex7p (*62-64*). Although other *PEX* gene products may not be involved in the protein transport machinery, the import of proteins into peroxisomes of these mutants is presumably inhibited by indirect factors such as peroxisomal membrane biogenesis, peroxisome proliferation, and peroxisome inheritance. We are now examining whether the *ped2* mutant has a defect in the import of only PTS2-containing proteins or of both PTS1-containing proteins and PTS2-containing proteins. In the former case, the PTS2 receptor is a candidate for the protein encoded by the *PED2* gene, while in the latter case, the *PED2* gene may be involved in regulating the biogenesis of plant peroxisomes. Identification of the genes

encoded by *ped2* as well as *ped3* are now in progress.

The collecting of the mutants that have a defect in glyoxysomal fatty acid β-oxidation is also still pursued in this laboratory. Such mutants will give us new insights into the regulatory mechanisms involved in the correct functioning of plant peroxisomes.

ACKNOWLEDGMENTS

We thank Prof. R. R. Theimer (Botanishes Institut der Universität, München, Germany) for useful discussion and critical reading of the manuscript. This work was supported in part by a grant from the Research for the Future Program of the Japanese Society for the Promotion of Science (JSPS-RFTF96L00407), and by grants-in-aid for scientific research from the Ministry of Education, Science and Culture of Japan (09274101, 09274103, 09440271 to M.N. and 09740606 to M.H.) and by a grant from the Nissan Science Foundation (Tokyo, Japan) to M.H.

REFERENCES

1. Beevers, H. (1979) Microbodies in higher plants. *Annu. Rev. Plant Physiol.* **30,** 159-193.

2. Beevers, H. (1982) Glyoxysomes in higher plants. *Annu. NY Acad. Sci.* **386,** 243-251.

3. Huang, A. H. C., Trelease, R. N. and Moore, T. S. (1983) *Plant Peroxisomes.* Academic Press, New York, NY

4. Kindl, H. (1993) Fatty acid degradation in plant peroxisomes: function and biosynthesis of the enzymes involved. *Biochimie* **75,** 225-30.

5. Hayashi, H., De Bellis, L., Yamaguchi, K., Kato, A., Mano, S., Hayashi, M., Nishimura, M. (1998) Molecular characterization of a glyoxysomal long-chain acyl-CoA oxidase that is synthesized as a precursor of higher molecular mass in pumpkin. *J. Biol. Chem.* **273,** 8301-8307.

6. Hooks, M. A., Bode, K. and Couee, I. (1996) Higher-plant medium- and short-chain acyl-CoA oxidases: Identification, purification and characterization of two novel enzymes of eukaryotic peroxisomal β-oxidation. *Biochem. J.* **320,** 607-614.

7. Osumi, T. and Hashimoto, T. (1978) Acyl-CoA oxidase of rat liver: a new enzyme for fatty acid oxidation. *Biochem. Biophys. Res. Commun.* **83,** 479-485.

8. Eaton, S., Bartlett, K. and Pourfarzam, M. (1996) Mammalian mitochondrial β-

oxidation. *Biochem. J.* **320,** 345-357.

9. Kindl H. (1984) Lipid degradation in higher plants, in *Fatty acid metabolism and its regulation* (Numa S., ed.) Elsevier, Amsterdam, pp. 181-204.

10. Hoppe, A. and Theimer, R. R. (1997) Enzymes for lipolysis and fatty acid metabolism in different organelle fractions from rape seed cotyledons. *Planta* **202,** 227-234.

11. Masterson, C., Wood, C. and Thomas, D. R. (1990) β-Oxidation enzymes in the mitochondria of *Arum* and oilseed rape. *Planta* **182,** 129-135.

12. Preisig-Muller, R., Guhnemann-Schafer, K. and Kindl, H. (1994) Domains of the tetrafunctional protein acting in glyoxysomal fatty acid β-oxidation. Demonstration of epimerase and isomerase activities on a peptide lacking hydratase activity. *J. Biol. Chem.* **269,** 20475-20481.

13. Preisig-Muller, R. and Kindl, H. (1993) Thiolase mRNA translated *in vitro* yields a peptide with a putative N-terminal presequence. *Plant Mol. Biol.* **22,** 59-66.

14. Kato, A., Hayashi, M., Takeuchi, Y. and Nishimura, M. (1996) cDNA cloning and expression of a gene for 3-ketoacyl-CoA thiolase in pumpkin cotyledons. *Plant Mol. Biol.* **31,** 843-852.

15. Comai, L., Baden, C. S. and Harada, J. J. (1989) Deduced sequence of a malate synthase polypeptide encoded by a subclass of the gene family. *J. Biol. Chem.* **264,** 2778-2782.

16. Graham, I. A., Smith, L. M., Brown, J. W., Leaver, C. J. and Smith S. M. (1989) The malate synthase gene of cucumber. *Plant Mol. Biol.* **13,** 673-684.

17. Mori, H., Takeda-Yoshikawa, Y., Hara-Nishimura, I. and Nishimura, M. (1991) Pumpkin malate synthase: Cloning and sequencing of the cDNA and Northern blot analysis. *Eur. J. Biochem.* **197,** 331-336.

18. Rodriguez, D., Ginger, R. S., Baker, A. and Northcote, D. H. (1990) Nucleotide sequence analysis of a cDNA clone encoding malate synthase of castor bean (*Ricinus communis*) reveals homology to DAL7, a gene involved in allantoin degradation in *Saccharomyces cerevisiae*. *Plant Mol. Biol.* **15,** 501-504.

19. Turley, R. B., Choe, S. M., Ni, W. and Trelease, R. N. (1990) Nucleotide sequence of cottonseed malate synthase. *Nucleic Acids Res.* **18,** 3643.

20. Beeching, J. R. and Northcote, D. H. (1987) Nucleic acid (cDNA) and amino acid sequences of isocitrate lyase from castor bean. *Plant Mol. Biol.* **8,** 471-475.

21. Mano S., Hayashi M., Kondo M. and Nishimura M. (1996) cDNA cloning and expression of a gene for isocitrate lyase in pumpkin cotyledons. *Plant Cell Physiol.* **37,** 941-948.

22. Turley, R. B., Choe, S. M. and Trelease, R. N. (1990) Characterization of a cDNA clone encoding the complete amino acid sequence of cotton isocitrate lyase. *Biochim. Biophys. Acta* **1049,** 223-226.

23. Zhang, J. Z., Gomez, P. M., Baden, C. S. and Harada, J. J. (1993) Two classes

of isocitrate lyase genes are expressed during late embryogeny and postgermination in *Brassica napus* L. *Mol. Gen. Genet.* **238,** 177-184

24. Gietl, C. (1990) Glyoxysomal malate dehydrogenase from watermelon is synthesized with an amino-terminal transit peptide. *Proc. Natl. Acad. Sci. USA* **87,** 5773-5777.

25. Kato, A., Takeda-Yoshikawa, Y., Hayashi, M., Kondo, M., Hara-Nishimura, I. and Nishimura, M. (1998) Glyoxysomal malate dehydrogenase in pumpkin: cloning of a cDNA and functional analysis of its presequence. *Plant Cell Physiol.* **39,** 186-195.

26. Kato, A., Hayashi, M., Mori, H. and Nishimura, M. (1995) Molecular characterization of a glyoxysomal citrate synthase that is synthesized as a precursor of higher molecular mass in pumpkin. *Plant Mol. Biol.* **27,** 377-390.

27. Hayashi, M., De Bellis, L., Alpi, A. and Nishimura, M. (1995) Cytosolic aconitase participates in the glyoxylate cycle in etiolated pumpkin cotyledons. *Plant Cell Physiol.* **36,** 669-680.

28. Peyret, P., Perez, P. and Alric, M. (1995) Structure, genomic organization, and expression of the Arabidopsis thaliana aconitase gene - Plant aconitase show significant homology with mammalian iron-responsive element-binding protein. *J. Biol. Chem.* **270,** 8131-8137.

29. De Bellis, L., Hayashi, M., Biagi, P. P., Hara-Nishimura, I., Alpi, A. and Nishimura, M. (1994) Immunological analysis of aconitase in pumpkin cotyledons - The absence of aconitase in glyoxysomes. *Physiol. Plant.* **90,** 757-762.

30. Courtois-Verniquet, F. and Douce, R. (1993) Lack of aconitase in glyoxysomes and peroxisomes. *Biochem. J.* **294,** 103-107.

31. Tolbert N. E. (1981) Metabolic pathways in peroxisomes and glyoxysomes. *Annu. Rev. Biochem.* **50,** 133-157.

32. Tsugeki R., Hara-Nishimura I., Mori H., Nishimura M. (1993) Cloning and sequencing of cDNA for glycolate oxidase from pumpkin cotyledons and Northern blot analysis. *Plant Cell Physiol.* **34,** 51-57.

33. Volokita, M. and Somerville, C. R. (1987) The primary structure of spinach glycolate oxidase deduced from the DNA sequence of a cDNA clone. *J. Biol. Chem.* **262,** 15825-15828.

34. Greenler, J. M., Sloan, J. S., Schwartz, B. W. and Becker, W. M. (1989) Isolation, characterization and sequence analysis of a full-length cDNA clone encoding NADH-dependent hydroxypyruvate reductase from cucumber. *Plant Mol. Biol.* **13,** 139-150.

35. Hayashi, M., Tsugeki, R., Kondo, M., Mori, H. and Nishimura, M. (1996) Pumpkin hydroxypyruvate reductases with and without a putative C-terminal signal for targeting to microbodies may be produced by alternative splicing. *Plant Mol. Biol.* **30,** 183-189.

36. Nishimura, M., Hayashi, M., Kato, A., Yamaguchi, K. and Mano, S. (1996) Functional transformation of microbodies in higher plant cells. *Cell Struct. Funct.* **21,** 387-393.

37. Nishimura, M., Yamaguchi, J., Mori, H., Akazawa, T. and Yokota, S. (1986) Immunocytochemical analysis shows that glyoxysomes are directly transformed to leaf peroxisomes during greening of pumpkin cotyledons. *Plant Physiol.* **80,** 313-316.

38. Titus, D. E. and Becker, W. M. (1985) Investigation of the glyoxysome-peroxisome transition in germinating cucumber cotyledons using double-label immunoelectron microscopy. *J. Cell. Biol.* **101,** 1288-1299.

39. De Bellis, L. and Nishimura, M. (1991) Development of enzymes of the glyoxylate cycle during senescence of pumpkin cotyledons. *Plant Cell Physiol.* **32,** 555-561.

40. De Bellis, L., Tsugeki, R. and Nishimura, M. (1991) Glyoxylate cycle enzymes in peroxisomes isolated from petals of pumpkin (*Cucurbita* sp.) during senescence. *Plant Cell Physiol.* **32,** 1227-1235.

41. Kudielka, R. A., Theimer, R. R. (1983) Repression of glyoxysomal enzyme activities in anise (*Pimpinella anisum* L.) suspension cultures. *Plant Sci. Lett.* **31**. 245-252.

42. Sarah, C. J. and Graham, I. A. and Reynolds, S. J. and Leaver, C. J., Smith, S. M. (1996) Distinct cis-acting elements direct the germination and sugar responses of the cucumber malate synthase gene. *Mol. Gen. Genet.* **250,** 153-161.

43. Mori, H. and Nishimura, M. (1989) Glyoxysomal malate synthase is specifically degraded in microbodies during greening of pumpkin cotyledons. *FEBS Lett.*

244, 163-166.

44. Olsen, L. J. and Harada, J. J. (1995) Peroxisomes and their assembly in higher plants. *Annu. Rev. Plant Physiol. Plant Mol. Biol.* **46,** 123-146.

45. De Hoop, M. J. and Ab, G. (1992) Import of proteins into peroxisomes and other microbodies. *Biochem. J.* **286,** 657-669.

46. Subramani, S. (1992) Targeting of proteins into the peroxisomal matrix. *J. Membr. Biol.* **125,** 99-106.

47. Hayashi, M., Aoki, M., Kato, A., Kondo, M. and Nishimura, M. (1996) Transport of chimeric proteins that contain a carboxy-terminal targeting signal into plant microbodies. *Plant J.* **10,** 225-234.

48. Hayashi, M., Aoki, M., Kondo, M. and Nishimura, M. (1997) Changes in targeting efficiencies of proteins to plant microbodies caused by amino acid substitutions in the carboxy-terminal tripeptide. *Plant Cell Physiol.* **38,** 759-768.

49. Nguyen, T., Zelechowska, M., Foster, V., Bergmann, H. and Verma, D. (1985) Primary structure of the soybean nodulin-35 gene encoding uricase II localized in the peroxisomes of uninfected cell of nodules. *Proc. Natl. Acad. Sci. USA* **82,** 5040-5044.

50. Mullen, R. T., Lee, M. S., Flynn, C. R. and Trelease, R. N. (1997) Diverse amino acid residues function within the type1 peroxisomal targeting signal. *Plant Physiol.* **115,** 881-889.

51. Kato, A., Hayashi, M., Kondo, M. and Nishimura, M. (1996) Targeting and processing of a chimeric protein with the N-terminal presequence of the precursor to glyoxysomal citrate synthase. *Plant Cell* **8,** 1601-1611.

52. Kato, A. and Hayashi, M. and Kondo, M., Nishimura, M. (1998) Transport of peroxisomal proteins that are synthesized as large precursors in plants. *ibid.*

53. Olsen, L. J., Ettinger, W. F., Damsz, B., Matsudaira, K., Webb, M. A. and Harada, J. J. (1993) Targeting of glyoxysomal proteins to peroxisomes in leaves and roots of a higher plant. *Plant Cell* **5,** 941-952.

54. Onyeocha, I., Behari, R., Hill, D. and Baker, A. (1993) Targeting of castor bean glyoxysomal isocitrate lyase to tobacco leaf peroxisomes. *Plant Mol. Biol.* **22,** 385-396.

55. Hayashi, M., Toriyama, K., Kondo, M. and Nishimura, M. (1998) 2,4-Dichlorophenoxybutyric acid-resistant mutants of Arabidopsis have defects on glyoxysomal fatty acid β-oxidation. *Plant Cell* **10,** 183-195.

56. Wain R. L. and Wightman F. (1954) The growth-regulating activity of certain ω-substituted alkyl carboxylic acids in relation to their β-oxidation within the plant. *Proc. Roy. Soc. Lond. Biol. Sci.* **142,** 525-536.

57. Distel, B., Erdmann, R., Gould, S. J., Blobel, G., Crane, D. I., Cregg, J. M., Dodt, G., Fujiki, Y., Goodman, J. M., Just, W. W., Kiel, J. A. K. W., Kunau, W. H., Lazarow, P. B., Mannaerts, G. P., Moser, H. W., Osumi, T., Rachubinski, R. A., Roscher, A., Subramani, S., Tabak, H. F., Tsukamoto, T., Valle, D., Vanderklei, I., Vanveldhoven, P. P. and Veenhuis, M. (1996) Unified

nomenclature for peroxisome biogenesis factors. *J. Cell Biol.* **135,** 1-3.

58. Subramani, S. (1997) *PEX* genes on the rise. *Nat Genet* **15,** 331-333.

59. Marzioch, M., Erdmann, R., Veenhuis, M. and Kunau, W. H. (1994) *PAS7* encodes a novel yeast member of the WD-40 protein family essential for import of 3-oxoacyl-CoA thiolase, a PTS2-containing protein, into peroxisomes. *EMBO J.* **13,** 4908-4918.

60. Zhang, J. W. and Lazarow, P. B. (1995) *PEB1* (*PAS7*) in *Saccharomyces cerevisiae* encodes a hydrophilic, intra-peroxisomal protein that is a member of the WD repeat family and is essential for the import of thiolase into peroxisomes. *J. Cell Biol.* **129,** 65-80.

61. McNew, J. A. and Goodman, J. M. (1996) The targeting and assembly of peroxisomal proteins: Some old rules do not apply. *Trends Biochem. Sci.* **21,** 54-58.

62. Erdmann, R. and Blobel, G. (1996) Identification of Pex13p, a peroxisomal membrane receptor for the PTS1 recognition factor. *J. Cell Biol.* **135,** 111-121.

63. Albertini, M., Rehling, P., Erdmann, R., Girzalsky, W., Kiel, J. A. K. W., Veenhuis, M. and Kunau, W. H. (1997) Pex14p, a peroxisomal membrane protein binding both receptors of the two PTS-dependent import pathways. *Cell* **89,** 83-92.

64. Komori, M., Rasmussen, S. W., Kiel, J. A. K. W., Baerends,R. J. S., Cregg, J. M., Van der Klei, I. J. and Veenhuis, M. (1997) The *Hansenula polymorpha*

PEX14 gene encodes a novel peroxisomal membrane protein essential for peroxisome biogenesis. *EMBO J.* **16,** 44-53.

65. Purdue, P. E., Lazarow, P. B. (1994) Peroxisomal biogenesis: Multiple pathways of protein import. *J. Biol. Chem.* **269,** 30065-30068.

FIGURE LEGENDS

Fig. 1. Effect of 2,4-dichlorophenoxybutyric acid (2,4-DB) and sucrose on the growth of wild-type Arabidopsis and *ped* mutants. Upper panel, seedlings grown for 7 days on growth medium containing 0.2 μg/ml of 2,4-DB. Lower panel, seedlings grown for 7 days on growth medium without sucrose. Photographs were taken after the seedlings has been removed from the media and rearranged on agar plates. Bar = 1 cm. WT; wild type.

Fig. 2. Immunodetection of thiolase in etiolated cotyledons of wild-type Arabidopsis and *ped* mutants. Extracts were prepared from 5-day-old etiolated cotyledons of wild-type Arabidopsis (WT) and *ped* mutants. For each sample, 5 μg of total protein was subjected to SDS-PAGE and immunoblot analysis was performed using an antibody raised against thiolase. The arrow indicates the positions of thiolase; arrowhead indicates the position of the precursor form of thiolase.

Fig. 3. Ultrastructure of peroxisomes in the cells of 5-day-old etiolated cotyledons. (A) A cotyledonary cell of a wild-type plant. (B) A cotyledonary cell of the *ped1* mutant. (C) A cotyledonary cell of the *ped2* mutant. Arrowhead; peroxisome, M; mitochondrion, Ep; etioplast, V; vacuole. Bar = 1 μm.

Table 1. Sequence specificity of carboxy-terminal tripeptide for PTS1 in plant (*48*) and other organisms (*65*). The sequences shown in this table have been demonstrated to be sufficient to target reporter proteins to peroxisomes in these cells. Underlined sequences have not yet found on a peroxisomal protein in that species. Asterisks indicate sequences that have been found on a peroxisomal protein but whose function has not been directly tested.

Plants	Mammals	*S. cerevisiae*	*H. polymorpha*	Trypanosomes
SRL	SRL			SRL
SRM				
SRI				
SKL	SKL	SKL	SKL	SKL
				SKM
			SKI	SKI
				SKY
		SKF		
	SHL			SHL
				SSL
	SQL*			S-M/N/Q-L
ARL				
ARM				
	AKL			AKL
		AKI		
			ARF	
PRL				
PRM				
CRL				
	CKL			CKL
	NKL*		NKL	NKL
				G/H/P/T-KL

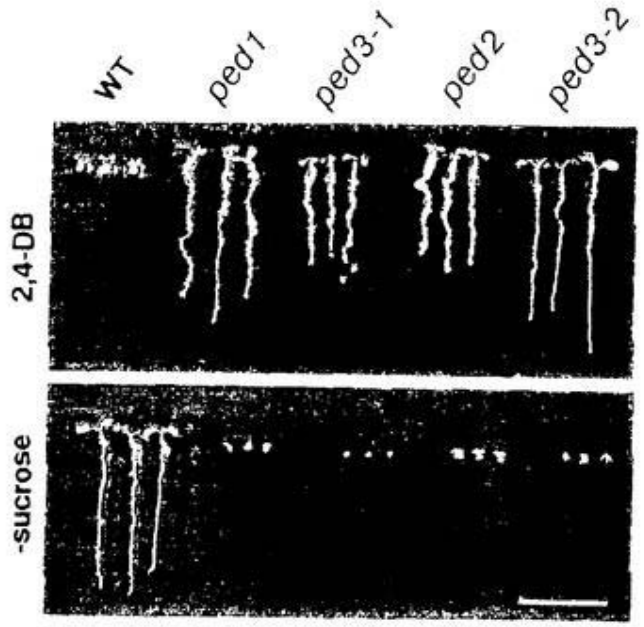

Fig. 1

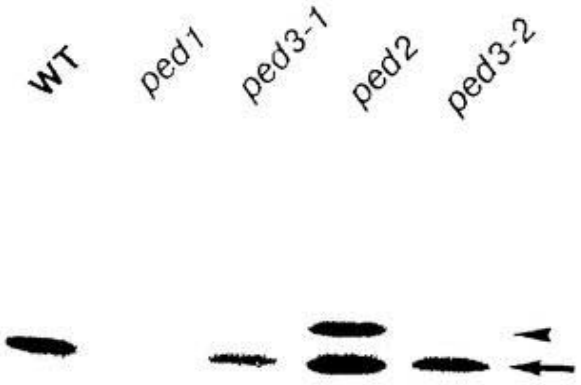

Fig. 2

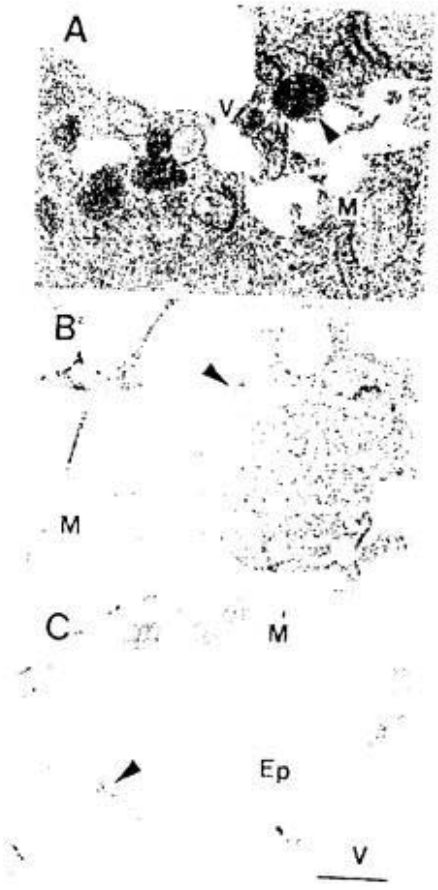

Fig. 3